

1 A multi-kingdom genetic barcoding system for 2 precise target clone isolation

3
4 Soh Ishiguro^{1,15,19}, Kana Ishida^{2,19}, Rina C. Sakata^{1,19}, Hideto Mori³⁻⁵, Mamoru Takana³,
5 Samuel King¹, Omar Bashteh¹, Minori Ichiraku⁶, Nanami Masuyama^{1,4,5}, Ren Takimoto¹, Yusuke
6 Kijima^{1,7}, Arman Adel¹, Hiromi Toyoshima³, Motoaki Seki³, Ju Hee Oh⁸, Anne-Sophie
7 Archambault⁸, Keiji Nishida^{9,10}, Akihiko Kondo⁹⁻¹¹, Satoru Kuhara¹², Hiroyuki Aburatani¹³,
8 Ramon I. Klein Geltink⁸, Yasuhiro Takashima⁶, Nika Shakiba¹, and Nozomu Yachie^{1,3,14,16-18*}

- 9
10 1. School of Biomedical Engineering, Faculty of Applied Science and Faculty of Medicine, The
11 University of British Columbia, Vancouver, Canada.
12 2. Spiber Inc., Tsuruoka, Japan.
13 3. Synthetic Biology Division, Research Center for Advanced Science and Technology, The
14 University of Tokyo, Tokyo, Japan.
15 4. Institute for Advanced Biosciences, Keio University, Tsuruoka, Japan.
16 5. Systems Biology Program, Graduate School of Media and Governance, Keio University, Fujisawa,
17 Japan.
18 6. Center for iPS Cell Research and Application, Kyoto University, Kyoto, Japan.
19 7. Department of Aquatic Bioscience, Graduate School of Agricultural and Life Sciences, The
20 University of Tokyo, Tokyo, Japan.
21 8. BC Children's Hospital Research Institute, Department of Pathology and Laboratory Medicine,
22 The University of British Columbia, Vancouver, Canada.
23 9. Engineering Biology Research Center, Kobe University, Kobe, Japan.
24 10. Graduate School of Science, Technology and Innovation, Kobe University, Kobe, Japan.
25 11. Department of Chemical Science and Engineering, Graduate School of Engineering, Kobe
26 University, Kobe, Japan.
27 12. Graduate School of Bioresource and Bioenvironmental Sciences, Faculty of Agriculture, Kyushu
28 University, Fukuoka, Japan.
29 13. Genome Science Division, Research Center for Advanced Science and Technology, The
30 University of Tokyo, Tokyo, Japan.
31 14. Premium Research Institute for Human Metaverse Medicine (WPI-PRIMe), Osaka University,
32 Suita, Osaka, Japan
33 15. Twitter: @soh_i
34 16. Twitter: @nzmyachie
35 17. Twitter: @yachielab
36 18. Mastodon: scencemastodon.com/@nzm
37 19. These authors contributed equally.
38
39 *Corresponding author: nozomu.yachie@ubc.ca.

40
41 **Teaser:** A multi-kingdom CRISPR-activatable barcoding system enables the precise isolation of target
42 barcode-labeled clones from a complex cell population.

43 **Clonal heterogeneity underlies diverse biological processes, including cancer progression, cell**
44 **differentiation, and microbial evolution. Cell tagging strategies with DNA barcodes have recently**
45 **enabled analysis of clone size dynamics and clone-restricted transcriptomic landscapes of**
46 **heterogeneous populations. However, isolating a target clone that displays a specific phenotype**
47 **from a complex population remains challenging. Here, we present a new multi-kingdom genetic**
48 **barcoding system, CloneSelect, in which a target cell clone can be triggered to express a**
49 **reporter gene for isolation through barcode-specific CRISPR base editing. In CloneSelect, cells**
50 **are first barcoded and propagated so their subpopulation can be subjected to a given experiment.**
51 **A clone that shows a phenotype or genotype of interest at a given time can then be isolated from**
52 **the initial or subsequent cell pools stored throughout the experimental timecourse. This novel**
53 **CRISPR-barcode genetics platform provides many new ways of analyzing and manipulating**
54 **mammalian, yeast, and bacterial systems.**

55
56 Cells are not homogeneous in any system. Although they proliferate and replicate the genome that
57 encodes molecular regulatory programs into their progenies, they also change their statuses according
58 to the dynamic response of gene expression patterns to environmental signals. As typically shown in
59 multicellular organisms, cells self-organize through mutual molecular and mechanical communications
60 and dynamically create complex structures. In these processes, spontaneous mutations in the genome
61 sometimes impair the cellular program and cause cellular malfunction. Conversely, some other
62 mutations confer growth or survival advantages to the cells, which can be beneficial or catastrophic to
63 the system.

64 During cancer chemotherapy, resistant clones arise and expand with unique genetic, epigenetic,
65 and cellular statuses, contributing to cancer recurrence and metastasis (1-4). In hematopoiesis, stem
66 cells of an analytically indistinguishable group show fate-restricted differentiation patterns, in which
67 some cells seem to be primed for specific lineages by incompletely understood factors (5-8). Similarly,
68 *in vitro* stem cell differentiation and direct reprogramming experiments have demonstrated that “elite”
69 clones reproducibly transform into target cell states (9-11). In laboratory microbial evolution experiments,
70 different cells within the initial population dynamically expand and shrink their clone sizes through the
71 acquisition of new mutations over multiple generations (12-16).

72 These views on clonal heterogeneity and cell lineage bias have been rapidly shaped by approaches
73 that use DNA barcodes and deep sequencing for high-resolution clonal cell tagging. DNA barcoding
74 involves integrating short and unique variable fragments of DNA—so-called “barcodes”—to individual
75 cells by lentiviral transduction, transposon-mediated delivery, site-specific DNA recombination in the
76 host genome, or plasmid transformation. In a given assay, the change in abundance of the barcoded
77 clones is traced *en masse* by subsampling the cell populations and quantifying the DNA barcodes by
78 deep sequencing read counts. Furthermore, the combination of barcode transcription and single-cell
79 RNA sequencing (scRNA-seq) allows clonal lineages to be analyzed alongside cell states, revealing cell
80 lineage-restricted state trajectories (9, 17-23). However, these measurements only provide snapshots
81 of clone population sizes and gene expression statuses at the time of observation (24), limiting the
82 analysis of the early causal molecular and/or environmental factors that derive specific fate outcomes
83 of clones.

84 Did the chemotherapy-resistant clones exist in the initial cell population with the genetic mutations
85 or altered cell state from the beginning? Did any molecular factor(s) underlie the observed stem cell
86 differentiation fates? Was the progression of the specific clone conditional on the existence of any other
87 clones? Flow cytometry cell sorting with immunostaining and emerging image cytometry cell sorting
88 technologies enable the dissociation of heterogeneous cell populations into single cells with their
89 observed phenotypes (25-28) but cannot do the same for a population of clones before they exhibit a
90 phenotype of interest. Furthermore, any current high-content omic measurement requires the
91 destruction of samples at the time of observation, which precludes the analysis of dynamic molecular
92 and cellular behaviors within the same biological systems. The new concept of “retrospective clone
93 isolation” has recently emerged to tackle the above-raised questions (29-33). In such a system, a
94 barcoded cell population is first propagated, and its subpopulation is subjected to a given assay (Fig.
95 1A). After identifying a barcoded clone of interest, the same clone (or its close relative) is isolated in a

96 barcode-specific manner from the initial or any other subpopulation stored during the experiment. The
97 isolated live clone can then be subjected to any following experiments, including omics measurements
98 and reconstitution of a synthetic cell population with the isolates.

99 The idea of retrospective clone isolation has been implemented using CRISPR–Cas9 genome
100 editing. In one form of the CRISPR activation (CRISPRa)-based approach (29), cells are tagged with
101 DNA barcodes that are located upstream of a fluorescent reporter gene with a minimal promoter
102 sequence. The barcoded cells are designed not to express the reporter gene before the guide RNA
103 (gRNA)-induced transcription activation is triggered. Once a barcoded clone is identified for isolation, a
104 gRNA targeting its barcode is introduced to the cell population with catalytically dead Cas9 (dCas9)
105 fused to transcriptional activator(s) to trigger reporter expression of the target clone. This approach
106 suffers from low specificity due to leaky expression of the reporter in the non-activated condition,
107 presumably because of the effect of another constitutively active promoter neighboring the reporter. This
108 effect can be mitigated by barcoding cells with a gRNA library pool and then labeling a target cell by
109 delivering a plasmid that only encodes a reporter targeted by its corresponding gRNA, with no additional
110 promoters present (30, 31). However, this strategy prohibits selection of the cells harboring the reporter
111 plasmid using a secondary selectable marker. The CRISPRa-based approach requires continuous
112 activation and maintenance of all components when a downstream experiment necessitates reporter
113 expression in isolated cells. Furthermore, CRISPRa-based retrospective clone isolation has only been
114 demonstrated in mammalian cell systems.

115 Genetic circuits based on DNA code alteration generally show highly specific input responses (34).
116 A wild-type Cas9-based retrospective clone isolation has also been prototyped as a DNA code
117 alteration-based approach (32). In this system, an out-of-frame start codon is followed by in-frame stop
118 codons and a DNA barcode is encoded upstream of a reporter gene, whose translation is inactivated.
119 The reporter translation can be restored by Cas9-induced double-stranded DNA break (DSB) and
120 deletion through non-homologous end-joining (NHEJ) DNA repair at the barcode region, which
121 stochastically removes the stop codons and brings the start codon into the coding frame. While this
122 does not usually show unexpected reporter activation for non-target clones and confers permanent
123 labeling of a target clone, the system's sensitivity relies on stochastic DNA deletion, which can be a
124 bottleneck to efficiency. Cas9-induced DSB is also cytotoxic and potentially impairs the target clone
125 during the reporter activation procedure (35, 36).

126 Another approach has been proposed using RNA fluorescence *in situ* hybridization (FISH), where
127 barcoded cells are first fixed, and a target transcribing barcoded clone can be labeled with a fluorophore
128 probe and isolated by cell sorting (37). While RNA FISH is specific and sensitive, the isolated cells
129 cannot be used for cell culture-based assays due to the fixation of the analyte.

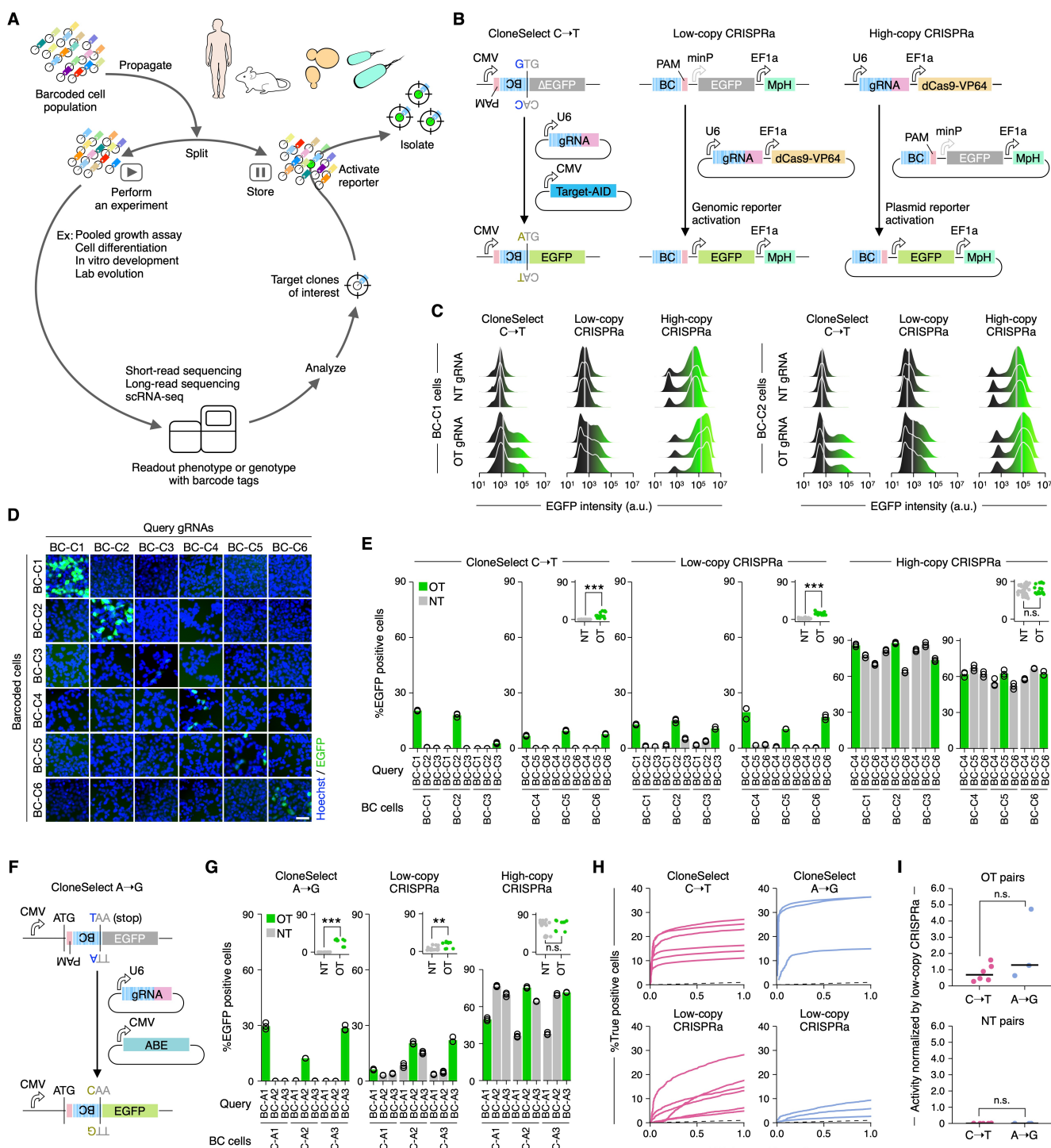
130 Here, we report a new CRISPR base editing-based approach, CloneSelect, that overcomes the
131 current technical constraints. CloneSelect is based on the restoration of reporter protein translation by
132 base editing of an impaired start codon or an upstream stop codon in a barcode-specific manner. The
133 new method is highly scalable, programmable, and compatible with scRNA-seq. Its specificity markedly
134 surpasses other CRISPR-based systems. We also present the versatility of the method by implementing
135 CloneSelect in human embryonic kidney (HEK) cells, mouse embryonic stem cells (mESCs), human
136 pluripotent stem cells (hPSCs), yeast cells, and bacterial cells.

137

138 Results

139 Mammalian CloneSelect by C→T base editing

140 CRISPR base editing has widely been used to induce a single nucleotide substitution at a target genomic
141 site without DSB (38). We first hypothesized that a C→T base editor (CBE)-based circuit (39) would
142 enable highly sensitive, precise barcode-specific clone isolation with better performance than the
143 previous CRISPR-based methods. In this CloneSelect C→T system, a barcode is encoded immediately
144 upstream of a reporter gene whose start codon is mutated to GTG (Fig. 1B left). A constitutively active
145 promoter transcribes the reporter-encoding region, but the impaired start codon makes its translation
146 inactive. C→T base editing at the target barcode site enables the antisense strand of the first guanine
147 (cytosine) to be substituted into thymine, restores ATG on the sense strand, and activates the reporter



149
150

151 **Fig. 1. The CloneSelect circuit.** (A) Conceptual diagram of retrospective clone isolation. (B) Different barcode-
152 specific gRNA-dependent reporter activation circuits. CloneSelect C→T, low-copy CRISPRa, and high-copy
153 CRISPRa. (C) Flow cytometry analysis of single-cell EGFP activation levels. (D) Barcode-dependent reporter
154 activation of six barcoded cell lines by CloneSelect C→T. Scale bar, 50 μm. (E) Comparison of CloneSelect C→T,
155 low-copy CRISPRa, and high-copy CRISPRa across the same barcode-gRNA pairs (n=3). For each approach,
156 Welch's t-test was performed to compare on-target (OT) and non-target (NT) activations. (F) CloneSelect A→G.
157 (G) Comparison of CloneSelect A→G, low-copy CRISPRa, and high-copy CRISPRa across the same barcode-
158 gRNA pairs (n=3). Welch's t-test was performed to compare OT and NT activations. (H) ROC curves along varying
159 EGFP intensity thresholds for target barcoded cells. Left, CloneSelect C→T and low-copy CRISPRa by the same
160 targeting gRNAs. Right, CloneSelect A→G and low-copy CRISPRa for the same set of targeting gRNAs. (I)

161 Performance comparison of CloneSelect C→T and CloneSelect A→G. Activated cell frequencies of OT and NT
162 barcodes were normalized by activated cell frequencies of OT barcodes conferred by low-copy CRISPRa using
163 the same targeting gRNA. The Mann-Whitney U test was performed to compare the two groups of datasets. * $P <$
164 0.05; ** $P < 0.01$; *** $P < 0.001$.

165

166

167 translation. To achieve this, we employed Target-AID, one of the CBEs with a narrow C→T base editing
168 window in the gRNA target site (36, 38).

169 To examine the performance of CloneSelect C→T employing EGFP (enhanced green fluorescent
170 protein) as a reporter, we compared it with two CRISPRa-based approaches. In the low-copy CRISPRa
171 approach, cells are lentivirally labeled by barcoded CRISPRa reporters, each consisting of a barcode
172 followed by a minimal promoter and EGFP with an MCP-p65-HSF1 (MpH) transcriptional activator
173 expression unit encoded on the same vector (Fig. 1B middle). The reporter can be activated by
174 introducing catalytically dead Cas9 (dCas9) fused to VP64 and a targeting gRNA fused to MS2 hairpins,
175 interacting with the MCP (MS2 coat protein) domain of MpH to recruit transcriptional activators (40). In
176 the high-copy CRISPRa approach, cells are labeled by gRNAs, in which gRNA spacers serve as
177 barcodes (Fig. 1B right). Upon transfection of the high-copy CRISPRa reporter-encoding plasmids, the
178 reporter expression can be induced in the cell encoding the targeting gRNA.

179 CloneSelect C→T was more sensitive than low-copy CRISPRa and more specific than high-copy
180 CRISPRa in HEK293T cells. For each of the three approaches, we prepared two cell lines with the same
181 set of barcodes (BC-C1 and BC-C2). CloneSelect C→T with on-target gRNAs activated the reporter
182 expression in 19.17% (BC-C1) and 17.89% (BC-C2) of target cells while minimizing the activation by
183 non-targeting gRNAs to less than 0.1% (Fig. 1C and Fig. S1A). Low-copy CRISPRa showed a lower
184 reporter activation rate of 5.24–6.26% (Fig. 1C and Fig. S1B), and high-copy CRISPRa showed a very
185 high background activation rate of 52.12–62.15% by non-targeting gRNAs (Fig. 1C and Fig. S1C). The
186 reporter intensity of activated cells for CloneSelect C→T was slightly but significantly higher (1.76-fold)
187 than that of low-copy CRISPRa (Fig. S1D). The sensitivity of CloneSelect C→T using Target-AID
188 constructed based on a nickase Cas9 (nCas9) was higher than that constructed based on dCas9 (Fig.
189 S1E). CloneSelect C→T was also demonstrated to activate the reporter expression in HeLa cells in a
190 barcode-specific manner (Fig. S1F).

191 To systematically examine the orthogonality between barcodes and gRNAs across the three
192 approaches, we expanded the analysis to six barcodes (Fig. 1D and Fig. S2A and B) and demonstrated
193 that CloneSelect C→T and low-copy CRISPRa both specifically activated the reporter expression of
194 target barcoded cells, where 2.81–20.46% and 10.39–19.53% of target cells were EGFP positive,
195 respectively, with minimal non-target activation (Fig. 1E). Consistent with the preceding result,
196 CloneSelect C→T exhibited significantly higher overall reporter expression level than low-copy
197 CRISPRa (Fig. S2C) and the least false positive rate (Fig. S2D). High-copy CRISPRa showed
198 substantially lower orthogonality (Fig. 1E and Fig. S2B and D), indicating that this approach is not
199 practical for retrospective clone isolation. For CloneSelect C→T, we also optimized the input DNA
200 amount without elevating the minimal false positive rate (Fig. S2E and F).

201 We also tested a wild-type CRISPR-based system in which the reporter expression interrupted by
202 an upstream stop codon is removed by the barcode-specific DSB, followed by its stochastic deletion
203 with NHEJ (Fig. S3A). The reporter activation rate of this approach remained at 2.14–2.30% for target
204 barcoded cells with a relatively high-false positive rate of 0.51–0.56 % for non-target barcoded cells (Fig.
205 S3B and C). Additionally, as an alternative to the EGFP reporter, we attempted to develop an mCherry
206 reporter for CloneSelect C→T (Fig. S4A). However, the mutation of the start codon did not inactivate
207 the fluorescent expression of the wild-type, presumably because the second methionine served as a
208 start codon (Fig. S4B and C). We found that a stringent barcode-specific gRNA-dependent reporter
209 activation can be established with the M1V (GTG)+M9A mutant without losing the fluorescence intensity
210 level (Fig. S4D).

211

212 **Mammalian CloneSelect by A→G base editing**

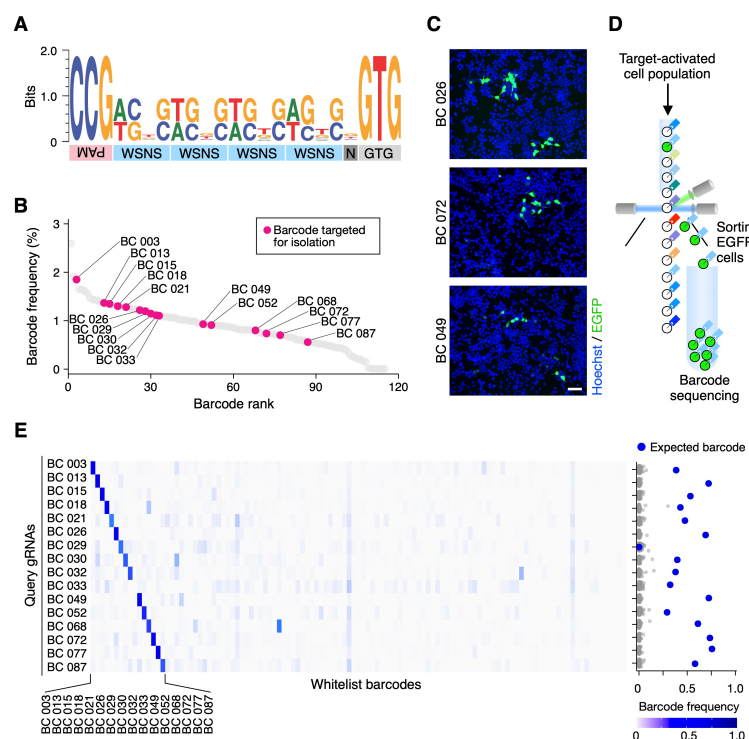
213 While exhibiting high efficiency and specificity in human cells, CloneSelect C→T is not applicable for
214 clone isolation of bacterial species as they use GTG to initiate protein translation (41). We thus designed

215 another system, CloneSelect A→G, using an adenine base editor ABE-7.10 that induces A→G base
216 substitution at the gRNA target sequence (42). In CloneSelect A→G, following a constitutively active
217 promoter and a start codon, a barcode encoding a TAA stop codon prevents downstream reporter
218 translation (Fig. 1F). The stop codon can be removed in a gRNA-dependent manner by mutating the
219 antisense strand of the thymine (adenine) to guanine, converting the stop codon into CAA (Proline). We
220 compared the performance of CloneSelect A→G, low-copy CRISPRa, and high-copy CRISPRa (Fig.
221 1G and Fig. S5A–F) for three arbitrarily designed barcodes in HEK293T cells. Similar to CloneSelect
222 C→T, CloneSelect A→G activated the reporter expression for 12.27–31.47% of on-target cells, whereas
223 the non-target activation was maintained below 0.5% with high orthogonality of barcodes and gRNAs.
224 Low-copy CRISPRa also exhibited barcode-specific reporter activation, but despite a lower reporter
225 expression level, its overall false positive rate was higher than CloneSelect A→G (Fig. S5H). High-copy
226 CRISPRa again showed a high background activation level.

227 To quantitatively compare the performances of CloneSelect C→T, CloneSelect A→G, low-copy
228 CRISPRa, and high-copy CRISPRa, we analyzed reporter activation frequencies of on-target barcoded
229 cells when a stringent false positive rate of 0.5% was permitted. CloneSelect C→T and CloneSelect
230 A→G exhibited 10.05–24.88% and 14.12–35.19%, respectively (Fig. 1H). Low-copy CRISPRa
231 examined with the same barcode sets also used for CloneSelect C→T and CloneSelect A→G exhibited
232 2.71–22.37% and 1.92–6.60%, respectively (Fig. 1H). In contrast, high-copy CRISPRa did not show
233 reporter-activated cells at this threshold. The efficacy of the gRNA to recruit the effector Cas9, in general,
234 has been known to depend highly on its
235 targeting sequence (43, 44). To compare
236 CloneSelect C→T and CloneSelect
237 A→G, their cell activation frequencies for
238 different target barcodes were
239 normalized by those of low-copy
240 CRISPRa for the same barcodes. As a
241 result, we did not observe a marked
242 difference in normalized performance
243 between CloneSelect C→T and
244 CloneSelect A→G (Fig. 1I).

245 Isolation of barcoded human cells 246 from a heterogeneous population

247 To examine if CloneSelect C→T can
248 isolate target barcoded cells from a
249 complex population, we next generated
250 a barcoded lentiviral library by pooled
251 ligation of barcoded EGFP fragments
252 (Fig. S6A). The barcoded EGFP
253 fragments were amplified by PCR using
254 an upstream forward primer pool
255 encoding semi-random barcodes and a
256 common reverse primer (Fig. S6A and
257 B). The barcode sequences were
258 designed to be WSNS repeats (W=A or
259 T; S=G or C) to avoid additional start
260 codons from appearing. The ligation
261 product was used to transform
262 *Escherichia coli* (*E. coli*) cells, and
263 transformant colonies on an agar plate
264 were scraped to purify a lentiviral
265 barcode library pool. We estimated that
266 our protocol normally confers a barcode
267



268 **Fig. 2. Barcode-dependent cell isolation from a HEK293T cell**
269 **population.** (A) Nucleotide compositions of barcodes in the
270 mammalian CloneSelect C→T plasmid mini-pool. Five barcodes
271 that had unexpected lengths were excluded from this
272 visualization. The full barcode sequence list can be found in
273 Table S1. (B) Barcode abundances in the cell population labeled
274 by the mini-lentiviral barcode pool of CloneSelect C→T. (C)
275 gRNA-dependent labeling of target barcoded cells in a
276 population. (D) Flow cytometry cell sorting of reporter-activated
277 cells. (E) Barcode enrichment analysis after cell sorting of the
278 reporter-activated cells. Each row represents the barcode
279 enrichment profile for each target isolation assay.

268 complexity of multiple hundreds of thousands (Fig. S6C) and confirmed most of them to have barcodes
269 by DNA restriction digestion (Fig. S6D).

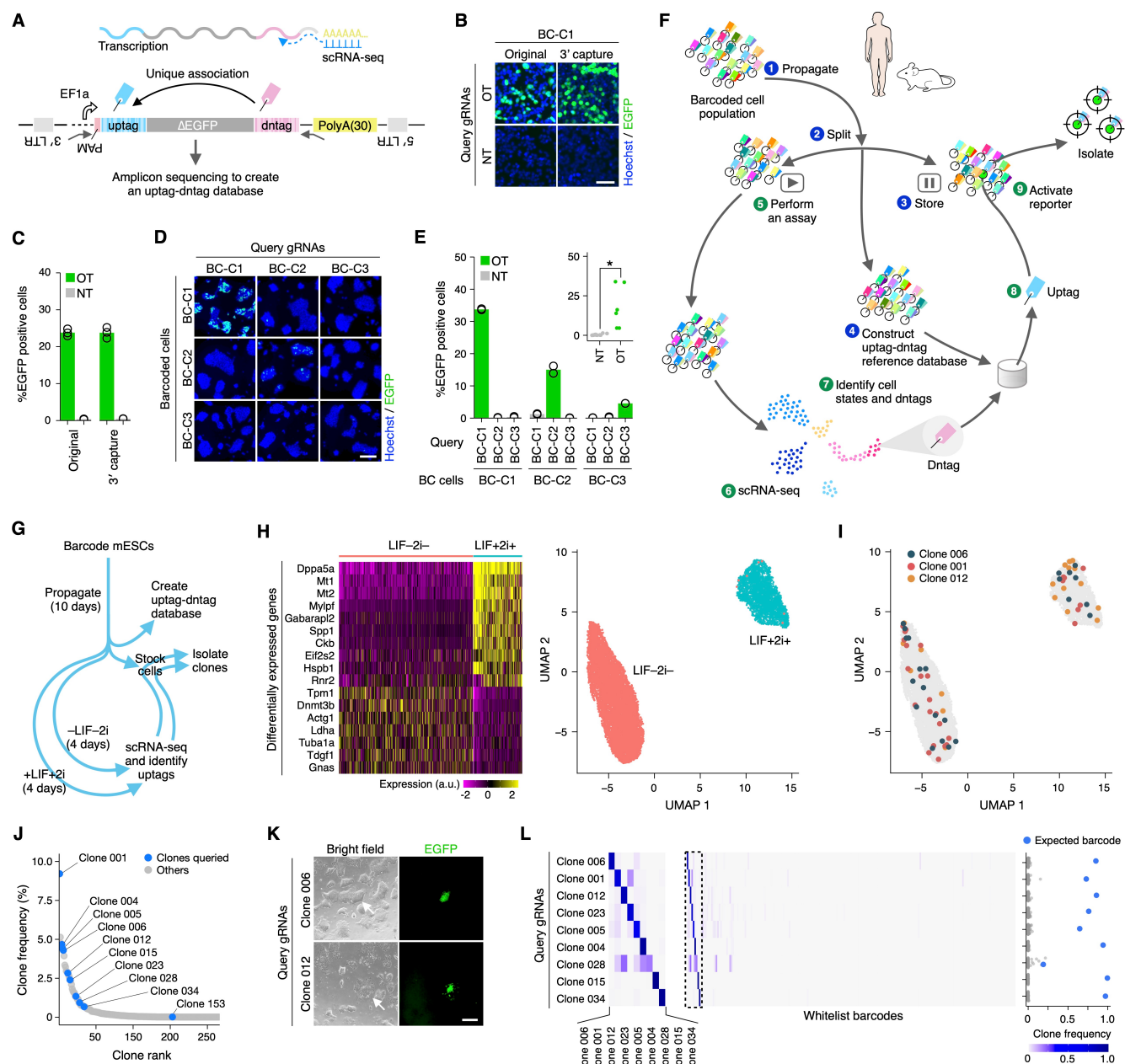
270 To perform a proof-of-principle demonstration, we transformed *E. coli* cells again with the
271 constructed library pool, isolated barcoded plasmid clones into a 96-well plate, and pooled 93 that were
272 confirmed to have single barcodes by Sanger sequencing (Fig. S6E). The plasmid mini-pool was used
273 to transduce HEK293T cells with a low multiplicity of infection (MOI) of <0.1, ensuring a single barcode
274 was introduced to each cell. We amplified the barcode region from the plasmid mini-pool and the
275 transduced cells by PCR and analyzed them by high-throughput sequencing. We identified 115
276 barcodes (Fig. 2A) and found that the variation in barcode abundance was replicable in two independent
277 sequencing library preparations (Fig. S6F) and largely inherited from that in the plasmid pool (Fig. S6G
278 and H), suggesting no substantial barcode-dependent bias in lentiviral packaging and transduction.

279 We then tested if we could enrich cells with 16 arbitrarily selected barcodes of different abundances
280 in the cell population (Fig. 2B). For each target barcode, the cell population was co-transfected with the
281 gRNA and Target-AID plasmids. After four days, we observed EGFP-positive cells in each assay (Fig.
282 2C) and sorted them by flow cytometry cell sorting (Fig. 2D). For each target barcode, its enrichment in
283 the sorted cell population was analyzed by PCR and high-throughput sequencing (Fig. 2E). In sum, we
284 succeeded in enriching the target barcoded cells in 15 out of 16 experiments (93.75%) with a relative
285 barcode abundance of 29.18–75.75% after sorting. For the 15 successful targets, the mutated start
286 codon was restored to ATG with an efficiency of 91.63–99.85% (Fig. S6I). A fraction of cells with the
287 expected barcodes did not demonstrate the GTG→ATG mutation, suggesting that the cytidine
288 deamination by Target-AID on the antisense strand might be sufficient to express the codon-repaired
289 reporter transcripts.

290 291 Isolation of clones identified in a scRNA-seq platform

292 To extend the utility of CloneSelect to isolate living clones identified according to their high-dimensional
293 transcriptome profiles from a cell population, we made CloneSelect C→T compatible with 3' capture
294 scRNA-seq platforms and established scCloneSelect. In scCloneSelect, the barcode located upstream
295 of the reporter with the mutated start codon (hereafter referred to as “uptag”) is paired with another
296 barcode (“dntag”) downstream of the reporter followed by a hard-coded 30-nt poly(A) sequence (Fig.
297 3A). The dntag is captured as part of the short-read scRNA-seq reads through the common poly(A)-
298 tailed 3' enrichment strategy (45, 46) and used to refer its corresponding uptag for the reporter start
299 codon restoration. This change in the circuit design did not affect the reporter activation performance of
300 CloneSelect C→T in HEK293T cells (Fig. 3B and C and Fig. S7A and B) as well as the high orthogonality
301 between barcodes and gRNAs (Fig. S7C and D). We also confirmed that dntag barcodes were
302 transcribed (Fig. S7E) and efficiently captured by a scRNA-seq platform (Fig. S7F).

303 One intriguing application of scCloneSelect would be to study the fate-determining factors of stem
304 cell differentiation and cell reprogramming. scCloneSelect can be used to retrospectively isolate, from
305 the initial population, cell clones whose states have been identified using scRNA-seq after differentiation.
306 These clones could then be subjected to further analyses. We therefore tested if the scCloneSelect
307 system is functional in selectively labeling target barcoded cells in mouse embryonic stem cell (mESC)
308 and human pluripotent stem cell (hPSC) populations. In one of our approaches, a constitutively active
309 Target-AID expression cassette was first stably integrated into a cell population by piggyBac
310 transposon-based genomic integration, followed by lentiviral transduction of the cells with a
311 scCloneSelect barcode library (Fig. S7G). The reporter activation was then triggered by introducing a
312 targeting gRNA by lentiviral transduction or lipofectamine transfection. In mESCs, both of the gRNA
313 reagent delivery methods activated the reporter expression in a barcode-dependent manner with no
314 marked false positive activation, but lentiviral delivery of the gRNA showed an overall higher cell
315 activation of 4.57–33.76% in comparison to 2.91–15.77% by the lipofectamine-based plasmid delivery
316 method (Fig. 3D and E and Fig. S7H). The barcode-specific reporter activation was also successful in
317 hPSCs, where targeting gRNA reagents were delivered by transfection (Fig. S7I). Additionally, we tested
318 an approach that required a minimal number of steps, where hPSCs were first lentivirally barcoded, and
319 the reporter was activated by electroporation with the targeting gRNA and Target-AID delivered together
320 (Fig. S7J). This also enabled barcode-dependent reporter activation in hPSCs (Fig. S7K).



321

322

Fig. 3. Isolation of live stem cell clones characterized by scRNA-seq. (A) scCloneSelect. (B and C) Barcode-specific gRNA-dependent reporter activation of the original CloneSelect C→T and scCloneSelect in HEK293T cells ($n=3$). Scale bar, 50 μ m. (D and E) Barcode-specific gRNA-dependent reporter activation of three barcoded mESC lines by scCloneSelect. Target-AID was stably integrated prior to the barcoding. gRNAs were delivered by lentiviral transduction. Scale bar, 100 μ m. Welch's t-test was performed to compare on-target (OT) and non-target (NT) activations. * $P < 0.05$; ** $P < 0.01$; *** $P < 0.001$. (F) Schematic diagram of a scCloneSelect workflow to retrospectively isolate a cell clone demonstrating a gene expression profile of interest from a cell population stored before they demonstrate the target gene expression pattern. (G) mESC cell culture assays and clone isolation performed in this work. (H) scRNA-seq of mESC populations treated with LIF and 2i and those without LIF or 2i. (I) Distribution of cells for arbitrarily selected clones in the two-dimensional embedding of high-dimensional gene expression space by UMAP (uniform manifold approximation and projection). (J) Abundance of barcoded cell clones in the mESC population. The data was generated based on dntags identified by reamplifying the dntag reads from the original scRNA-seq libraries. (K) gRNA-specific activation of target barcoded clones in the mESC population. Scale bar, 50 μ m. (L) Barcode enrichment analysis after cell sorting of the reporter-activated cells. Each row represents the barcode enrichment profile for each target isolation assay. The left heatmap was expanded from the dashed box area of the right heatmap.

339 To demonstrate that barcoded cell clones identified with single-cell transcriptomes can be isolated
340 from a barcoded cell pool sub-populated in parallel with the one used in scRNA-seq, we set up the
341 following experiments using mESCs (Fig. 3F and Fig. S8A). In this experimental pipeline, a ΔEGFP (no
342 start codon) fragment reporter is first amplified with forward primers encoding semi-random uptags of
343 WSNS repeats accompanying a mutated start codon and reverse primers encoding random dntags.
344 They are cloned into a common backbone plasmid *en masse* (Fig. S8B and C), and the constructed
345 barcode plasmid pool is used to lentivirally barcode cells. Barcoded cells are then cultured to propagate
346 cell clones (Step 1) and separated into three groups of sub-pools (Step 2). The first group is stored for
347 later clone isolation (Step 3). The second group is used to identify the uptag-dntag combination
348 reference database by PCR amplification and high-throughput sequencing (Step 4). The last group is
349 subjected to a given assay, during which intermediate subpopulations can be stored at any point (Step
350 5). A cell population obtained during the assay is then analyzed by scRNA-seq to identify high-content
351 gene expression profiles of single cells (Step 6). For a single cell demonstrating a cell state of interest,
352 its dntags can be identified (Step 7), and the corresponding uptag can be retrieved from the uptag-dntag
353 combination reference database (Step 8). Finally, using a gRNA targeting the identified uptag, the
354 reporter expression of the clone containing the dntag is activated and isolated by cell sorting (Step 9).
355 Because retroviral transduction, in general, is prone to having chimeric products of input vector
356 sequences integrated into the genome through its high recombination activity (47, 48), the uptag-dntag
357 database of the analyte population needs to be determined every time after the pooled transduction.
358 We optimized the PCR protocol for the amplicon sequencing that identifies this database by minimizing
359 chimeric PCR artifact products (Fig. S8D and E).

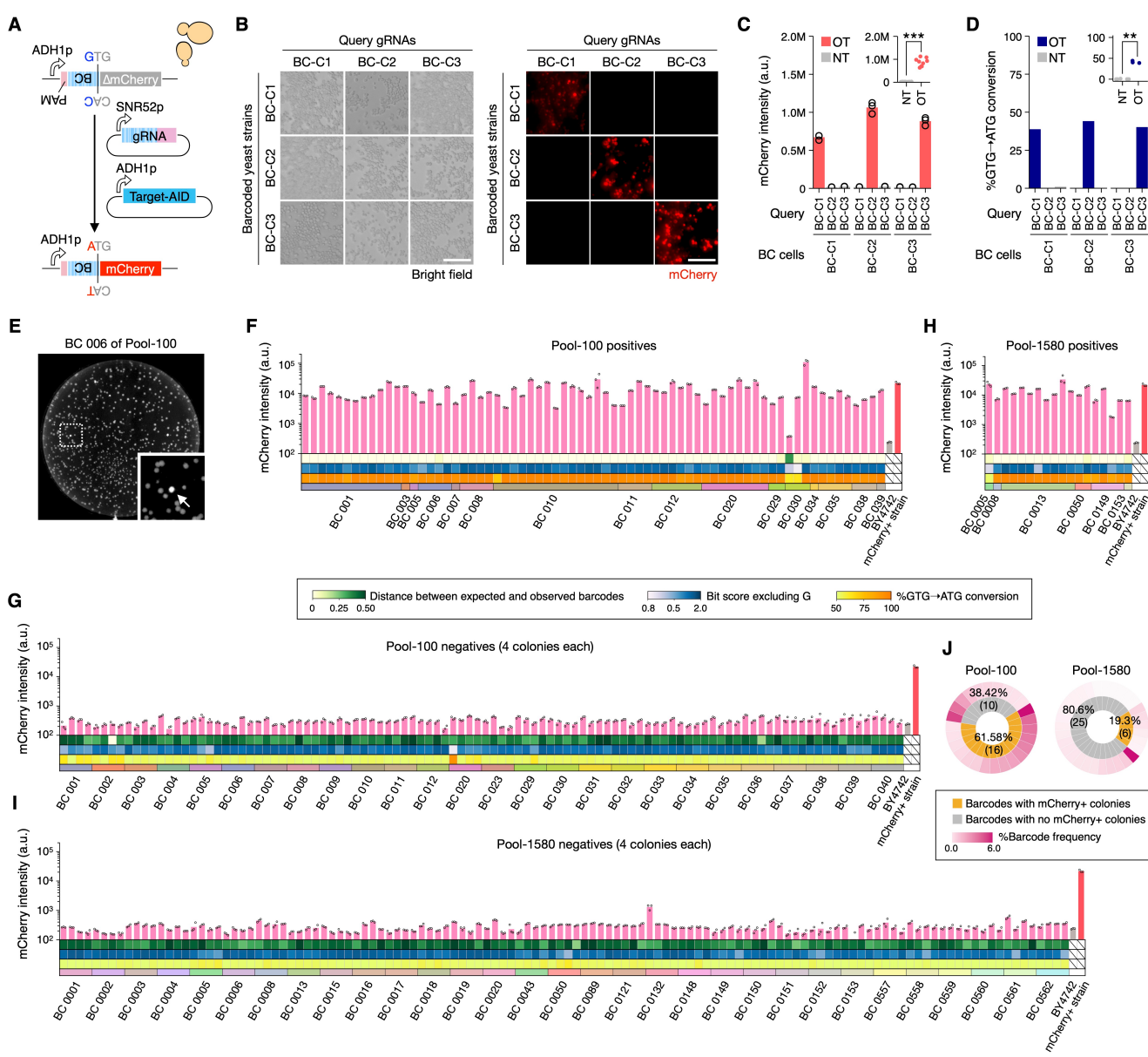
360 Using a plasmid pool with a barcode complexity of ~150,000, we lentivirally transduced mESCs with
361 Target-AID at an MOI of <0.1. Following the creation of a clone variation bottleneck by sparse sampling
362 and 10 days of expansion, a subpopulation of the barcoded cells was used to construct the uptag-dntag
363 database, in which 216 unique barcode pairs were identified (Fig. 3G). After preserving another
364 subpopulation, the remaining cells were cultured with serum with LIF and 2i (LIF+2i+) or serum without
365 LIF or 2i (LIF–2i–), to maintain or to lose pluripotency, respectively. Four days after, scRNA-seq was
366 performed independently for the two conditions. While the RNA capture rates per cell of the two datasets
367 were similar (Fig. S9A), the gene expression profiles of single cells were clustered into two distinct
368 groups along with the culture conditions (Fig. 3H and Fig. S9B). Pluripotency marker genes, such as
369 *Dppa5a*, were highly expressed in the pluripotency maintenance condition, whereas differentiation
370 marker genes, such as *Tpm1*, were enriched in the non-pluripotent condition. Although the barcoded
371 clones did not show a significantly biased distribution between the two conditions, we attempted to
372 isolate the top 10 abundant clones in the scRNA-seq datasets (Fig. 3I and Fig. S9C and D) from the
373 initial barcoded population. The abundances of these clones varied from 0.0133% to 9.21% in the initial
374 population according to the analysis determined by the uptag-dntag database (Fig. 3J). Except for one
375 experiment targeting Clone 153, we obtained a sufficient number of EGFP-positive cells after introducing
376 the targeting gRNA using lentivirus followed by flow cytometry cell sorting (Fig. 3K and Fig. S9E). For
377 each of the remaining nine clone isolation attempts, eight showed target clone enrichment with relative
378 target abundances of 64.8–99.4%, whereas one (Clone 028) showed an enrichment degree of 18.9%
379 (Fig. 3L). Furthermore, we isolated single cells from the EGFP-positive cell samples obtained for Clone
380 006 and Clone 012, expanded them (Fig. S9F), and confirmed the purification of the isolated clones
381 (Fig. S9G). Accordingly, scCloneSelect was demonstrated to greatly enrich a target clone identified by
382 scRNA-seq from a complex population with a success rate of 80% (eight out of 10).

384 Yeast CloneSelect

385 Clonal barcoding approaches have also been used in microorganisms, such as yeast *Saccharomyces*
386 *cerevisiae* (*S. cerevisiae*) and *E. coli*, to study their laboratory evolution and the genomic mutations
387 accompanying clonal expansions of cells (14, 16). However, the analysis methods have been limited to
388 time-course tracing of clone size dynamics. No technology has been developed to explore genetic,
389 epigenetic, and other molecular factors contributing to laboratory evolution.

390 We next extended the CloneSelect C→T system for the yeast *S. cerevisiae* using mCherry as a
391 fluorescent reporter (Fig. 4A). Like the mCherry reporter in mammalian cells, we also needed to truncate

392 the first nine amino acids of mCherry to establish the reporter system (Fig. S10A). CBEs, including
 393 Target-AID, developed for mammalian species normally accompany uracil glycosylase inhibitor (UGI)
 394 to inhibit the base excision repair pathway, enhancing both the efficacy and purity of C→T substitution
 395 at the target site (38). However, Target-AID has been tested in yeast without UGI and was demonstrated
 396 to confer C→D (non-C) substitution at the target sequence at a high rate (36). We, therefore, constructed
 397
 398
 399



400
 401
 402 **Fig. 4. Yeast CloneSelect.** (A) Yeast CloneSelect C→T circuit. (B and C) Barcode-specific gRNA-dependent
 403 reporter activation. Scale bar, 25 μm. Mean mCherry intensity measured by a plate reader was normalized by
 404 OD_{595 nm} (n=3). Welch's t-test was performed to compare on-target (OT) and non-target (NT) activities. (D)
 405 GTG→ATG editing frequencies observed by high-throughput sequencing. Welch's t-test was performed to
 406 compare OT and NT datasets. (E) Yeast colonies formed on a 10-cm agar plate after performing a target clone
 407 labeling in the yeast cell population of Pool-100. (F–J) Analysis of colonies isolated after clone labeling using each
 408 targeting gRNA. (F) mCherry positive isolates from Pool-100. (G) mCherry negative isolates from Pool-100. (H)
 409 mCherry positive isolates from Pool-1580. (I) mCherry negative isolates from Pool-1580. (J) Summary of the
 410 analysis results. *P < 0.05; **P < 0.01; ***P < 0.001.

411 a yeast Target-AID with UGI and found that it did not largely impair the base editing activity (Fig. S10B–
412 D) but as expected, greatly enhanced the frequency of resulting thymine at the target sequence (Fig.
413 S10E). The efficient yeast CloneSelect C→T reporter activation was only possible by the addition of
414 UGI (Fig. S10F). Similar to mammalian CloneSelect systems, yeast CloneSelect C→T was also
415 demonstrated to activate barcoded cells in a highly target-specific manner with a sensitivity of 38.80–
416 44.13% by co-transformation of Target-AID and gRNA plasmids (Fig. 4B–D and Fig. S10G). Unlike
417 mammalian cells, the labeled clones could be isolated by picking fluorescent colonies formed on a solid
418 agar plate (Fig. 4E).

419 To test the sensitivity of the clone isolation strategy, we generated a barcode plasmid pool by a
420 pooled ligation of semi-random barcode fragments to a backbone vector (Fig. S11A and B). Following
421 a quality control of the pooled cloning reaction (Fig. S11C), *E. coli* cells were then transformed with the
422 plasmid pool, and either 100 or ~1,580 colonies were pooled to prepare barcode plasmid pools of
423 defined complexities (hereafter referred to as Pool-100 and Pool-1580, respectively). After establishing
424 the barcoded yeast cell populations of Pool-100 and Pool-1580 by yeast plasmid transformation, we
425 arbitrarily targeted 26 and 31 barcodes of a range of abundances (0.83–5.79% for Pool-100 and 0.12–
426 0.37% for Pool-1580) to be isolated (Fig. S11D). For each barcoded clone isolation, its corresponding
427 gRNA plasmid and Target-AID plasmid was co-transformed into the barcoded yeast cells, and
428 fluorescent colonies were isolated, if any, together with four non-fluorescent colonies. The colony
429 isolates were then cultured in liquid selective media in a microwell plate to measure the fluorescence
430 intensities by a plate reader and barcode sequences were examined by PCR followed by Sanger
431 sequencing (Fig. 4F–I). For Pool-100, 16 out of the 26 attempts (61.58%) conferred positive colonies,
432 all of which, except for one of the three positive colonies obtained for BC 030, had the expected
433 barcodes with a GTG→ATG conversion rate of 48.92–97.41% (Fig. 4J). For Pool-1580, six out of the
434 31 attempts (19.35%) conferred positive colonies, and all of them had the expected barcodes with a
435 GTG→ATG conversion rate of 81.51–97.20%. The abundance of these successful barcodes in the Pool-
436 100 and Pool-1580 yeast pools ranged from 0.120% and 5.78%, respectively, demonstrating that yeast
437 CloneSelect can also isolate rare clones.

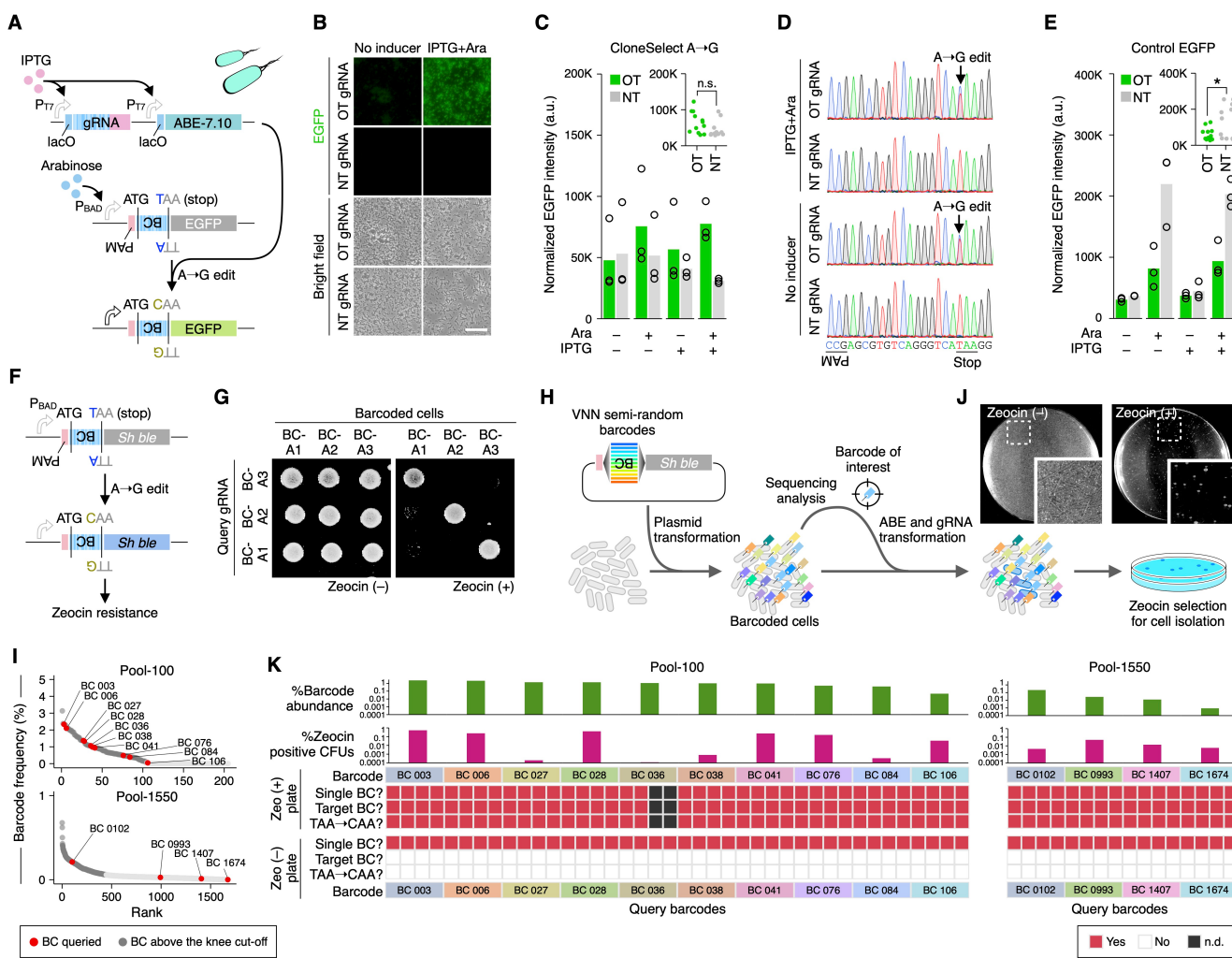
438 **Bacterial CloneSelect**

439 Lastly, we also established a bacterial CloneSelect system for *E. coli* clone isolation. We first
440 implemented CloneSelect A→G using an arabinose-inducible promoter for the EGFP reporter and an
441 IPTG (Isopropyl β-d-1-thiogalactopyranoside)-inducible promoter for both the gRNA and ABE (Fig. 5A).
442 The inducible promoter circuits showed an overall higher reporter expression in a barcode-specific
443 manner (Fig. 5B). At the same time, the EGFP expression level by a targeting gRNA was higher than
444 that by a non-targeting gRNA regardless of IPTG induction (Fig. 5C). The expected A→G substitution
445 was also observed in a target barcode-dependent manner even for the no IPTG condition (Fig. 5D).
446 These results collectively suggest that the background expression levels of the genome editing reagents
447 with no inducer were sufficient to confer the base editing. Furthermore, when the EGFP positive control
448 reporter was used, the arabinose-induced reporter intensity was suppressed by the targeting gRNA (Fig.
449 5E and Fig. S12A and B), suggesting a transcriptional silencing effect by ABE recruited at the target
450 site.

451 Because the fold change in EGFP reporter intensity for the targeting gRNA compared to the non-
452 targeting gRNA was not high (0.901–2.52 fold), we then sought to establish a drug-selectable system
453 for bacterial CloneSelect. We first realized that when a Zeocin resistance gene (*Sh ble*) (49) was used
454 for the barcode-specific reporter system (Fig. 5F), a constitutively active J23119 promoter conferred cell
455 growth under the selective condition regardless of the upstream TAA stop codon (Fig. S12C). In contrast,
456 the arabinose-inducible promoter was selective for the stop codon removal even without the arabinose
457 supplement, suggesting that a small gene expression level is sufficient for drug resistance. We also
458 found that targeting gRNA expression from the T7 promoter substantially dropped the number of colony-
459 forming units (Fig. S12D), presumably because nickase Cas9 has known to be toxic to the bacterial
460 cells (50, 51). Finally, we found that using the same setup as EGFP for the Zeocin resistance reporter
461 with no inducer condition demonstrated cell growth in a gRNA-dependent manner (Fig. S12E). A

463 Blasticidin S-resistance gene (*Bsr*) (52) also showed utility for gRNA-dependent cell growth with a similar
 464 experimental setup (Fig. S12F and G).

465 The Zeocin reporter system enabled the isolation of different barcoded strains with high specificity
 466 (Fig. 5G). To demonstrate barcoded cell isolation from a complex population, we constructed a pooled
 467 plasmid library for semi-random barcodes of VNN repeats (V=non-T), preventing the appearance of stop
 468 codons (Fig. S13A), and prepared sub-pool libraries by pooling 100 and ~1,550 colonies, respectively
 469 (Fig. S13B; hereafter referred as to Pool-100 and Pool-1550). After establishing barcoded *E. coli* cell
 470
 471
 472



473
 474
 475 **Fig. 5. Bacterial CloneSelect.** (A) Bacterial CloneSelect A→G circuit. ABE and gRNA expressions were
 476 controlled by IPTG-inducible promoters, and the EGFP reporter expression was controlled by an arabinose-
 477 inducible promoter. (B and C) EGFP reporter activation of *E. coli* cells under different inducer conditions. Scale
 478 bar, 25 μm. Mean EGFP intensity measured by a plate reader was normalized by OD_{595 nm} (n=3). Welch's t-test
 479 was performed to compare on-target (OT) and non-target (NT) activities. (D) Base editing outcomes analyzed by
 480 Sanger sequencing. (E) Activities of the positive control EGFP reporter under the same conditions tested for (C)
 481 (n=3). Welch's t-test was performed to compare OT and NT activities. (F) Zeocin resistance marker-based circuit.
 482 (G) Barcode-specific gRNA-dependent Zeocin resistance reporter activation. (H) Schematic diagram of a bacterial
 483 CloneSelect workflow using a drug selective condition for the target barcoded cell isolation. (I) Abundance of
 484 barcoded cells in Pool-100 and Pool-1550. (J) Colonies formed on Zeocin-selective and non-selective solid agar
 485 plates after performing the reporter activation of Clone 106 in the *E. coli* cell population of Pool-100. (K) Analysis
 486 of colonies isolated from Zeocin selective and non-selective plates obtained after clone labeling using each
 487 targeting gRNA. *P < 0.05; **P < 0.01; ***P < 0.001.

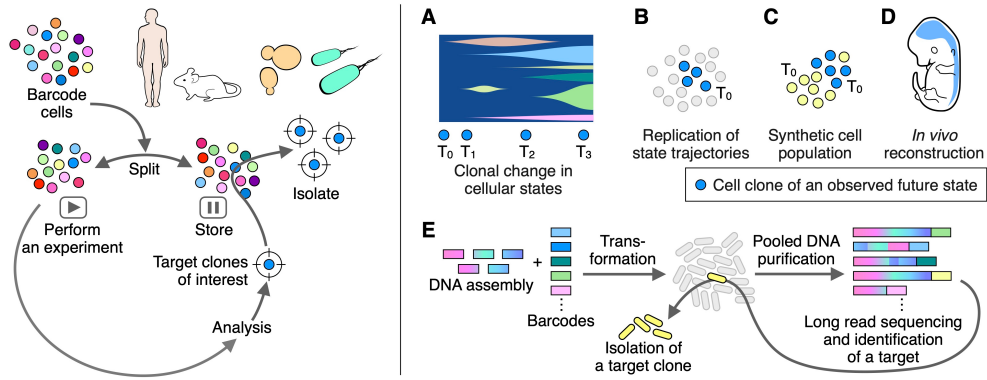
488 populations of Pool-100 and Pool-1550, we arbitrarily selected target barcodes and attempted to select
489 cells having each of those barcodes by co-transforming the targeting gRNA and ABE, followed by Zeocin
490 selection (Fig. 5H). We targeted 10 and four barcodes of a range of abundances in Pool-100 (0.047–
491 2.33%) and Pool-1550 (0.00089–0.211%), respectively (Fig. 5I). In every isolation experiment, the
492 Zeocin selective conditions showed a substantially lower number of colonies than the non-selective
493 conditions (Fig. 5J and K). For each of the successful target barcodes, except for BC 036 of Pool-100
494 in which we obtained only two colonies in the selective condition, four and four colonies were isolated
495 from the selective and non-selective conditions, respectively, and their barcodes and base editing
496 patterns were analyzed by Sanger sequencing. All isolates from the selective conditions had the
497 expected barcodes and all of the isolates from the non-selective conditions had non-targeted barcodes.
498 Accordingly, bacterial CloneSelect with the drug resistance marker system demonstrated great
499 sensitivity and was able to isolate clones that were extremely low in frequency.
500

501 Discussion

502 We describe a method, CloneSelect, which enables the isolation of target barcoded cells from a complex
503 population using CRISPR base editing. Compared to the CRISPRa and wild-type Cas9-based systems
504 tested in this study, CloneSelect demonstrated an ability to isolate cells with a higher sensitivity when a
505 certain degree of false positive isolation was permitted. The low-copy CRISPRa experiments confirmed
506 the reporter expression leak in similar existing methods (29). High background activity observed in the
507 high-copy CRISPRa experiments supports the utility of a strategy implemented in the approaches
508 COLBERT (30) and ClonMapper (31), whereby cells are labeled with gRNAs as barcodes, and target
509 barcoded clones are activated by provision of a plasmid that encodes only the target gRNA-
510 corresponding reporter with no constitutively active promoters. However, this approach of barcoding
511 cells using gRNAs does not allow selected cells to maintain reporter activation for subsequent
512 experiments, when necessary. CloneSelect largely benefits from the precision of base editing and the
513 simplicity of altering the genetic code, while a CRISPRa-based system involves more additional
514 endogenous factors to be coordinated for the target barcode-dependent reporter activation. Furthermore,
515 engineering evolutionarily prevalent rules of the genetic code enabled us to implement the same idea
516 across diverse species. We demonstrated the retrospective isolation of barcoded cells from complex
517 yeast populations for the first time. While the isolation of barcoded *E. coli* cells has recently been
518 demonstrated using barcode-specific CRISPR interference of a counter selection marker (53), we have
519 shown that bacterial CloneSelect achieves the isolation of target barcoded cells at unprecedented
520 sensitivity and selectivity.

521 When practically examining its ability to isolate target barcoded cells from complex populations,
522 CloneSelect was able to retrieve rare, barcoded cells whose estimated abundances were as small as
523 0.558%, 0.013%, 0.120%, and 0.00089% in the human HEK293T, mouse ESC, yeast, and *E. coli*
524 populations, respectively. The theoretical complexity of semi-random barcodes is limited to 4.19×10^6
525 and 2.54×10^8 for CloneSelect C→T and CloneSelect A→G, respectively. The sensitivities to obtain
526 target barcoded cells that align with the same possible minimal abundance thresholds above are
527 93.75%, 90.00%, 61.56%, and 100.00%, respectively. The limited sensitivity per isolation attempt could
528 be explained by the general gRNA-dependent genome editing efficacy (43) since isolation success did
529 not correlate well with the abundance of the target in a population. We suggest that the current sensitivity
530 range of CloneSelect is sufficient in most prospective assays, with the expectation that multiple
531 independent clones show a phenotype of interest that allows the user to have multiple attempts. More
532 enhanced genetic circuits can be considered to improve sensitivity and specificity. We tested an OR-
533 gate with C→T base editing of tandemly arrayed barcodes (Fig. S14A) and an AND-gate with A→G
534 base editing of tandemly arrayed barcodes (Fig. S14B). The OR-gate did not function well and enabled
535 an efficient reporter activation for only one of the three barcodes. The AND-gate enabled the three-
536 input-dependent reporter activation, but exhibited a tight trade-off with the sensitivity, as expected. Given
537 the high specificity of the system, introducing multiple independent CloneSelect barcodes per cell might
538 be a solution to increase the sensitivity if necessary.
539

540 With CloneSelect, new wide-ranging experiments can be conceived in broad fields of biology. A
541 CloneSelect-barcoded cell population can be subjected to any assay. Existing time-course scRNA-seq
542 measurement strategies enable interrogation of different clonal lineages in a barcoded population
543 alongside the dynamic changes in their gene expression landscapes, if the clone population sizes are
544 not too small (9). In contrast, CloneSelect would allow the clones isolated from different time points from
545 the progressing population to be analyzed by diverse approaches (Fig. 6A). Such non-transcriptomic
546 analyses could include morphological analyses under a microscope and molecular analyses available
547 for small amounts of input cells, but any currently available methods should be applicable for the
548 downstream analysis if the isolated clones can be propagated for the given hypothesis.
549
550
551



552
553
554 **Fig. 6. New biology directions made possible by CloneSelect.** (A) Clonal analysis of molecular profiles in a
555 complex population. (B) Replication of cell state trajectories. (C) Reconstitution of synthetic cell populations. (D)
556 Transplantation of a fate-mapped clone. (E) New DNA assembly strategy.

557 Cells isolated by CloneSelect are alive. The clones isolated from the initial stage of a once-
558 performed assay can be tested to see if they take the same developmental trajectories (Fig. 6B) or used
559 to reconstitute a synthetic population with another cell population or other isolated clones (Fig. 6C). For
560 example, a variety of hPSC lines have been reported to be favorable for different cell differentiation and
561 organoid models (54-58), suggesting that there could also be fate priming of stem cell clones due to
562 undiscovered intrinsic factors. CloneSelect enables mapping of cell states after differentiation and their
563 subsequent isolation from the initial population. The fate-mapped stem cell clones could be used to
564 engineer new stem cell-based models or high-quality stem cell therapeutics. Cell clones isolated from
565 diverse systems can also be transplanted into animal models (Fig. 6D). Examples include
566 xenotransplantation of a cancer stem cell clone and aggregation of a fate-mapped stem cell clone with
567 an early embryo. As opposed to the CRISPRa-based system, the barcode-dependent reporter activation
568 is irreversible. When a fluorescent reporter gene is used, the spatial distribution of the targeted clone
569 and their interaction with others in a complex biological system can be traced.

570 In alignment with having DNA sequencing as a readout, CloneSelect would also promote the
571 genetic engineering of cells and DNA assembly (59-63). Any cell engineering cannot be perfect—only
572 a fraction of cells that go through an engineering process will harbor the target genetic product.
573 Therefore, obtaining successful cells becomes difficult when their fractions in the reaction pool are very
574 small. In such a task, through the barcoding and sequencing of the product cells, CloneSelect could
575 retrieve target cells with the desired genetic engineering outcome. We also envision CloneSelect to
576 largely improve DNA assembly in general (Fig. 6E). Currently, it is common practice to transform a DNA
577 assembly reaction sample into *E. coli* cells in order to clone each assembly product, followed by colony
578 isolation and sequencing-based confirmation. A pool of CloneSelect barcodes can be used to
579 molecularly tag DNA assembly products. In this framework, the assembly products are used to transform
580 *E. coli*, followed by the pooling of transformants and extraction of the pooled plasmid products from its
581 582

583 subpopulation. The pooled plasmid product is then sequenced by long-read DNA sequencing to identify
584 barcodes assigned to the desired product. Finally, the clone harboring the target product can be isolated
585 using CloneSelect in a target barcode-specific manner. This strategy would enable the utilization of even
586 inefficient DNA assembly protocols.

587 Accordingly, CloneSelect is a new way to precisely isolate target cell clones from complex
588 populations. Its performance demonstrated in multi-kingdom species opens a vast array of possibilities
589 to answer complex questions in diverse areas of biology.

590

591 **Acknowledgments**

592 We thank the members of the Yachie lab at the University of British Columbia and the University of
593 Tokyo, especially Sanchit Chopra, Sean Okawa, Sofia Romero, Yin Liu, Yeganeh Dorri, Madina Kagineva,
594 and Rina Yogo, for their constructive feedback. We also thank Kaori Shiina, Shiro Fukuda, and Tara
595 Stach for their technical support in high-throughput sequencing and Andy Johnson for the flow cytometry
596 cell sorting. This study was funded by the New Energy and Industrial Technology Development
597 Organization (NEDO), the Japan Agency for Medical Research and Development (AMED), the Japan
598 Science and Technology Agency (JST), the Takeda Science Foundation, the SECOM Science and
599 Research Foundation, the Canada Foundation for Innovation (CFI), the Canadian Institutes of Health
600 Research (CIHR) CoVaRR-Net Project (all to N.Y.), and the Allen Institute Allen Distinguished
601 Investigator Award (to N.Y. and N.S.). Authors were also supported by the JST PRESTO program (N.Y.),
602 the Canada Research Chair program (N.Y.), the Ryoichi Sasakawa Young Leaders Fellowship (S.I.),
603 the Taikichiro Mori Memorial Research Fund (S.I., H.M., and N.M.), the Japan Society for the Promotion
604 of Science (JSPS) DC Fellowship (S.I., H.M., Y.K., and N.M.), the JSPS Overseas Research Fellowships
605 (S.I.), Japan Student Services Organisation (R.S.), the Funai Overseas Scholarship (R.S.), the
606 Takenaka Scholarship Foundation (R.T.), the Ministry of Science and Education (MEXT) Research
607 Scholarship (A.A.), the Natural Sciences and Engineering Research Council of Canada (NSERC)
608 Undergraduate Student Research Award (S.King), Michael Smith Health Research BC Scholar Award
609 (R.I.K.G.), and the Michael Smith Health Research BC Trainee Award (A.-S.A.). High-throughput
610 sequencing data analysis was performed using the SHIROKANE Supercomputer at the University of
611 Tokyo Human Genome Center.

612

613 **Author contributions**

614 S.I. and N.Y. conceived the study. S.I., R.S., and M.T. performed all the major mammalian cell
615 experiments. K.I. and M.T. performed all the yeast and bacterial experiments. O.B., N.S., M.I., and Y.T.
616 performed a part of the experiments using mESCs and hPSCs. S.I., H.M., H.T., R.S., Y.K., and H.A.
617 performed the high-throughput sequencing analyses. R.T., A.A., and N.M. performed preliminary assays
618 and contributed to the design of the system. J.H.O., A.-S.A., and R.I.K.G. contributed to the optimization
619 of the system. S.King supported the plasmid construction. K.N., A.K., and S.Kuhara also provided
620 substantial ideas in designing the proposed system. M.S. supported the flow cytometry cell sorting. H.A.
621 supported the high-throughput sequencing, the flow cytometry analysis, and the microscope imaging.
622 S.I., R.S., K.I., and N.Y. wrote the manuscript.

623

624 **Competing interests**

625 K.I. is an employee of Spiber Inc. The other authors declare no competing interests.

626

627 **Materials and Methods**

628 **Plasmids**

630 Oligonucleotides were chemically synthesized by FASMAC, Integrated DNA Technologies, or Eurofins
631 Genomics. All the oligonucleotides and cloning procedures used to construct the plasmids in this study
632 can be found in Table S2. We used QUEEN version 1.2.0 (<https://github.com/yachielab/QUEEN>) to
633 describe each plasmid construction and generate the annotated plasmid files in the GenBank (gbk) file
634 format, embedding the full construction procedure (Table S2). A QUEEN-generated gbk file behaves as
635 a quine code, where the QUEEN simulation code that generated the gbk file can perfectly be
636 reconstructed from the file itself (64). We believe that providing the QUEEN-generated gbk files satisfies
637 the mandate of reporting the reproducible protocols for the newly constructed plasmids. We also
638 provided natural language descriptions for each plasmid construction step in the QUEEN code, allowing
639 the user to retrieve the natural language description of materials and methods for each plasmid by
640 simply executing "QUEEN --protocol_description --input [gbk file]" in a QUEEN-installed environment. A
641 custom QUEEN wrapper that generated all QUEEN-generated gbk files can be found at
642 https://github.com/yachielab/CloneSelect_v1/tree/main/QUEEN. We, therefore, do not provide the
643 plasmid construction protocols here. All plasmid DNA sequences were confirmed by Sanger sequencing.
644 The representative plasmids are in the process of being deposited to Addgene with their QUEEN-
645 generated gbk files, which Addgene agreed to accommodate.

646

647

648 **Mammalian CloneSelect**

649 **Cell culture**

650 HEK293T and HeLa cells. Human embryonic kidney 293Ta (HEK293Ta) and HEK293T Lenti-X cells
651 were purchased from GeneCopoeia (#LT008) and Takara (#632180), respectively. Cells were cultured
652 in Dulbecco's Modified Eagle Medium (DMEM) (Sigma-Aldrich #11965084) supplemented with 10%
653 Fetal bovine serum (FBS) (Gibco #16000044) and 1% Penicillin-Streptomycin (Wako #168-23191) at
654 37°C with 5% CO₂ in a cell culture incubator. Cells were detached and passaged using 0.25 w/v%
655 Trypsin-EDTA (Wako #203-20251) once the cells reached 70–90% confluence. The cell lines were
656 regularly tested for mycoplasma contamination. When microscope imaging of HEK293T cells was
657 performed with Hoechst 33342 (Invitrogen #H3570) counterstain, 100–200 µL of Collagen-I (Nippi
658 #PSC-1-100-100) diluted in 5 mM acetic acid was added to each cell culture plate well, incubating for
659 30 min at 37°C. The collagen-coated plate wells were washed by 100–200 µL of 1x PBS before use.

660

661 mESCs. Under the approval by the Institutional Animal Care Committee of the University of Tokyo
662 (RAC180003), mESCs were established from embryos of a 129(+Ter)/SvJcl (female) x C57BL/6NJcl
663 (male) cross and maintained in Dulbecco's Modified Eagle Medium - low glucose (Sigma-Aldrich
664 #D6046-500ML) supplemented with 1% Penicillin-Streptomycin (Gibco #15140122), 1% MEM Non-
665 essential Amino Acids (Wako #139-15651), 1% GlutaMAX Supplement (Gibco #35050061), 1% Sodium
666 Pyruvate (Gibco #11360070), 15% FBS (Gibco #16000044), 100 µM/mL 2-Mercaptoethanol (Wako
667 #131-14572), 10³ units/mL ESGRO Recombinant Mouse LIF Protein (Millipore #ESG1107), 3.0 µM
668 CHIR99021 (GSK-3 inhibitor) (Wako #038-23101), and 1.0 µM PD0325901 (MEK inhibitor) (Toris
669 #4423). A sufficient volume of 0.1% Gelatin (Sigma-Aldrich #G9391) in 1x Phosphate-buffered saline
670 (PBS) (Takara #T9181 or Gibco #70011044) was added to each well such that the liquid could cover
671 the entire surface and be aspirated after one hour at 37°C before plating cells. Cells were cultured in a
672 cell culture incubator at 37°C with 5% CO₂. The cell culture medium was replaced at least once every
673 two days. The cell line was regularly tested for mycoplasma contamination.

674

675 hPSCs. CA1 human PSC (hPSC) line was used after approval by the Canadian Institutes of Health
676 Research Stem Cell Oversight Committee. CA1 hPSCs were cultured using mTeSR Plus (STEMCELL
677 Technologies #100-0276) cell culture medium in a humidified incubator at 37°C with 21% O₂ and 5%
678 CO₂. Culture plates were coated with Geltrex LDEV-Free Reduced Growth Factor Basement Membrane

679 Matrix (Gibco #A1413201). Dulbecco's Modified Eagle Medium/Nutrient Mixture F-12 (DMEM/F12)
680 (Gibco #11320033) was used to make a working solution of Geltrex (Gibco #A1413201) with 1:100
681 dilution. A sufficient volume of Geltrex was added to each well such that the liquid could cover the entire
682 surface and be aspirated after one hour incubation at 37°C before plating cells. The cell culture medium
683 was exchanged every other day after plating the cells. Regularly, cells were passaged as medium-sized
684 clumps. Upon aspiration of the media, ReLeSR (STEMCELL Technologies #05872) was added, and
685 cells were incubated at room temperature for about 1 min before the second aspiration. Cells were then
686 placed inside the incubator for 4-5 min, added fresh media, and dissociated by pipetting up and down.
687 Cells were then plated and placed inside the incubator. For single-cell passaging, we used TrypLE
688 Express (Gibco #12604021). Cells were then placed inside the incubator for four min before adding a
689 sufficient fresh media to stop the activity of TrypLE Express. Cells were then collected in centrifuge
690 tubes, dissociated by pipetting up and down, and passed through a 40 µm cell strainer (Sarstedt
691 #83.3945.040) to remove cell clumps. The tubes were then centrifuged at 300–400 g for 5 min and the
692 supernatant was aspirated. The pellets were resuspended in a fresh media supplemented with 10 µM
693 ROCK inhibitor Y-27632 (Tocris Bioscience #1254) for 24 hours to promote the survival of the single
694 cells. For culturing H1 hPSCs, we used StemFit AK02N cell culture medium (REPROCELLAHS
695 #RCAK02N) with Y-27632 (Cayman #10005583) added for one or two days after plating. Culture plates
696 were coated with the recombinant Laminin-511 E8 fragment using iMatrix-511 Silk (MAX #892021). The
697 cell lines were tested for mycoplasma contamination.
698

699 **Mammalian CloneSelect barcode libraries**

700 CloneSelect C→T barcode library. To generate the CloneSelect C→T barcode library, a semi-random
701 oligo pool SI#679 encoding 5'-CCGWSNSWSNSWSNSNGTG-3' was first chemically
702 synthesized (Table S2), where the antisense strand sequence of the 5'-CGG-3' PAM sequence and a
703 quadruple repeat of WSNS (W=A or T; S=G or C) were followed by a mutated start codon (GTG). The
704 WSNS repeat restricts additional start codons from appearing before the downstream reporter. An
705 EGFP coding sequence was then amplified from pLV-eGFP (Addgene #36083) in 25 separate PCR
706 reactions, each in 50 µL volume, composed of 1 ng/µL of pLV-eGFP template plasmid, 1.25 µL of 20
707 µM SI#679 oligo pool as a forward primer, 1.25 µL of 20 µM SI#680 as a common reverse primer, 0.5
708 µL of Phusion High-fidelity DNA Polymerase (NEB #M0530), 10 µL of 5x Phusion HF Buffer (NEB
709 #B0518S), and 5 µL of 2.5 mM dNTPs (Takara #4025), with the following thermal cycle condition: 98°C
710 for 30 s, 30 cycles of 98°C for 10 s, 72°C for 10 s, and 72°C for 60 s, and then 72°C for 5 min for the
711 final extension. The amplified fragment was digested by DpnI (NEB #R0176) for an hour at 37°C, pooled
712 into a single tube (1,250 µL in total), and column purified using FastGene PCR/Gel Extraction Kit (Nippon
713 Genetics #FG-91302). The purified fragment was then subjected to EcoRI-HF (NEB #R3101S) and XbaI
714 (NEB #R0145S) digestion overnight at 37°C and purified again by FastGene PCR/Gel Extraction Kit
715 (Nippon Genetics #FG-91302). To obtain a highly complex lentiviral plasmid pool, we performed a total
716 of five ligation reactions using PCR strip tubes, each for a 50-µL reaction containing ~30 fmol of EcoRI-
717 XbaI digested pLV SIN-CMV-Pur backbone plasmid (Takara #6183), ~300 fmol of the insert fragment,
718 2.5 µL of T4 DNA Ligase (NEB #M0202), and 5 µL of 10x T4 DNA Ligase Buffer (NEB #B0202). The
719 reaction samples were incubated at room temperature for two hours and purified by FastGene PCR/Gel
720 Extraction Kit (Nippon Genetics #FG-91302). The ligation sample was then used to transform NEB
721 Stable Competent *E. coli* cells (NEB #C3040I). The transformation was performed in five reactions, each
722 with 1,250 ng of the ligation sample transformed to 200 µL of the competent cells according to the
723 manufacturer's high-efficiency transformation protocol. Following one-hour outgrowth in SOC medium
724 (NEB #B9020) at 37°C, cells were spun down and plated on a total of 25 LB agar plates containing 100
725 µg/mL Ampicillin (Wako #014-23302). After overnight incubation at 37°C, colonies formed on the plates
726 were scraped by adding 1–2 mL ddH2O, pooled into a flask, and further incubated with 200–300 mL of
727 LB liquid medium containing 100 µg/mL Ampicillin (Wako #014-23302) overnight at 37°C. We plated the
728 transformation sample on agar plates with 500-fold dilution in triplicate and estimated the barcode
729 complexity of the constructed library to be ~6.8 × 10⁵. The plasmid library was finally purified by
730 NucleoBond Midi-prep Kit (Macherey-Nagel #740410) and stored at –20°C before use. We performed
731 the isolation of 16 random clones and triple restriction enzyme digestion using BsrGI-HF (NEB

732 #R3575S), Clal (NEB #R0197S), and Pvul-HF (NEB #R3150S), and confirmed that all the tested clones
733 (16/16) contained the expected barcode inserts. To generate a low-complexity library for the proof-of-
734 concept assays using HEK293T cells, we examined barcode sequences of 96 isolated clones by Sanger
735 sequencing using a sequencing primer SI#471. After removing three clones observed to have mixed
736 Sanger sequencing spectra in the barcode region, barcoded plasmids were pooled with an equimolar
737 ratio and subjected to high-throughput sequencing and lentiviral packaging.
738

739 scCloneSelect barcode library. The scCloneSelect barcode library was prepared similarly to the
740 CloneSelect C→T barcode library. An EGFP coding sequence was first amplified by PCR from pLV-CS-
741 112 (Addgene #131127) using the semi-random oligo pool SI#679 as a forward primer and another oligo
742 pool RS#244 as a reverse primer. The PCR was performed in 25 separate reactions, each in 40 μL
743 reaction volume, composed of 0.12 μL of 10 ng/μL pLV-CS-112 template plasmid, 2 μL each of forward
744 and reverse primers, 0.6 μL of Phusion High-fidelity DNA Polymerase (NEB M0530), 8 μL of 5x Phusion
745 HF Buffer (NEB #B0518S), and 3.2 μL of 2.5 mM dNTPs (NEB #N0447) with the following thermal cycle
746 condition: 98°C for 30 s, 30 cycles of 98°C for 10 s, 65°C for 10 s, and 72°C for 60 s, and then 72°C for
747 5 min for the final extension. The amplified barcode-EGFP fragment was pooled into a single tube (1,000
748 μL in total) and digested with 12.5 μL of DpnI (NEB #R0176) at 37°C for 1 hour. The digested product
749 was then size-selected using FastGene PCR/Gel Extraction Kit (Nippon Genetics #FG-91302). The
750 purified product was subjected to EcoRI-HF (NEB #R3101S) and XbaI (NEB #R0145) digestion
751 overnight at 37°C and purified again by FastGene PCR/Gel Extraction Kit (Nippon Genetics #FG-91302).
752 For backbone preparation, 25 μg of pRS193 lentiviral cloning backbone plasmid was digested by EcoRI-
753 HF (NEB #R3101S) and XbaI (NEB #R0145) at 37°C overnight and size-selected using FastGene
754 PCR/Gel Extraction Kit (Nippon Genetics #FG-91302). 1.25 μg of the digested backbone, 320 ng of the
755 purified insert, 25 μL of T4 DNA Ligase (Nippon Gene #317-00406), and 25 μL of 10x T4 DNA Ligase
756 Buffer (NEB #B0202) were mixed in a total volume of 250 μL and incubated overnight at 16°C. The
757 ligation sample was then used to transform NEB Stable Competent *E. coli* cells (NEB # C3040I). The
758 transformation was performed in a total of 17 reactions, each with 4 μL of the ligation sample
759 transformed to 50 μL of the competent cells according to the manufacturer's high-efficiency
760 transformation protocol. Following one-hour outgrowth in SOC medium (NEB #B9020) at 37°C, cells
761 were spun down and plated on a total of 15 LB agar plates containing 100 μg/mL Ampicillin (Wako #014-
762 23302). After overnight incubation at 37°C, colonies formed on the solid agar plates were scraped by
763 adding 1–2 mL ddH2O, pooled into a flask, and further incubated with 200–300 mL of LB liquid medium
764 containing 100 μg/mL Ampicillin (Wako #014-23302) overnight at 37°C. We plated the transformation
765 sample on agar plates with 300-fold dilution in duplicate and estimated the barcode complexity of the
766 constructed library to be ~1.5 × 10⁵. The plasmid library was finally purified by NucleoBond Midi-prep
767 Kit (Macherey-Nagel #740410) and stored at –20°C before use. We performed the isolation of 20
768 random clones and confirmed the expected fragment insertion for 17/20 by genotyping PCR using the
769 primer pair RS#147 and SI#514. From the same 20 clones, we selected six (including the three that did
770 not yield the expected genotyping PCR bands), performed double digestion using EcoRI-HF (NEB
771 #R3101S) and BamHI-HF (NEB #R3136S), and Sanger sequencing using sequencing primers SI#514
772 and RS#147 for uptag and dntag, respectively, and confirmed that all the tested clones contained the
773 expected uptag and dntag inserts.
774

775 **Lentiviral barcoding**

776 Virus packaging. HEK293T cells were plated on either a 10-cm cell culture dish at a density of ~2 × 10⁶
777 cells with 10 mL of the culture medium or 6-well cell culture plate wells at a density of ~2 × 10⁵ cells/well
778 with 2 mL of the culture medium one day before plasmid transfection. For packaging using a 10-cm cell
779 culture dish, 3.0 μg transgene vector, 2.25 μg psPAX2 (Addgene #12260), 0.75 μg pMD2.G (Addgene
780 #12259), and 18 μL of 1 mg/mL PEI MAX (Polysciences #24765-100) were dissolved in 1,000 μL of 1x
781 PBS and applied to the cell culture. For packaging using a 6-well cell culture plate well, 489 ng transgene
782 plasmid, 366.7 ng psPAX2, 122.3 ng pMD2.G, and 2.93 μL of 1 mg/mL PEI MAX (Polysciences #24765-
783 100) were dissolved in 300 μL of 1x PBS and applied to the cell culture. The culture medium was
784 changed to a fresh medium one day after transfection. The transfected cells were further incubated for

785 48–72 hours. The cell culture supernatant was then harvested and filtered with 0.22 µm pore size sterile
786 syringe filters. The recombinant lentivirus sample was then aliquoted 500–1,000 µL each into 1.5-mL
787 test tubes and stored at –80°C.
788

789 **Virus concentration.** To increase virus infection titer, we concentrated harvested virus samples using a
790 polyethylene glycol (PEG)-based method (65) using PEG 6000 (Wako #169-09125) or Lenti-X
791 Concentrator (Takara #631231). When PEG 6000 was used, ~10 mL of recombinant virus sample was
792 mixed with 2.55 mL of 50 w/v% PEG 6000, 1.085 mL of 4M NaCl, and 1.365 mL of 1x PBS in a 50 mL
793 tube. The sample was continuously mixed using a rotator at 4°C for 90 min and centrifuged at 4,000 g
794 and 4°C for 20 min. The supernatant was discarded, and the precipitated virus pellet was resuspended
795 with 1.1 mL of Opti-MEM (Gibco #31985062) by pipetting and vortexing until fully dissolved, resulting in
796 a 10-fold concentration of the virus sample. The virus concentration using Lenti-X Concentrator was
797 performed with the manufacturer's protocol and dissolved in Opti-MEM (Gibco #31985062) to yield a
798 10- or 15-fold concentration. The concentrated virus samples were stored at –80°C.
799

800 **Transduction of HEK293T and HeLa cells.** Cells were seeded on 6-well cell culture plate wells at a density of ~2 x 10⁵ cells/well with 2 mL of the culture medium one day before transduction. A total of 801 1,000 µL transduction mix containing 1 µL of 2 µg/mL Polybrene (Sigma-Aldrich #TR-1003),
802 recombinant lentivirus, and the cell culture medium was applied to each well alongside non-virus
803 controls. One day after transduction, cells were trypsinized and plated on 96-well cell culture plate wells
804 at a density of ~5 x 10³ cells/well for a virus titer measurement. The next day, the culture medium was
805 exchanged with a fresh medium containing 2.0 µg/mL Puromycin (Gibco #A1113803) or 5.0 µg/mL
806 Blasticidin S (Wako #029-18701) to select the infected cells for two to five days. After drug selection,
807 cell viability was measured using CellTiter-Glo (Promega #G7570) according to the manufacturer's
808 protocol. The luminescence was quantified using Infinite 200 PRO plate reader (TECAN). The
809 background luminescence from wells without cell samples was used to subtract the signals. For each
810 condition, the multiplicity of infection (MOI) was determined by the fraction of the survived cells
811 compared to the non-selective condition control. The samples with an MOI close to but not over 0.1 was
812 used for the following analyses, where most of the selected cells were expected to have a single viral
813 integration according to Poisson statistics.
814

815 **Transduction of mESCs.** Cells were seeded on 6-well cell culture plate wells at a density of ~2 x 10⁵
816 cells/well with 2 mL of the culture medium one day before transduction. For cell transduction,
817 recombinant virus samples with volume of 10–100 µL were thawed on ice, mixed with 1.5 µL of 8 µg/mL
818 Polybrene (Sigma-Aldrich #TR-1003) and 1.5 mL of fresh cell culture medium, and applied to the cells.
819 To select the transduced cells, the culture media was exchanged with a fresh media containing 1.0
820 µg/mL Puromycin (Gibco #A1113803) two days after infection, followed by incubation for three days.
821 Survived cells were detached, and cell counts were measured using Automated Cell Counter TC20
822 (BioRad). The MOI was determined by the fraction of the survived cells compared to the non-selective
823 condition control. The samples with an MOI close to but not over 0.1 was used for the following analyses.
824

825 **Transduction of hPSCs.** Cells were seeded on 6-well cell culture plate wells at a density of ~1 x 10⁵
826 cells/well with 2 mL of the culture medium one day before transduction. For cell transduction,
827 recombinant virus samples with volume of 10–100 µL were thawed on ice, mixed with 1.5 µL of 8 µg/mL
828 Polybrene (Sigma-Aldrich #TR-1003) and 1.5 mL of fresh cell culture medium, and applied to the cells.
829 After 48 hours of infection, the culture media was exchanged with a fresh media containing 1.0 µg/mL
830 of Puromycin (Gibco #A1113803) for three days. The reporter-integrated cells were dissociated into
831 single cells and subjected to flow cytometry cell sorting to enrich EGFP-negative cells. The sorted cells
832 were maintained with StemFit AK02N culture media (REPROCELL #RCAK02N).
833

834 **Preparing cells with stably integrated Target-AID**

835 **mESCs.** The mESC line with stably integrated Target-AID was established by electroporation using
836 NEPA21 Super Electroporator (NEPAGENE). After detaching cells from cell culture plate wells, ~2 x 10⁶
837

838 cells were mixed with 100 μ L of Opti-MEM (Gibco #31985062), 2.0 μ g of pNM1325, and 0.7 μ g of a
839 Super piggyBac transposase vector (SBI #PB210PA-1), and transferred to an electroporation cuvette
840 (NEPAGENE #EC-002S). The electroporation was done by two poring pulses of positive electric polarity
841 with 115 V for 5 ms with 50-ms intervals and 10% decay rate, and five transfer pulses each for positive
842 and negative electric polarities with 20 V for 50 ms with 50-ms intervals and 40% the decay rate. After
843 electroporation, cells were transferred to a 10-cm cell culture dish with a fresh culture medium. The
844 medium was exchanged with a fresh medium one day after electroporation. Two days post
845 electroporation, the medium was exchanged again with medium containing 5 μ g/mL of Blasticidin S
846 (Wako #029-18701) to select cells with stable integration. The cells were incubated for about two weeks
847 in the selection medium.

848
849 hPSCs. To establish an hPSC line with stably integrated Target-AID, CA1 cells were seeded on 24-well
850 cell culture plate wells at a density of \sim 5 \times 10⁴ cells/well with 1 mL of the culture medium one day before
851 transfection. The next day, the medium was exchanged to remove Y-27632. The transfection mix was
852 prepared by combining 450 ng of pNM1325 (CAGp-Target-AID-2A-Blast), 50 ng of a hyperactive
853 PiggyBac transposase plasmid, 1 μ L of Lipofectamine Stem Transfection Reagent (Invitrogen
854 #STEM00001), and 49 μ L of Opti-MEM (Gibco #31985062) and applied to the wells after 10 min
855 incubation. The next day, the culture medium was exchanged with a fresh medium to remove the
856 transfection reagent. Three days after transfection, the medium was exchanged with a fresh medium
857 containing 5 μ g/mL of Blasticidin S to start selection for 24 hours. Another selection was performed two
858 days until confluent and cells were passaged into a new cell culture plate. One extra selection was
859 conducted to ensure a positive selection of the cells.
860

861 **Transient plasmid delivery**

862 Transfection of HEK293T and HeLa cells. Cells were seeded on 24-well cell culture plate wells at a
863 density of \sim 5 \times 10⁴ cells/well with 500 μ L of the culture medium or 6-well cell culture plate wells at a
864 density of \sim 2 \times 10⁵ cells/well with 2,000 μ L of the culture medium one day before transfection. For regular
865 transfection in a 24-well plate, a total of 400 ng of plasmids (3:1 volume of Cas9-based enzyme plasmid
866 to gRNA plasmid when they were mixed), 1.2 μ L of 1 mg/mL PEI MAX (Polyscience #24765), and 100
867 μ L of 1x PBS were mixed, incubated for 5 or 10 min at room temperature, and applied to each well. The
868 dose-dependent activation assay with the different Target-AID expression plasmid was performed using
869 a 24-well plate with the plasmid amount per well ranging from 50–800 ng and 1 mg/mL of PEI MAX
870 whose volume was adjusted to be 3 μ L per 1 μ g of the plasmid. For isolating barcoded HEK293T cells
871 using CloneSelect C→T, we used 6-well cell culture plates, and a total of 800 ng of plasmids encoding
872 both Target-AID and gRNA were combined with 2.5 μ L of 1 mg/mL PEI MAX (Polyscience #24765) and
873 200 μ L of 1x PBS and applied to each well after 5–10 min incubation at room temperature.
874

875 Transfection of mESCs. Cells were seeded on 48-well cell culture plate wells at a density of \sim 6 \times 10⁴
876 cells with 200 μ L of the culture medium. For each reaction, a total of 200 ng of plasmids were diluted in
877 20 μ L of Opti-MEM (Gibco #31985062), and 0.6 μ L of Lipofectamine 2000 (Invitrogen #11668019) was
878 combined with 19.4 μ L of Opti-MEM (Gibco #31985062) as a transfection mix. The plasmid and
879 transfection mix were then combined and applied to each well after 5 min incubation at room
880 temperature.
881

882 Electroporation of hPSCs. For the gRNA-dependent reporter activation of the barcoded CA1 hPSCs
883 with the stably integrated Target-AID, we used Neon Transfection System (Invitrogen MPK5000) to
884 deliver the gRNA plasmid by electroporation. Cells were detached from cell culture plate wells, and \sim 1
885 \times 10⁵ cells were mixed with 100 μ L of Neon Resuspension Buffer and 2.0 μ g of gRNA plasmid. The
886 electroporation was done by 1,200 V for 30 ms with one pulse. In the co-delivery of Target-AID and
887 gRNA expression plasmids to the barcoded H1 hPSCs, \sim 1 \times 10⁵ cells were mixed with 100 μ L of Neon
888 Resuspension Buffer, 3.0 μ g of Target-AID plasmid, and 3.0 μ g of gRNA plasmid, and the
889 electroporation was done by 1,200 V for 20 ms with two pulses.
890

891 **Preparing microscope imaging samples**

892 For imaging HEK293T cells, 25 µL of 0.1 mg/mL Hoechst 33342 (Invitrogen #H3570) dissolved in DMEM
893 was directly added to each well of 24-well cell culture plates three days after transfection for nuclear
894 counterstaining. The specimens were incubated at room temperature for 10 min, followed by removal
895 of the culture medium. Cells were gently washed with fresh 500-µL of DMEM once and filled with 500
896 µL of fresh DMEM before imaging. For imaging HeLa cells, cells were first washed with 500 µL of 1x
897 PBS, added 25 µL of 0.1 mg/mL Hoechst 33342 dissolved in 475 µL of DMEM and incubated at room
898 temperature for 10 min. Cells were gently washed with 500 µL of 1x PBS and filled with 500 µL of fresh
899 DMEM. For mESCs, 5.0 µg/mL Hoechst 33342 (Invitrogen #H3570) dissolved in the cell culture medium
900 was directly added to each well and incubated at room temperature for 10 min to proceed with imaging.
901 All live cell imaging was performed using BZ-X710 (Keyence), InCellAnalyzer 6000 (GE Healthcare), or
902 IX83 (Olympus) with a 4x, 10x, or 20x objective lens. The contrast and brightness of the images obtained
903 in a single batch of the experiment were uniformly adjusted using ImageMagick (Version 7.1.0-20) or
904 Fiji (Version 1.0).

905

906 **Flow cytometry analysis**

907 Cells were detached by 0.25 w/v% Trypsin-EDTA (Wako #201-18841), incubated at 37°C for 5 min,
908 collected into a 1.5-mL tube or a 96-well round-bottom plate, and centrifuged at 1,000 rpm and room
909 temperature for 5 min. After aspirating the supernatant, cell pellets were gently resuspended with 150–
910 500 µL of ice-cold FACS buffer consisting of 2% FBS in 1x PBS. The samples were immediately placed
911 on ice until flow cytometry analysis. The flow cytometry analysis was performed with BD FACSVerso
912 Cell Analyzer (BD Biosciences) or CytoFLEX Flow Cytometer (Beckman Coulter). The samples were
913 mixed gently by pipetting or vortexing immediately before the analysis. Approximately 10,000–20,000
914 raw events were acquired for each sample. The data analysis was performed with custom R scripts
915 using flowWorkspace (version 0.5.40) (<https://github.com/RGLab/flowWorkspace>), flowCore (version
916 1.11.20) (<https://github.com/RGLab/flowCore>) and CytoExploreR (version 1.1.00)
917 (<https://github.com/DillonHammill/CytoExploreR>) or a Python package FlowCytometryTools (version
918 0.5.0) (<https://github.com/eyurtsev/FlowCytometryTools>). Codes are available at
919 https://github.com/yachielab/CloneSelect_v1/tree/main/FACS.

920

921 **Flow cytometry cell sorting**

922 HEK293T cells. Four days after the transfection of Target-AID and gRNA plasmids for barcode-specific
923 cell isolation, cells were detached by 0.25 w/v% Trypsin-EDTA (Wako #201-18841), incubated at 37°C
924 for 5 min, collected into a 1.5-mL tube, and centrifuged at 1,000 rpm and room temperature for 5 min,
925 followed by resuspension into a 5-mL polystyrene round-bottom tube (FALCON) containing 150–500 µL
926 of 1% FBS in 1x PBS. The cell suspension was immediately placed on ice until sorting. The sorting was
927 performed using BD FACSJazz (BD Biosciences) with 1.0 Drop Single Sort mode. Cells were first gated
928 using FSC-A and SSC-A, and the gate for EGFP+ cells was determined to obtain those having high
929 FITC-A intensities that were not observed in a control cell sample transfected with Target-AID and NT
930 gRNA plasmids. EGFP+ cells were sorted into 8-strip PCR tubes (Nippon Genetics #FG-018WF), each
931 containing 2.5 µL of 1x PBS. For good cell recovery, the cell destination position in the collecting tube
932 was adjusted manually for each sample. The sample was immediately placed on an ice-cold 96-well
933 aluminum block. Although the EGFP+ cell rate varied across the samples, approximately 50–600
934 EGFP+ cells were recovered from each experiment.

935

936 mESCs. Three days after the transduction of a query gRNA, each cell sample was expanded in a 10-
937 cm cell culture dish. Cells were detached by 0.25 w/v% Trypsin-EDTA (Gibco #25200072), incubated
938 at 37°C for 5 min, collected into a 1.5-mL tube, and centrifuged at 1,000 rpm and room temperature for
939 5 min, followed by resuspension to ~1 x 10⁶ cells in 1x PBS containing 2% FBS in a 5-mL polystyrene
940 round-bottom tube (Falcon #352054). The cell suspension was immediately placed on ice until sorting.
941 The sorting was performed using MoFlo Astrios EQ Cell Sorter (Beckman Coulter). Cells were first gated
942 using FSC-A and SSC-A, and the gate for EGFP+ cells was determined to obtain those having high
943 FITC-A intensities that were not observed in a non-transduction control cell sample. EGFP+ positive

944 cells were single-cell sorted into 96-well plate wells, with the rest sorted in bulk to a single well of 96-
945 well plate, each with 100 μ L of the mESC culture media. Approximately 100–1,000 EGFP+ cells were
946 recovered from each experiment, except for Clone 153, for which EGFP+ cells above the gating
947 threshold could not be observed.

948

949 **Barcode sequencing library preparation**

950 CloneSelect C→T plasmid library and barcoded cell population. To identify barcodes of the CloneSelect
951 C→T plasmid library by high-throughput sequencing, ~10 ng of plasmid DNA (~1.0 x 10⁹ molecules)
952 was used as a PCR template. To identify barcodes of the initial barcoded HEK293Ta cell population,
953 genomic DNA was purified using NucleoSpin Tissue (Macherey Nagel #740952) according to the
954 manufacturer's protocol, and 119 ng of the extracted genomic DNA (4 x 10⁴ molecules; 400-fold to the
955 estimated barcode complexity) was used as a PCR template. The sequencing libraries were prepared
956 by a two-step PCR method. The first-round PCR was performed in triplicate, each in 20 μ L volume,
957 composed of template DNA, 0.5 μ L each of 20 μ M forward (SI#682) and reverse (SI#683) primers, 0.2
958 μ L of Phusion High-Fidelity DNA Polymerase (NEB #M0530), 4 μ L of Phusion HF Buffer (NEB #B0518S),
959 2 μ L of 2 mM dNTPs (Takara #4025), and 0.6 μ L of 100% DMSO (NEB #12611P), with the following
960 thermal cycle condition: 98°C for 10 s, 30 cycles of 98°C for 10 s, 61°C for 10 s, and 72°C for 30 s, and
961 then 72°C for 5 min for the final extension. Each PCR product was size-selected using 2% agarose gel,
962 purified using PCR/Gel Extraction Kit (Nippon Genetics #FG-91302). To provide Illumina sequencing
963 adapters and custom indices, the second-round PCR was performed to amplify each first-round PCR
964 replicate product in 20 μ L volume, composed of 2.5 ng of the 1st PCR product, 1 μ L each of 10 μ M P5
965 and P7 custom index primers, 0.2 μ L of Phusion High-Fidelity DNA Polymerase (NEB #M0530), 4 μ L of
966 Phusion HF Buffer (NEB #B0518S), 2 μ L of 2 mM dNTPs (Takara #4025), and 0.6 μ L of 100% DMSO
967 (NEB #12611P), with the following thermal cycle condition: 98°C for 10 s, 20 cycles of 98°C for 10 s,
968 61°C for 10 s, and 72°C for 30 s, and then 72°C for 5 min for the final extension. Custom indices assigned
969 to the second-round PCR products can be found in Table S3. The second-round PCR products were
970 size-selected and purified using PCR/Gel Extraction Kit (Nippon Genetics #FG-91302). The samples
971 were pooled, quantified by qPCR using KAPA Library Quantification Kit Illumina (KAPA BIOSYSTEMS
972 #KK4824), and analyzed by paired-end sequencing using Illumina MiSeq.

973

974 Sorted HEK293T cells. For the amplicon sequencing-based identification of barcodes in low-volume
975 cells sorted after gRNA-dependent barcode-specific clone isolation using CloneSelect C→T, we
976 prepared a cell lysate for each sample as a PCR template. The sequencing library of each sample was
977 prepared by modifying the two-step PCR protocol described for purified DNA as a PCR template. Cells
978 in 8-strip PCR tubes were first incubated with 2.0 μ L of lysis buffer, including 600 mM KOH, 10 mM
979 EDTA, and 100 mM DTT. The samples were then neutralized with 2.0 μ L of neutralization buffer
980 composed of 0.4 μ L of 1M Tris-HCl and 1.6 μ L of 3 M HCl. The first-round PCR was performed by
981 replacing the template with 2.0 μ L of the cell lysate. Although we did not observe visible gel
982 electrophoresis bands for the first-round PCR products, the PCR product of the expected size were size-
983 selected using 2% agarose gel, purified and eluted into 15 μ L of ddH₂O using PCR/Gel Extraction Kit
984 (Nippon Genetics #FG-91302). The PCR products were quantified using Quant-iT PicoGreen dsDNA
985 Assay Kit (Thermo Fisher Scientific #P7589) and Infinite 200 PRO plate reader (TECAN) using Tecan
986 i-control software (version 1.10.4.0). The second-round PCR was performed for 2.0 ng of the first-round
987 PCR product. Custom indices assigned to the second-round PCR products can be found in Table S3.
988 The second-round PCR products were size-selected and purified using PCR/Gel Extraction Kit (Nippon
989 Genetics #FG-91302). The samples were pooled into a DNA LoBind 1.5-mL tube (Eppendorf #13-698-
990 791), quantified by qPCR using KAPA Library Quantification Kit Illumina (KAPA BIOSYSTEMS
991 #KK4824), and analyzed by paired-end sequencing using Illumina MiSeq.

992

993 Uptag-dntag combination reference database. To identify the uptag-dntag combination reference
994 database of the mESC population tagged using the scCloneSelect barcode library, genomic DNA was
995 first extracted from 1 x 10⁵ cells using NucleoSpin Tissue (MACHEREY-NAGEL #740952) according to
996 the manufacturer's protocol. The sequencing libraries were prepared by a two-step PCR method. A total

997 of 50 ng genomic DNA was used for each PCR reaction. The first-round PCR was performed in duplicate,
998 each in 20 μ L volume, composed of template DNA, 0.7 μ L each of 10 μ M forward (SI#682) and reverse
999 (RS#250) primers, 0.2 μ L of Phusion High-Fidelity DNA Polymerase (NEB #M0530), 4.5 μ L of Phusion
1000 HF Buffer (NEB #B0518S), 1.6 μ L of 2.5 mM dNTPs (NEB #N0447), with the following thermal cycle
1001 condition: 98°C for 10 s, 30 cycles of 98°C for 10 s, 60°C for 10 s, and 72°C for 2 min, and then 72°C
1002 for 5 min for the final extension. Each PCR product was size-selected using 2% agarose gel, purified,
1003 and eluted into 20 μ L of ddH₂O using PCR/Gel Extraction Kit (Nippon Genetics #FG-91302). To provide
1004 Illumina sequencing adapters and custom indices, the second-round PCR was performed to amplify
1005 each first-round PCR replicate product in 20 μ L volume, composed of 20-fold dilution of the first-round
1006 PCR product, 0.7 μ L each of 10 μ M P5 and P7 custom index primers, 0.2 μ L of Phusion High-Fidelity
1007 DNA Polymerase (NEB #M0530), 4.5 μ L of Phusion HF Buffer (NEB #B0518S), 1.6 μ L of 2.5 mM dNTPs
1008 (NEB #N0447), with the following thermal cycle condition: 98°C for 10 s, 20 cycles of 98°C for 10 s, 60°C
1009 for 10 s, and 72°C for 30 s, and then 72°C for 5 min for the final extension. Custom indices assigned to
1010 the second-round PCR products can be found in Table S3. The second-round PCR products were size-
1011 selected and purified using PCR/Gel Extraction Kit (Nippon Genetics #FG-91302). The samples were
1012 pooled, quantified by qPCR using KAPA Library Quantification Kit Illumina (KAPA BIOSYSTEMS
1013 #KK4824), and analyzed by paired-end sequencing using Illumina MiSeq.

1014
1015 Sorted mESCs. For the amplicon sequencing-based identification of barcodes in cells sorted after
1016 gRNA-dependent barcode-specific clone isolation using scCloneSelect, we prepared a cell lysate for
1017 each sample as a PCR template. The sequencing library of each sample was prepared by modifying
1018 the two-step PCR method described for the identification of the uptag-dntag combination reference
1019 database. Sorted mESC samples were expanded in 96-well culture plate wells until confluent. After
1020 aspirating the culture medium, 20 μ L of 50 mM NaOH was added to each well and transferred into a 96-
1021 well PCR plate for direct cell lysis. The samples were then heated at 95°C for 15 min, followed by cooling
1022 down on ice. The samples were neutralized with 2.0 μ L of 1 M Tris-HCl (pH 8.0). The first-round PCR
1023 was performed in 40 μ L volume replacing the template with 3.5 μ L of cell lysate. The second-round PCR
1024 was performed in 20 μ L volume replacing the template with a 10-fold dilution of the first-round PCR
1025 product. Custom indices assigned to the second-round PCR products can be found in Table S3. The
1026 second-round PCR products were size-selected and purified using GeneJET Gel Extraction Kit (Thermo
1027 Fisher Scientific #K0691). The samples were pooled into a DNA LoBind 1.5-mL tube (Eppendorf
1028 #0030108051), quantified by qPCR using KAPA Library Quantification Kit Illumina (KAPA
1029 BIOSYSTEMS #KK4824), and analyzed by paired-end sequencing using Illumina HiSeq2500.

1030
1031 Reamplification of scCloneSelect dntags from Drop-seq library. To increase the sensitivity of identifying
1032 dntags associated with single cells and their transcriptome profiles, we selectively reamplified the DNA
1033 fragments encoding dntags and cell IDs from the intermediate Tn5 transposon-fragmented library of the
1034 Drop-seq process and sequenced them separately. The reamplification PCR was performed in 20 μ L
1035 volume, composed of 1 ng of the cDNA library quantified using TapeStation with High Sensitivity D5000
1036 ScreenTape (Agilent #5067-559 and #5067-5593), 0.7 μ L each of 20 μ M forward primer P5-TSO_Hybrid
1037 (45) and reverse primer SI#682, 0.2 μ L of Phusion High-Fidelity DNA Polymerase (NEB #M0530), 4.5
1038 μ L of 5x Phusion HF Buffer (NEB #B0518), and 1.6 μ L of 2.5 mM dNTPs (NEB #N0447) with the
1039 following thermal cycle condition: 95°C for 30 s, 30 cycles of 98°C for 30 s, 60°C for 10 s, and 72°C for
1040 2 min, and 72°C for 5 min for the final extension. The first-round PCR product was purified and eluted
1041 into 20 μ L of ddH₂O using GeneJET Gel Extraction Kit (Thermo Fisher Scientific #K0691). The second-
1042 round PCR was then reamplified in 20 μ L volume, composed of 10-fold dilution of the first-round PCR
1043 product, 0.7 μ L each of 10 μ M P5 and P7 custom dual index primers, 0.2 μ L of Phusion High-Fidelity
1044 DNA Polymerase (NEB #M0530), 4.5 μ L of 5x Phusion HF Buffer (NEB #B0518), 1.6 μ L of 2.5 mM
1045 dNTPs (NEB #N0447), with the following thermal cycle condition: 95°C for 30 s, 15 cycles of 98°C for
1046 10 s, 65°C for 10 s, and 72°C for 2 min, and 72°C for 5 min for the final extension. Custom indices
1047 assigned to the second-round PCR products can be found in Table S3. The second-round PCR products
1048 were size-selected using 2% agarose gel and purified using GeneJET Gel Extraction Kit (Thermo Fisher
1049 Scientific #K0691). The samples were pooled, quantified by qPCR using KAPA Library Quantification

1050 Kit Illumina (KAPA BIOSYSTEMS #KK4824), and analyzed by paired-end sequencing using Illumina
1051 HiSeq2500.
1052

1053 **Drop-seq**

1054 scRNA-seq was performed by Drop-seq. The Drop-seq platform was set up using devices manufactured
1055 by Dolomite Bio following the manufacturer's protocol. The microfluidic devices were fabricated by
1056 YODAKA Co., Ltd. Cell samples were prepared at a concentration of $\sim 2 \times 10^5$ cells/mL for analysis.
1057 Sequencing libraries were prepared following the original Drop-seq paper (45). In brief, following
1058 emulsion breakage and reverse transcription, "single-cell transcriptomes attached to microparticles"
1059 (STAMPs) were washed and proceeded to the Exonuclease I (NEB #M0293L) treatment. A total of
1060 $\sim 2,000$ STAMPs were used for the whole cDNA amplification of each sample. After second-strand
1061 synthesis, the library DNA was purified using AMPure XP beads (Beckman Coulter #A63881), quantified
1062 using TapeStation with High Sensitivity D5000 ScreenTape (Agilent #5067-5592 and #5067-5593), and
1063 fragmented by Tn5 transposon using Nextera XT DNA Library Preparation Kit (Illumina #FC-131-1024)
1064 according to the manufacturer's protocol. The fragmented sequencing library was then purified using
1065 AMPure XP beads (Beckman Coulter #A63881) and quantified by TapeStation with High Sensitivity
1066 D5000 ScreenTape (Agilent #5067-5592 and #5067-5593). We confirmed each average library size to
1067 be ~ 500 bp. Multiple scRNA-seq libraries were pooled and subjected to high-throughput sequencing
1068 using Illumina MiSeq or HiSeq2500. The sequencing library index information can be found in Table S3.
1069

1070 **mESC differentiation assay**

1071 For the establishment of a barcoded mESC population, cells were seeded on 6-well cell culture plate
1072 wells at a density of $\sim 2 \times 10^5$ cells/well with 2 mL of the culture medium containing 10^3 units/mL ESGRO
1073 Recombinant Mouse Leukemia inhibitory factor (LIF) (Millipore #ESG1107) and 2i (1.0 μ M PD0325901
1074 Toris #4423 and 3.0 μ M CHIR99021 Wako #038-23101). The next day, cells were transduced with 500
1075 μ L of 15-fold concentrated barcoded lentivirus pool of scCloneSelect. Two days after, the culture
1076 medium was exchanged with a fresh medium containing 1.0 μ g/mL of Puromycin (Gibco #A1113803).
1077 To restrict the clone complexity for the downstream cell differentiation and clone isolation assays, a
1078 clonal population bottleneck was created where $\sim 1,000$ cells were seeded on a 6-well cell culture plate
1079 well and cultured for ten days. Cells were then split as follows: $\sim 1 \times 10^4$ cells were seeded into the
1080 culture medium with LIF and 2i (LIF+2i+), $\sim 1 \times 10^4$ cells were seeded into the culture medium without
1081 LIF or 2i (LIF-2i-), two samples of $\sim 1 \times 10^5$ cells each were used for the identification of uptag-dntag
1082 combination reference database, and five replicates of $\sim 1 \times 10^5$ cells were stored at -80°C using
1083 CELLBANKER 1 freeze media (ZENOAQ #11910). Four days later, the cell cultures of the LIF+2i+ and
1084 LIF-2i- conditions were subjected to scRNA-seq.
1085

1086 **RT-PCR-based analysis of barcode transcription**

1087 The transcription of polyadenylated scCloneSelect barcode products was analyzed by RT-PCR and gel
1088 electrophoresis. Total RNA was first extracted using ISOSPIN Cell & Tissue RNA Kit (Nippon Gene
1089 #314-08211) according to the manufacturer's protocol. The RNA sample was then subjected to DNase
1090 I treatment (Takara #2270B) to remove DNA and purified again using ISOSPIN Cell & Tissue RNA Kit
1091 (Nippon Gene #314-08211). The first-strand cDNA was synthesized using High-Capacity cDNA Reverse
1092 Transcription Kit (Applied Biosciences #4368814). The reaction was performed in 10 μ L volume,
1093 composed of 5 μ L of DNase I treated RNA (~ 1 μ g), 0.5 μ L of 100 μ M oligo dT primer SI#4, 0.5 μ L of
1094 MultiScribe Reverse Transcriptase, 1 μ L of 10x RT buffer, 0.4 μ L of 100 mM dNTP, and 0.5 μ L of RNase
1095 Inhibitor (Applied Biosciences #N8080119), with the following thermal cycler condition: 25°C for 10 min,
1096 37°C for 12 min, and 85°C for 5 min. Lastly, the transcription of the target barcode was tested by PCR
1097 along with a GAPDH control. The PCR was performed in 20 μ L volume, composed of 2 μ L of 50-fold
1098 diluted first-strand cDNA, 2.8 μ L total of a primer pair SI#116–SI#7 to amplify the dntag or a primer pair
1099 RS#507–RS#508 to amplify GAPDH, 0.2 μ L of Phusion DNA Polymerase (NEB #M0530S), 4 μ L of 5x
1100 Phusion HF Buffer (NEB #B0518), and 1.6 μ L of 2.5 mM dNTPs (NEB #N0447), with the following
1101 thermal cycler condition: 98°C for 30 s, 30 cycles of 98°C for 10 s, 60°C for 10 s, and 72°C for 30 s, and

1102 then 72°C for 5 min for the final extension. The resulting PCR products were analyzed with 2% agarose
1103 gel.
1104
1105
1106 **Yeast CloneSelect**

1107 **Strains**

1108 *Saccharomyces cerevisiae* BY4741 (*MATa his3Δ0 leu2Δ0 met15Δ0 ura3Δ0*) was used for the
1109 experiments using yeast CloneSelect system.
1110

1111 **Yeast CloneSelect library**

1112 To generate the yeast CloneSelect barcode library, a semi-random oligo pool KI#200 encoding 5'-
1113 CCGWSNSWSNSWSNSWSNSNGT-3' was first chemically synthesized (Table S2) and amplified by
1114 PCR in 40 μL volume, composed of 2 μL of 0.01 μM template, 2 μL each of 10 μM forward primer SI#368
1115 and 10 μM reverse primer SI#369, 0.8 μL of Phusion High-fidelity DNA Polymerase (NEB #M0530S), 8
1116 μL of 5x Phusion HF Buffer (NEB #B0518S), and 2 μL of 2 mM dNTPs, with the following thermal cycle
1117 condition: 98°C for 30 s, 35 cycles of 98°C for 10 s, 68°C for 20 s, and 72°C for 5 s, and then 72°C for
1118 5 min for the final extension. The PCR product was analyzed with 2% agarose gel and size-selected
1119 and purified using FastGene PCR/Gel Extraction Kit (Nippon Genetics #FG-91302). The purified
1120 barcode fragment was then assembled into the cloning backbone plasmid pKI110 by Golden Gate
1121 Assembly (66) using BsmBI (NEB #R0580S). We performed two assembly reactions, each in 25 μL
1122 volume, composed of 500 fmol barcode fragments, 50 fmol backbone plasmid, 0.5 μL of BsmBI (NEB
1123 #R0580S), 0.5 μL of T4 DNA Ligase (Nippon Gene #317-00406), 2.5 μL of 10x T4 DNA Ligation
1124 Reaction Buffer (NEB #B0202S), and 0.125 μL of 60 mg/mL BSA (NEB #B9001S) with the following
1125 thermal cycle condition: 15 cycles of 37°C for 5 min and 20°C for 5 min, and then 55°C for 30 min for
1126 complete backbone digestion. For the bacterial transformation, 5 μL of the assembly product was used
1127 to transform 50 μL of DH5α chemically competent cells (NEB #C2987I) according to the manufacturer's
1128 high-efficiency transformation protocol. Following one-hour outgrowth in 1 mL of SOC medium (NEB
1129 #B9020S) at 37°C, cells were plated on a total of four LB agar plates containing 100 μg/mL Ampicillin
1130 (Wako #014-23302). The cell sample was also diluted and spread on the selective plates to estimate
1131 the clone complexity. To check assembly efficiency, random clones were isolated to perform genotyping
1132 PCR with a primer pair of KI#169 and KI#170, validating each clone to have an expected barcode insert.
1133 To construct Pool-100, 100 colonies were isolated, dissolved in 80 μL each of LB medium containing
1134 100 μg/mL Ampicillin (Wako #014-23302), combined 5 μL each, and cultured overnight at 37°C. The
1135 plasmid DNA was extracted using FastGene Plasmid Mini Kit (Nippon Genetics #FG-90502). Pool-1580
1136 was constructed by scraping and harvesting colonies from a plate with colony forming units close to
1137 1,000 by adding 1.5 mL of LB media containing 100 μg/mL Ampicillin (Wako #014-23302). The resulting
1138 cell samples were centrifuged at 13,000 rpm for 2 min to discard supernatant. The plasmid DNA pools
1139 were then purified from the collected cells using FastGene PCR/Gel Extraction Kit (Nippon Genetics
1140 #FG-91302).
1141

1142 **Barcoding of cells and introduction of genome editing reagents**

1143 For the barcoding of cells and introduction of genome editing reagents by transformation, we used the
1144 Frozen-EZ Yeast Transformation II kit (Zymo Research #T2001) with slight modifications. Cells were
1145 first pre-cultured in 5 mL of YPDA or SC-Dropout medium (complying with the auxotrophic requirement
1146 for plasmid maintenance in the host cells) in a cell culture tube rotating overnight at 30°C. The next day,
1147 cells were cultured in 5 mL of a fresh YPDA medium with a starting OD_{600 nm} of 0.3 and incubated until
1148 the OD_{600 nm} reached 0.8–1.0. After making competent cells according to the manufacturer's protocol,
1149 plasmid DNA and 50 μL of competent cells were added into a 1.5-mL tube, mixed thoroughly with 500
1150 μL of EZ3 solution according to the manufacturer's protocol, and incubated at 30°C for an hour with
1151 rotation. The cell sample was centrifuged at 13,000 rpm for 2 min, and the supernatant was discarded,
1152 followed by the addition of 2.5 mL of YPDA medium for recovery. After two-hour outgrowth at 30°C with
1153 rotation, cells were centrifuged to remove the medium and washed with 1,000 μL of 1x TE twice. Cells
1154 were then spread on SC-Dropout agar plates and incubated for two–four days at 30°C.

1155

1156 Barcodeing of cells. When the background BY4741 cells were transformed using the barcode plasmid
1157 library containing *HIS3* marker, YPDA medium was used for pre-culturing and SC–His+Ade plates for
1158 selecting transformants. For the pooled barcoding of cells, the reaction was scaled to transform 250 μ L
1159 of competent cells using 200 ng of plasmid in total, and colonies formed on the selective plates were
1160 pooled and collected by scraping with 3–4 mL of SC–His+Ade. For the barcoding of cells using a single
1161 barcode plasmid clone, 200 ng of plasmid was used to transform 15 μ L of competent cells.

1162

1163 Introduction of genome editing reagents. When cells harboring the barcode plasmid containing *HIS3*
1164 marker were subjected to a clone isolation, cells were transformed twice, first with the constitutively
1165 active Target-AID plasmid pKI086 containing *LEU2* marker and next with the targeting gRNA expression
1166 plasmid encoding *URA3* marker. For the first transformation, we used SC–His+Ade medium for pre-
1167 culturing and SC–His–Leu+Ade plates for selecting transformants. For the second transformation, SC–
1168 His–Leu+Ade medium for pre-culturing and SC–His–Leu–Ura+Ade for selecting transformants. When
1169 the background BY4741 cells were transformed using one of the galactose-inducible Cas9-based
1170 enzyme plasmids (Cas9, dCas9, dCas9-PmCDA1, dCas9-PmCDA1-UGI, nCas9, nCas9-PmCDA1, and
1171 nCas9-PmCDA1-UGI) containing *LEU2* marker and a CAN1-targeting gRNA plasmid containing *URA3*
1172 marker, we used YPDA medium for pre-culturing and SC–Leu–Ura+Ade plates for selecting
1173 transformants. For the barcode-specific reporter activation in a complex barcoded population, the
1174 reaction was scaled to transform 250 μ L of competent cells using 200 ng of the enzyme plasmid and
1175 200 ng of the targeting gRNA plasmid in total. For the other small-scale transformations, 200 ng of the
1176 effector plasmid and 200 ng of the targeting gRNA plasmid were used to transform 15 μ L of competent
1177 cells.

1178

1179 **Barcode sequencing library preparation**

1180 To identify barcodes of the yeast CloneSelect plasmids introduced to the cells by high-throughput
1181 sequencing, we first extracted and purified the barcode plasmids. We first centrifuged cells at 15,000
1182 rpm for 3 min, followed by discarding the supernatant. The cell pellet was resuspended with 20 μ L of
1183 Zymolyase Buffer, containing 2.5 mg/mL Zymolyase (Zymo Research #E1005), 10 mM Sodium
1184 phosphate, and 1.2 M Sorbitol, and 500 μ L of Solution I Buffer (Supplied in Zymolyase #E1005),
1185 containing 0.1 M EDTA and 1 M Sorbitol. The sample was incubated at 37°C for one hour and
1186 centrifuged at 15,000 rpm for 1 min, followed by discarding the supernatant. The cell lysate sample was
1187 then incubated with 250 μ L of Solution II Buffer (Supplied in Zymolyase #E1005), containing 20 mM
1188 EDTA and 50 mM Tris-HCl, and 1% SDS, at 65°C for 30 min, followed by the addition of 100 μ L of 5 M
1189 potassium acetate. The sample was further incubated on ice for 30 min and centrifuged at 15,000 rpm
1190 for 3 min. The supernatant was transferred into a 1.5-mL tube, and the plasmid DNA was precipitated
1191 with the addition of 400 μ L of isopropanol, followed by cleanup with 400 μ L of 70% ethanol. The resulting
1192 DNA pellet was resuspended with 50 μ L of ddH₂O containing 10 μ g/mL RNase and incubated at 65°C
1193 for 10 min. Next, the barcode sequencing libraries were prepared by a two-step PCR method. The first-
1194 round PCR was performed in triplicate, each in 40 μ L volume, composed of 1.0 μ g of template DNA, 1
1195 μ L each of 10 μ M forward primer KI#169 and 10 μ M reverse primer KI#289, 0.4 μ L of Phusion High-
1196 Fidelity DNA Polymerase (NEB #M0530S), 8 μ L of Phusion HF Buffer (NEB #B0518S), and 0.8 μ L of
1197 10 mM dNTPs (Takara #4030), with the following thermal cycle condition: 98°C for 30 s, 20 cycles of
1198 98°C for 10 s, 61°C for 20 s, and 72°C for 25 s, and then 72°C for 5 min for the final extension. Each
1199 PCR product was size-selected using 2% agarose gel, purified, and eluted into 50 μ L of ddH₂O using
1200 PCR/Gel Extraction Kit (Nippon Genetics #FG-91302). To provide Illumina sequencing adapters and
1201 custom indices, the second-round PCR was performed to amplify each first-round PCR replicate product
1202 in 40 μ L volume, composed of 2 μ L of the first PCR product, 1 μ L each of 10 μ M P5 and P7 custom
1203 index primers, 0.4 μ L of Phusion High-Fidelity DNA Polymerase (NEB #M0530S), 8 μ L of 5x Phusion
1204 HF Buffer (NEB #B0518S), and 0.8 μ L of 10 mM dNTPs (Takara #4030), with the following thermal cycle
1205 condition: 98°C for 30 s, 15 cycles of 98°C for 10 s and 60°C for 10 s, and 72°C for 1 min, and then 72°C
1206 for 5 min for the final extension. Custom indices assigned to the second-round PCR products can be
1207 found in Table S3. The second-round PCR products were size-selected and purified using PCR/Gel

1208 Extraction Kit (Nippon Genetics #FG-91302). The sequencing libraries were pooled, quantified by qPCR
1209 using KAPA Library Quantification Kit Illumina (KAPA BIOSYSTEMS #KK4824), pooled with equimolar
1210 ratios, and analyzed by paired-end sequencing using Illumina HiSeq2500.
1211

1212 **Analysis of reporter activation efficiency**

1213 To analyze the efficiency of the gRNA-dependent barcode-specific mCherry reporter activation, we
1214 treated three independent barcoded cell samples, each by all three corresponding gRNAs (3x3 assay).
1215 Each sample was spread on SC–His–Leu–Ura+Ade agar plates, scraped and inoculated to a 1.5-mL
1216 tube containing 500 μ L of SC–His–Leu–Ura+Ade medium, and cultured for two–four days at 30°C. The
1217 20 μ L of pre-cultured cell sample was mixed with 180 μ L of SC–His–Leu–Ura+Ade media and
1218 transferred into a flat-bottom transparent 96-well plate (Greiner Bio-One #655090). Samples were then
1219 analyzed using Infinite 200 PRO plate reader (TECAN) using Tecan i-control software (version 1.10.4.0)
1220 to measure mCherry fluorescence intensities normalized by OD_{595 nm} values. For microscopic
1221 observation of cells, 2.5 μ L of cell sample was transferred on a glass slide, gently covered with a glass
1222 coverslip, and observed using BZ-X710 (Keyence) with 20x and 40x objective lenses. We also directly
1223 measured the GTG→ATG conversion rate of each sample by high-throughput sequencing. Cells were
1224 scraped and harvested from the selective plates and lysed by DNAZol (COSMO BIO #DN127) according
1225 to the manufacturer's protocol. The sequencing libraries were then prepared by a two-step PCR method.
1226 The first-round PCR was performed in 32 μ L volume, composed of 1.6 μ L of cell lysate, 1.6 μ L each of
1227 10 μ M forward primer KI#168 and 10 μ M reverse primer KI#169, 0.64 μ L of Phusion High-Fidelity DNA
1228 Polymerase (NEB #M0530S), 6.4 μ L of Phusion HF Buffer (NEB #B0518S), and 0.64 μ L of 10 mM
1229 dNTPs (Takara #4030), with the following thermal cycle condition: 98°C for 30 s, 30 cycles of 98°C for
1230 10 s, 61°C for 10 s, and 72°C for 1 min, and then 72°C for 5 min for the final extension. The remaining
1231 procedure was processed by the same protocols described for the barcode sequencing library
1232 preparation. Custom indices assigned to the second-round PCR products can be found in Table S3.
1233 The second-round PCR products were size-selected and purified using PCR/Gel Extraction Kit (Nippon
1234 Genetics #FG-91302). The samples were pooled, quantified by qPCR using KAPA Library Quantification
1235 Kit Illumina (KAPA BIOSYSTEMS #KK4824), and analyzed by paired-end sequencing using Illumina
1236 MiSeq.
1237

1238 **Isolation and analysis of barcoded colonies**

1239 After the barcode-specific reporter activation of a complex population, cells from test and control
1240 conditions were spread on SC–His–Leu–Ura+Ade agar plates and imaged under a blue light illuminator
1241 FAS-IV (Nippon Genetics) to distinguish mCherry+ and mCherry– colonies. Colonies were isolated into
1242 96-well cell culture plate wells containing 98 μ L of SC–His–Leu–Ura+Ade and cultured overnight at 30°C.
1243 Samples were then analyzed using Infinite 200 PRO plate reader (TECAN) using Tecan i-control
1244 software (version 1.10.4.0) to measure mCherry fluorescence intensities normalized by OD_{595 nm} values.
1245 The same colony isolates were also subjected to Sanger sequencing to identify their barcode sequences
1246 and base editing outcomes. Using the same cell lysis, first-round PCR, and PCR cleanup protocols as
1247 in the analysis of the reporter activation efficiency, we obtained barcode DNA fragments from each
1248 sample. Each PCR product was analyzed by Sanger sequencing using a sequencing primer SI#658.
1249 The Sanger sequencing trace was analyzed using PySanger (<https://github.com/ponnhide/PySanger>).
1250

1251 **Canavanine assay**

1252 Genome editing efficiencies of different Cas9-based genome editing enzymes (Cas9, dCas9, dCas9-
1253 PmCDA1, dCas9-PmCDA1-UGI, nCas9, nCas9-PmCDA1 and nCas9-PmCDA1-UGI) were estimated
1254 by Canavanine assay, where enzymes were introduced to the cells with a gRNA targeting an arginine
1255 transporter CAN1 and its knockout efficiency can be assessed by cell survival under the presence of a
1256 toxic arginine analog Canavanine. In this assay, Cas9-based enzyme expressions were regulated under
1257 a galactose-inducible GAL1/10 promoter. To induce genome editing, cells containing enzyme and gRNA
1258 plasmids were first cultured in SC–Leu–Ura medium containing 2% glucose at 30°C until saturation.
1259 Cells were then resuspended in SC–Leu–Ura medium containing 2% raffinose with 16-fold dilution and
1260 cultured at 30°C until saturation. Finally, cells were resuspended in SC–Leu–Ura medium containing

1261 2% raffinose and 0.02% galactose with 32-fold dilution and cultured at 30°C for two days. Each sample
1262 was then spread on SC–Leu–Ura–Arg+Ade and SC–Leu–Ura–Arg+Ade containing 60 mg/ml
1263 canavanine plates and cultured at 30°C for two–four days to estimate colony forming units and perform
1264 spot assays. Furthermore, we scraped and harvested colonies from the SC–Leu–Ura–Arg+Ade control
1265 plates to extract genomic DNA samples for the mutation spectra assay by high-throughput sequencing.
1266 We first lysed 20 µL of cells at OD_{600 nm} of 1.0 using 100 µL of DNAZol (COSMO BIO #DN127) followed
1267 by incubation at room temperature for 15 min. The lysate was mixed thoroughly with 30 µL of 1M NaCl
1268 and 50 µL of 100% ethanol and centrifuged at 14,000 rpm for 10 min. The supernatant was discarded,
1269 and the pellet was washed with 550 µL of 70% ethanol. After air-drying, the sample was resuspended
1270 in 50 µL of ddH₂O. We then prepared an amplicon sequencing library for each sample by a two-step
1271 PCR method in triplicate. The first-round PCR was in 40 µL volume, composed of 2 µL of template DNA,
1272 2 µL each of 10 µM forward primer #KN85F3 and 10 µM reverse primer #KN85R2, 0.8 µL of Phusion
1273 High-Fidelity DNA Polymerase (NEB #M0530S), 8 µL of Phusion HF Buffer (NEB #B0518S), and 0.8
1274 µL of 10 mM dNTPs (Takara #4030), with the following thermal cycle condition: 98°C for 30 s, 30 cycles
1275 of 98°C for 10 s, 60°C for 10 s, and 72°C for 1 min, and then 72°C for 5 min for the final extension. We
1276 also performed the same process using a primer pair #HO2F2–#HO2R2 to prepare control samples.
1277 The remaining procedure was processed by the same protocols described for the barcode sequencing
1278 library preparation. Custom indices assigned to the second-round PCR products can be found in Table
1279 S3. The second-round PCR products were size-selected and purified using PCR/Gel Extraction Kit
1280 (Nippon Genetics #FG-91302). The sequencing libraries were pooled, quantified by qPCR using KAPA
1281 Library Quantification Kit Illumina (KAPA BIOSYSTEMS #KK4824), pooled with equimolar ratios, and
1282 analyzed by paired-end sequencing using Illumina MiSeq.

1283
1284
1285 **Bacterial CloneSelect**

1286 **Preparation of cells for various bacterial CloneSelect systems**

1287 We prepared cell samples harboring single barcode plasmids for different variants of bacterial
1288 CloneSelect systems (Table S2). The plasmid for the EGFP reporter-based system was introduced to
1289 BL21(DE3) Competent *E. coli* cells (NEB #C2527I), and the plasmids for the Blasticidin and Zeocin
1290 resistance marker-based systems were introduced to T7 Express chemically competent cells (NEB
1291 #C2566I) according to the manufacturer's high-efficiency transformation protocols. The transformants
1292 were selected on LB agar plates containing 100 µg/mL Ampicillin (Wako #014-23302) and/or 50 µg/mL
1293 Kanamycin (Wako #111-00344).

1294
1295 **Bacterial CloneSelect library**

1296 To generate the bacterial CloneSelect barcode library for the Zeocin resistance marker, a semi-random
1297 oligo pool KI#405 encoding 5'-ATGCCGVNNVNNVNNVNNTAA-3' was chemically synthesized
1298 (Table S2), where a start codon ATG, the antisense strand sequence of 5'-CGG-3' PAM and a quintuple
1299 repeat of VNN (V=non-T) were followed by a TAA stop codon. The VNN repeat restricts additional stop
1300 codons from appearing in-frame to the downstream reporter. The semi-random oligo pool was amplified
1301 by PCR in 20 µL volume, composed of 1 µL of 1 µM template, 1 µL each of 10 µM forward primer SI#368
1302 and 10 µM reverse primer SI#369, 0.4 µL of Phusion High-fidelity DNA Polymerase (NEB #M0530L), 4
1303 µL of 5x Phusion HF Buffer (NEB #B0518S), and 0.4 µL of 10 mM dNTPs, with the following thermal
1304 cycle condition: 98°C for 30 s, 20 cycles of 98°C for 10 s, 68°C for 20 s, and 72°C for 20 s, and then
1305 72°C for 5 min for the final extension. The PCR product was analyzed with 2% agarose gel and size-
1306 selected and purified using FastGene PCR/Gel Extraction Kit (Nippon Genetics #FG-91302). The
1307 purified barcode fragment was then assembled into the cloning backbone plasmid pKI243 by Golden
1308 Gate Assembly using BsmBI (66). We performed the assembly in 12.5 µL volume, composed of 2.91
1309 fmol of barcode fragments, 14.9 fmol of backbone plasmid, 0.25 µL of BsmBI (NEB #R0580L), 0.5 µL
1310 of T4 DNA Ligase (Nippon Gene #317-00406), 1.25 µL of 10x T4 DNA Ligation Reaction Buffer (NEB
1311 #B0202S), and 0.62 µL of 2 mg/mL BSA (NEB #B9001S) with the following thermal cycle condition: 15
1312 cycles of 37°C for 5 min and 20°C for 5 min, and then 55°C for 30 min for complete backbone digestion.
1313 For the bacterial transformation, 3 µL of the assembly product was used to transform 65 µL of T7

1314 Express chemically competent cells (NEB #C2566I) according to the manufacturer's high-efficiency
1315 transformation protocol. Following one-hour outgrowth in 500 µL of SOC medium (NEB #B9020S) at
1316 37°C, the cell sample was plated 250 µL each on three LB agar plates containing 100 µg/mL Ampicillin
1317 (Wako #014-23302). The cell sample was also diluted and plated on the selective plates to estimate the
1318 clone complexity. To check assembly quality and efficiency, 12 random clones were isolated and
1319 subjected to Sanger Sequencing, validating that 11 out of 12 clones showed an expected clone barcode
1320 insert. To construct Pool-100, 100 colonies were isolated, dissolved in 80 µL each of LB medium
1321 containing 100 µg/mL Ampicillin (Wako #014-23302), combined 5 µL each, and cultured overnight at
1322 37°C. The plasmid DNA was extracted using FastGene Plasmid Mini Kit (Nippon Genetics #FG-90502).
1323 Pool-1550 was constructed by scraping and harvesting colonies from a plate with colony forming units
1324 close to 1,000 by adding 1.5 mL of LB media containing 100 µg/mL Ampicillin (Wako #014-23302). The
1325 barcode plasmid libraries were used to transform T7 Express chemically competent cells (NEB #C2566I)
1326 to establish barcoded *E. coli* cell populations.
1327

1328 **Barcode sequencing library preparation**

1329 For each of the Pool-100 and Pool-1550 barcode plasmid libraries, the barcode sequencing library was
1330 prepared in triplicate by a two-step PCR method. The first-round PCR was performed in five separate
1331 PCR reactions, each in 40 µL volume, composed of 2.0 ng of plasmid template DNA, 1 µL each of 10
1332 µM forward primer KI#403 and 10 µM reverse primer KI#404, 0.4 µL of Phusion High-Fidelity DNA
1333 Polymerase (NEB #M0530L), 8 µL of Phusion HF Buffer (NEB #B0518S), and 0.8 µL of 10 mM dNTPs
1334 (Takara #4030), with the following thermal cycle condition: 98°C for 30 s, 20 cycles of 98°C for 10 s,
1335 54°C for 20 s, and 72°C for 25 s, and then 72°C for 5 min for the final extension. For each replicate, the
1336 five PCR reaction products were pooled, size-selected using 2% agarose gel, purified, and eluted into
1337 30 µL of ddH2O using PCR/Gel Extraction Kit (Nippon Genetics #FG-91302). To provide Illumina
1338 sequencing adapters and custom indices, the second-round PCR was performed to amplify each first-
1339 round PCR replicate product in 40 µL volume, composed of 2 µL of the first PCR product, 1 µL each of
1340 10 µM P5 and P7 custom index primers, 0.4 µL of Phusion High-Fidelity DNA Polymerase (NEB
1341 #M0530L), 8 µL of 5x Phusion HF Buffer (NEB #B0518S), and 0.8 µL of 10 mM dNTPs (Takara #4030),
1342 with the following thermal cycle condition: 98°C for 30 s, 15 cycles of 98°C for 10 s, 60°C for 10 s, and
1343 72°C for 60 s, and then 72°C for 5 min for the final extension. Custom indices assigned to the second-
1344 round PCR products can be found in Table S3. The second-round PCR products were size-selected
1345 and purified using PCR/Gel Extraction Kit (Nippon Genetics #FG-91302). The sequencing libraries were
1346 pooled, quantified by qPCR using KAPA Library Quantification Kit Illumina (KAPA BIOSYSTEMS
1347 #KK4824), pooled with equimolar ratios, and analyzed by paired-end sequencing using Illumina MiSeq.
1348

1349 **Introduction of genome editing reagents**

1350 To introduce a plasmid containing ABE-7.10 and gRNA with given induction systems to barcoded cells,
1351 we used Mix&Go! *E. coli* Transformation Kit (Zymo Research #T3001) according to the manufacturer's
1352 protocol. To select successful transformants, the transformation reaction sample was plated on LB agar
1353 plates containing 100 µg/mL Ampicillin (Wako #014-23302) and 50 µg/mL Kanamycin (Wako #111-
1354 00344) and incubated overnight at 37°C. For the experiments that involved Arabinose (Sigma-Aldrich
1355 #A3256-10MG) and Isopropylthio-β-galactoside (IPTG) (ThermoFisher Scientific #15529019)
1356 inductions, cells were cultured in the medium containing 100 mM Arabinose and 0.1 mM IPTG overnight
1357 at 37°C prior to the analyses. For the barcoded cell isolation with the Zeocin-resistance marker-based
1358 system, we used a low-salt LB medium adjusted to pH 7.5 with 1 M NaOH (Nakalai #37421-05) for the
1359 Zeocin activity. We also decided to use 100 µg/mL Zeocin (Invitrogen #R25001) or 100 µg/mL Blasticidin
1360 S (Wako #029-18701) with no Arabinose or IPTG for genome editing and selecting reporter-activated
1361 cells, as leaky gene editing reagent expressions from the inducible promoters with the no inducer
1362 condition were sufficient and maximized the cell viability. The information on the genome editing
1363 plasmids used in this study can be found in Table S2.
1364

1365 **Analysis of reporter activation efficiency**

1366 To analyze the efficiency of the gRNA-dependent barcode-specific EGFP-reporter activation, 200 µL of
1367 cell samples were transferred into a flat-bottom transparent 96-well plate (Greiner Bio-One #655090)
1368 and analyzed using Infinite 200 PRO plate reader (TECAN) using Tecan i-control software (version
1369 1.10.4.0) to measure EGFP fluorescence intensities normalized by OD_{595 nm} values. For microscopic
1370 observation of cells, 2.5 µL of cell sample was transferred onto a glass slide (MATSUNAMI #S2441),
1371 gently covered with a glass coverslip, and observed using BZ-X710 (Keyence) with 20x and 40x
1372 objective lenses.

1373 **Isolation and analysis of barcoded colonies**

1374 After the barcode-specific Zeocin-resistance marker activation in the barcoded cell population, barcodes
1375 of colonies from test and control conditions were analyzed by Sanger sequencing. For each colony, the
1376 barcode region was amplified by PCR in 20 µL volume, composed of 1 µL of cell suspension, 0.5 µL
1377 each of 10 µM forward primer KI#403 and 10 µM reverse primer KI#404, 0.2 µL of Phusion High-Fidelity
1378 DNA Polymerase (NEB #M0530L), 4 µL of Phusion HF Buffer (NEB #B0518S), and 0.4 µL of 10 mM
1379 dNTPs (Takara #4030), with the following thermal cycle condition: 98°C for 30 s, 30 cycles of 98°C for
1380 10 s, 54°C for 20 s, and 72°C for 30 s, and then 72°C for 5 min for the final extension. The PCR products
1381 were analyzed with 2% agarose gel and transferred into 96-well PCR plate wells for clean-up with 20
1382 µL of AMPure XP beads (Beckman Coulter #A63881) according to the manufacturer's protocol. The
1383 Sanger sequencing was performed using a sequencing primer KI#403. The Sanger sequencing trace
1384 was analyzed using PySanger (<https://github.com/ponnhide/PySanger>).
1385

1386
1387 **High-throughput sequencing and data analysis**

1388 **High-throughput sequencing**

1389 The sequencing libraries were mixed with 20–30% of PhiX spike-in DNA control (Illumina #FC-110-
1390 3001) for better cluster generation on the flow cell and sequenced by Illumina MiSeq (MiSeq v3 150-
1391 cycles kit #MS-102-3001 or 300-cycles kit #MS-102-3003), HiSeq2500 (TruSeq rapid SBS kit v2 #FC-
1392 402-4022). Base calling was performed with bcl2fastq2 (version v2.20.0) to generate FASTQ files. The
1393 sequencing condition for each library and the NCBI Sequence Read Archive's ID to each raw FASTQ
1394 file can be found in Table S3.
1395

1396 **Barcode identification**

1397 **Mammalian CloneSelect C→T and yeast and bacterial CloneSelect.** Sequencing reads were aligned to
1398 the constant sequences of the designed library structure using NCBI BLAST+ (version 2.6.0) (67) with
1399 the blastn-short option to identify sample indices for demultiplexing and CloneSelect barcode sequences.
1400 To generate the barcode allowlist for the mammalian CloneSelect C→T mini-pool experiments, barcode
1401 sequences commonly identified in both the plasmid DNA library and genomic DNA library were first
1402 obtained. Their sequencing errors were then corrected using starcode (version 1.4)
1403 (<https://github.com/gui11aume/starcode>) with the maximum Levenshtein distance threshold of 4 to
1404 merge minor and major barcodes. The barcode counts of each sample were normalized by the total
1405 barcode count. To estimate barcode frequencies for a given cell or DNA pool sample, the barcode
1406 frequencies were averaged across replicates if any. The barcode sequence and frequency information
1407 obtained in this study can be found in Table S1. Codes are available at
1408 https://github.com/yachielab/CloneSelect_v1/tree/main/Barcode_identification/CloneSelect.
1409

1410 **scCloneSelect.** To identify uptag and dntag barcodes of the barcoded cells, we first demultiplexed the
1411 sequencing reads and used cutadapt v4.1 (<https://github.com/marcelm/cutadapt/>) to extract uptag and
1412 dntag sequences sandwiched between their 20-bp upstream and downstream constant sequences. The
1413 identified uptags and dtags were filtered with the Q-score threshold of 30, clustered, and further filtered
1414 with their lengths of 17-bp for uptags and 30-bp for dtags using bartender-1.1
1415 (<https://github.com/LaoZZZZZ/bartender-1.1>) (68). For the construction of the uptag-dtag combination
1416 reference database, uptags and dtags found in the same reads were first paired. We discarded
1417

1418 redundant uptag-dntag pairs whose uptag or dntag were found in more abundant pairs. For the mapping
1419 of dntag to the uptag-dntag database, we used symspellpy v6.7
1420 (<https://github.com/mammothb/symspellpy>) to find one with the shortest edit distance. In cases where
1421 multiple dntags in the database were found to be mapped by a query with the same edit distances, the
1422 dntag with the highest frequency in the database was chosen. To analyze uptag frequencies in a cell
1423 population obtained after gRNA-dependent barcode-specific EGFP reporter activation followed by flow
1424 cytometry cell sorting, we mapped the sequencing reads to the uptag-dntag database and obtained read
1425 counts for uptags recorded in the database using bartender-1.1 and symspellpy v6.7. Conflicts by the
1426 redundant hits to the database were resolved in the same way as those for dntags described above.
1427 Codes are available at
1428 [https://github.com/yachielab/CloneSelect_v1/tree/main/Barcode identification/scCloneSelect](https://github.com/yachielab/CloneSelect_v1/tree/main/Barcode%20identification/scCloneSelect).
1429

1430 **Drop-seq data analysis**

1431 After sample demultiplexing, FASTQ files were processed with Dropseq Tools v2.5.1
1432 (<https://github.com/broadinstitute/Drop-seq>) for base quality filtering, adapter trimming, and Cell ID and
1433 UMI extraction. Picard v2.18.14 (<https://github.com/broadinstitute/picard>) was used to convert BAM files
1434 to FASTQ files for the proceeding step. The filtered reads were aligned using STAR v2.7
1435 (<https://github.com/alexdobin/STAR>) (69) using the mm10 reference genome. The differential gene
1436 expression and clustering analysis were performed using Seurat v3 (<https://github.com/satijalab/seurat>)
1437 (70). After filtering cells with the thresholds of Feature_RNA > 200 & nFeature_RNA < 2500 & percent.mt
1438 < 5, their gene expression profiles were normalized before clustering with the Seurat::sctransform
1439 function. The dntags to be analyzed in this study were first determined in the first Drop-seq run based
1440 on their cumulative read count distribution of Cell IDs with the threshold determined by the knee point
1441 using the Python package kneed v0.8.1 (<https://github.com/arvkevi/kneed>). However, to map dntag
1442 distribution to the single-cell transcriptome data with high sensitivity, we also sequenced the dntag-
1443 reamplified library and identified the association of Cell IDs and dntags in the dntag-uptag combination
1444 reference database by the method described above for the scCloneSelect uptag and dntag identification.
1445 In cases where multiple dntags were found for a single Cell ID, the dntag with the most abundant UMI
1446 count was chosen. Codes are available at
1447 https://github.com/yachielab/CloneSelect_v1/tree/main/Drop-seq.
1448

1449 **Mutational spectra analysis**

1450 The amplicon sequencing reads obtained to analyze mutational patterns at the CAN1 target site
1451 conferred by each of the Cas9-based genome editing enzymes was processed by a pipeline described
1452 previously (39). Codes specific to this study are available at
1453 [https://github.com/yachielab/CloneSelect_v1/tree/main/Mutational Spectra Analysis](https://github.com/yachielab/CloneSelect_v1/tree/main/Mutational_Spectra_Analysis).
1454
1455

1456 **Statistical analysis**

1457 The statistical tests were performed using R (version 4.2.0). The details of each statistical test can be
1458 found in the corresponding figure legend. The statistical methods used in this study and *P*-values are
1459 also listed in Table S4.
1460
1461

1462 **Data and code availability**

1463 High-throughput sequencing data generated in this study are available at the NCBI Sequence Read
1464 Archive (PRJNA901977). All the codes used in this study are available at
1465 https://github.com/yachielab/CloneSelect_v1.
1466
1467

1468 **References**

- 1469
1470 1. H. E. Bhang *et al.*, Studying clonal dynamics in response to cancer therapy using high-complexity
1471 barcoding. *Nat Med* **21**, 440-448 (2015).
1472 2. A. N. Hata *et al.*, Tumor cells can follow distinct evolutionary paths to become resistant to
1473 epidermal growth factor receptor inhibition. *Nat Med* **22**, 262-269 (2016).
1474 3. U. Ben-David *et al.*, Genetic and transcriptional evolution alters cancer cell line drug response.
1475 *Nature* **560**, 325-330 (2018).
1476 4. L. V. Nguyen *et al.*, Barcoding reveals complex clonal dynamics of de novo transformed human
1477 mammary cells. *Nature* **528**, 267-271 (2015).
1478 5. W. Pei *et al.*, Polylox barcoding reveals haematopoietic stem cell fates realized in vivo. *Nature*
1479 **548**, 456-460 (2017).
1480 6. R. Lu, N. F. Neff, S. R. Quake, I. L. Weissman, Tracking single hematopoietic stem cells in vivo
1481 using high-throughput sequencing in conjunction with viral genetic barcoding. *Nat Biotechnol* **29**,
1482 928-933 (2011).
1483 7. S. H. Naik *et al.*, Diverse and heritable lineage imprinting of early haematopoietic progenitors.
1484 *Nature* **496**, 229-232 (2013).
1485 8. A. Gerrits *et al.*, Cellular barcoding tool for clonal analysis in the hematopoietic system. *Blood*
1486 **115**, 2610-2618 (2010).
1487 9. B. A. Biddy *et al.*, Single-cell mapping of lineage and identity in direct reprogramming. *Nature*
1488 **564**, 219-224 (2018).
1489 10. J. Hollmann *et al.*, Genetic barcoding reveals clonal dominance in iPSC-derived mesenchymal
1490 stromal cells. *Stem Cell Res Ther* **11**, 105 (2020).
1491 11. P. D. Tonge *et al.*, Divergent reprogramming routes lead to alternative stem-cell states. *Nature*
1492 **516**, 192-197 (2014).
1493 12. S. Venkataram *et al.*, Development of a Comprehensive Genotype-to-Fitness Map of Adaptation-
1494 Driving Mutations in Yeast. *Cell* **166**, 1585-1596 e1522 (2016).
1495 13. J. E. Barrick *et al.*, Genome evolution and adaptation in a long-term experiment with Escherichia
1496 coli. *Nature* **461**, 1243-1247 (2009).
1497 14. S. F. Levy *et al.*, Quantitative evolutionary dynamics using high-resolution lineage tracking.
1498 *Nature* **519**, 181-186 (2015).
1499 15. J. R. Blundell *et al.*, The dynamics of adaptive genetic diversity during the early stages of clonal
1500 evolution. *Nat Ecol Evol* **3**, 293-301 (2019).
1501 16. A. N. Nguyen Ba *et al.*, High-resolution lineage tracking reveals travelling wave of adaptation in
1502 laboratory yeast. *Nature* **575**, 494-499 (2019).
1503 17. A. E. Rodriguez-Fraticelli *et al.*, Single-cell lineage tracing unveils a role for TCF15 in
1504 haematopoiesis. *Nature* **583**, 585-589 (2020).
1505 18. C. Weinreb, A. Rodriguez-Fraticelli, F. D. Camargo, A. M. Klein, Lineage tracing on
1506 transcriptional landscapes links state to fate during differentiation. *Science* **367**, (2020).
1507 19. D. E. Wagner *et al.*, Single-cell mapping of gene expression landscapes and lineage in the
1508 zebrafish embryo. *Science* **360**, 981-987 (2018).
1509 20. A. E. Rodriguez-Fraticelli *et al.*, Clonal analysis of lineage fate in native haematopoiesis. *Nature*
1510 **553**, 212-216 (2018).
1511 21. Z. He *et al.*, Lineage recording in human cerebral organoids. *Nat Methods* **19**, 90-99 (2022).
1512 22. M. M. Chan *et al.*, Molecular recording of mammalian embryogenesis. *Nature* **570**, 77-82 (2019).
1513 23. B. Raj *et al.*, Simultaneous single-cell profiling of lineages and cell types in the vertebrate brain.
1514 *Nat Biotechnol* **36**, 442-450 (2018).
1515 24. S. Ishiguro, H. Mori, N. Yachie, DNA event recorders send past information of cells to the time
1516 of observation. *Curr Opin Chem Biol* **52**, 54-62 (2019).
1517 25. S. Ota *et al.*, Ghost cytometry. *Science* **360**, 1246-1251 (2018).
1518 26. D. Schraivogel *et al.*, High-speed fluorescence image-enabled cell sorting. *Science* **375**, 315-
1519 320 (2022).
1520 27. N. Nitta *et al.*, Intelligent Image-Activated Cell Sorting. *Cell* **175**, 266-276 e213 (2018).

- 1521 28. N. Hasle *et al.*, High-throughput, microscope-based sorting to dissect cellular heterogeneity. *Mol Syst Biol* **16**, e9442 (2020).
- 1522 29. C. Umkehrer *et al.*, Isolating live cell clones from barcoded populations using CRISPRa-inducible reporters. *Nat Biotechnol* **39**, 174-178 (2021).
- 1523 30. A. M. Al'Khafaji, D. Deatherage, A. Brock, Control of Lineage-Specific Gene Expression by Functionalized gRNA Barcodes. *ACS Synth Biol* **7**, 2468-2474 (2018).
- 1524 31. C. Gutierrez *et al.*, Multifunctional barcoding with ClonMapper enables high-resolution study of clonal dynamics during tumor evolution and treatment. *Nat Cancer* **2**, 758-772 (2021).
- 1525 32. D. Feldman *et al.*, CloneSifter: enrichment of rare clones from heterogeneous cell populations. *BMC Biol* **18**, 177 (2020).
- 1526 33. W. Chen *et al.*, Live-seq enables temporal transcriptomic recording of single cells. *Nature* **608**, 733-740 (2022).
- 1527 34. B. H. Weinberg *et al.*, Large-scale design of robust genetic circuits with multiple inputs and outputs for mammalian cells. *Nat Biotechnol* **35**, 453-462 (2017).
- 1528 35. C. Kuscu *et al.*, CRISPR-STOP: gene silencing through base-editing-induced nonsense mutations. *Nat Methods* **14**, 710-712 (2017).
- 1529 36. K. Nishida *et al.*, Targeted nucleotide editing using hybrid prokaryotic and vertebrate adaptive immune systems. *Science* **353**, (2016).
- 1530 37. B. L. Emert *et al.*, Variability within rare cell states enables multiple paths toward drug resistance. *Nat Biotechnol* **39**, 865-876 (2021).
- 1531 38. H. A. Rees, D. R. Liu, Base editing: precision chemistry on the genome and transcriptome of living cells. *Nat Rev Genet* **19**, 770-788 (2018).
- 1532 39. R. C. Sakata *et al.*, Base editors for simultaneous introduction of C-to-T and A-to-G mutations. *Nat Biotechnol*, (2020).
- 1533 40. S. Konermann *et al.*, Genome-scale transcriptional activation by an engineered CRISPR-Cas9 complex. *Nature* **517**, 583-588 (2015).
- 1534 41. A. Hecht *et al.*, Measurements of translation initiation from all 64 codons in *E. coli*. *Nucleic Acids Res* **45**, 3615-3626 (2017).
- 1535 42. N. M. Gaudelli *et al.*, Programmable base editing of A•T to G•C in genomic DNA without DNA cleavage. *Nature* **551**, 464-471 (2017).
- 1536 43. J. G. Doench *et al.*, Optimized sgRNA design to maximize activity and minimize off-target effects of CRISPR-Cas9. *Nat Biotechnol* **34**, 184-191 (2016).
- 1537 44. N. Kim *et al.*, Prediction of the sequence-specific cleavage activity of Cas9 variants. *Nat Biotechnol* **38**, 1328-1336 (2020).
- 1538 45. E. Z. Macosko *et al.*, Highly Parallel Genome-wide Expression Profiling of Individual Cells Using Nanoliter Droplets. *Cell* **161**, 1202-1214 (2015).
- 1539 46. G. X. Zheng *et al.*, Massively parallel digital transcriptional profiling of single cells. *Nat Commun* **8**, 14049 (2017).
- 1540 47. A. J. Hill *et al.*, On the design of CRISPR-based single-cell molecular screens. *Nat Methods* **15**, 271-274 (2018).
- 1541 48. M. Hegde, C. Strand, R. E. Hanna, J. G. Doench, Uncoupling of sgRNAs from their associated barcodes during PCR amplification of combinatorial CRISPR screens. *PLoS One* **13**, e0197547 (2018).
- 1542 49. R. P. Bennett, C. A. Cox, J. P. Hoeffler, Fusion of green fluorescent protein with the Zeocin-resistance marker allows visual screening and drug selection of transfected eukaryotic cells. *Biotechniques* **24**, 478-482 (1998).
- 1543 50. S. Banno, K. Nishida, T. Arazoe, H. Mitsunobu, A. Kondo, Deaminase-mediated multiplex genome editing in *Escherichia coli*. *Nat Microbiol* **3**, 423-429 (2018).
- 1544 51. R. M. Shelake, D. Pramanik, J. Y. Kim, In Vivo Rapid Investigation of CRISPR-Based Base Editing Components in *Escherichia coli* (IRI-CCE): A Platform for Evaluating Base Editing Tools and Their Components. *Int J Mol Sci* **23**, (2022).
- 1545 52. M. Izumi *et al.*, Blasticidin S-resistance gene (bsr): a novel selectable marker for mammalian cells. *Exp Cell Res* **197**, 229-233 (1991).

- 1574 53. J. Burian *et al.*, High-throughput retrieval of target sequences from complex clone libraries using
1575 CRISPRi. *Nat Biotechnol*, (2022).
- 1576 54. K. Kim *et al.*, Epigenetic memory in induced pluripotent stem cells. *Nature* **467**, 285-290 (2010).
- 1577 55. O. Bar-Nur, H. A. Russ, S. Efrat, N. Benvenisty, Epigenetic memory and preferential lineage-
1578 specific differentiation in induced pluripotent stem cells derived from human pancreatic islet beta
1579 cells. *Cell Stem Cell* **9**, 17-23 (2011).
- 1580 56. K. Kim *et al.*, Donor cell type can influence the epigenome and differentiation potential of human
1581 induced pluripotent stem cells. *Nat Biotechnol* **29**, 1117-1119 (2011).
- 1582 57. K. Osafune *et al.*, Marked differences in differentiation propensity among human embryonic stem
1583 cell lines. *Nat Biotechnol* **26**, 313-315 (2008).
- 1584 58. G. L. Boultling *et al.*, A functionally characterized test set of human induced pluripotent stem cells.
1585 *Nat Biotechnol* **29**, 279-286 (2011).
- 1586 59. A. Casini, M. Storch, G. S. Baldwin, T. Ellis, Bricks and blueprints: methods and standards for
1587 DNA assembly. *Nat Rev Mol Cell Biol* **16**, 568-576 (2015).
- 1588 60. C. A. Hutchison, 3rd *et al.*, Design and synthesis of a minimal bacterial genome. *Science* **351**,
1589 aad6253 (2016).
- 1590 61. Y. Shao *et al.*, Creating a functional single-chromosome yeast. *Nature* **560**, 331-335 (2018).
- 1591 62. D. G. Gibson *et al.*, Enzymatic assembly of DNA molecules up to several hundred kilobases. *Nat
1592 Methods* **6**, 343-345 (2009).
- 1593 63. D. G. Gibson, H. O. Smith, C. A. Hutchison, 3rd, J. C. Venter, C. Merryman, Chemical synthesis
1594 of the mouse mitochondrial genome. *Nat Methods* **7**, 901-903 (2010).
- 1595 64. H. Mori, N. Yachie, A framework to efficiently describe and share reproducible DNA materials
1596 and construction protocols. *Nat Commun* **13**, 2894 (2022).
- 1597 65. R. H. Kutner, X. Y. Zhang, J. Reiser, Production, concentration and titration of pseudotyped HIV-
1598 1-based lentiviral vectors. *Nat Protoc* **4**, 495-505 (2009).
- 1599 66. C. Engler, R. Kandzia, S. Marillonnet, A one pot, one step, precision cloning method with high
1600 throughput capability. *PLoS One* **3**, e3647 (2008).
- 1601 67. C. Camacho *et al.*, BLAST+: architecture and applications. *BMC Bioinformatics* **10**, 421 (2009).
- 1602 68. L. Zhao, Z. Liu, S. F. Levy, S. Wu, Bartender: a fast and accurate clustering algorithm to count
1603 barcode reads. *Bioinformatics* **34**, 739-747 (2018).
- 1604 69. A. Dobin *et al.*, STAR: ultrafast universal RNA-seq aligner. *Bioinformatics* **29**, 15-21 (2013).
- 1605 70. T. Stuart *et al.*, Comprehensive Integration of Single-Cell Data. *Cell* **177**, 1888-1902 e1821
1606 (2019).
- 1607

Supplementary Materials for

A multi-kingdom genetic barcoding system for precise target clone isolation

Soh Ishiguro^{1,15,19}, Kana Ishida^{2,19}, Rina C. Sakata^{1,19}, Hideto Mori³⁻⁵, Mamoru Takana³, Samuel King¹, Omar Bashteh¹, Minori Ichiraku⁶, Nanami Masuyama^{1,4,5}, Ren Takimoto¹, Yusuke Kijima^{1,7}, Arman Adel¹, Hiromi Toyoshima³, Motoaki Seki³, Ju Hee Oh⁸, Anne-Sophie Archambault⁸, Keiji Nishida^{9,10}, Akihiko Kondo⁹⁻¹¹, Satoru Kuhara¹², Hiroyuki Aburatani¹³, Ramon I. Klein Geltink⁸, Yasuhiro Takashima⁶, Nika Shakiba¹, and Nozomu Yachie^{1,3,14,16-18*}

1. School of Biomedical Engineering, Faculty of Applied Science and Faculty of Medicine, The University of British Columbia, Vancouver, Canada.
2. Spiber Inc., Tsuruoka, Japan.
3. Synthetic Biology Division, Research Center for Advanced Science and Technology, The University of Tokyo, Tokyo, Japan.
4. Institute for Advanced Biosciences, Keio University, Tsuruoka, Japan.
5. Systems Biology Program, Graduate School of Media and Governance, Keio University, Fujisawa, Japan.
6. Center for iPS Cell Research and Application, Kyoto University, Kyoto, Japan.
7. Department of Aquatic Bioscience, Graduate School of Agricultural and Life Sciences, The University of Tokyo, Tokyo, Japan.
8. BC Children's Hospital Research Institute, Department of Pathology and Laboratory Medicine, The University of British Columbia, Vancouver, Canada.
9. Engineering Biology Research Center, Kobe University, Kobe, Japan.
10. Graduate School of Science, Technology and Innovation, Kobe University, Kobe, Japan.
11. Department of Chemical Science and Engineering, Graduate School of Engineering, Kobe University, Kobe, Japan.
12. Graduate School of Bioresource and Bioenvironmental Sciences, Faculty of Agriculture, Kyushu University, Fukuoka, Japan.
13. Genome Science Division, Research Center for Advanced Science and Technology, The University of Tokyo, Tokyo, Japan.
14. Premium Research Institute for Human Metaverse Medicine (WPI-PRI^Me), Osaka University, Suita, Osaka, Japan
15. Twitter: @soh_i
16. Twitter: @nzmyachie
17. Twitter: @yachielab
18. Mastodon: scencemastodon.com/@nzm
19. These authors contributed equally.

*Corresponding author: nozomu.yachie@ubc.ca.

Table of Contents

Fig. S1	Supplementary data for developing CloneSelect C→T
Fig. S2	Supplementary data for comparing CloneSelect C→T with CRISPRa-based circuits
Fig. S3	DSB-based circuit
Fig. S4	mCherry reporter for CloneSelect C→T
Fig. S5	Supplementary data for comparing CloneSelect A→G with CRISPRa-based circuits
Fig. S6	Supplementary data for isolating barcoded cells using CloneSelect C→T
Fig. S7	Supplementary data for developing scCloneSelect
Fig. S8	The gene expression profile cytometry cell sorting concept
Fig. S9	Supplementary data for isolating barcoded cells identified in scRNA-seq data
Fig. S10	Supplementary data for developing yeast CloneSelect
Fig. S11	Preparation of yeast CloneSelect library
Fig. S12	Supplementary data for developing bacterial CloneSelect
Fig. S13	Preparation of <i>E. coli</i> CloneSelect library
Fig. S14	Multiple gRNA-input logic gates
Table S1	Barcode count distributions observed in this study
Table S2	Oligonucleotides and plasmids used in this study
Table S3	List of high-throughput sequencing datasets
Table S4	Statistical tests performed in this study and <i>P</i> -values

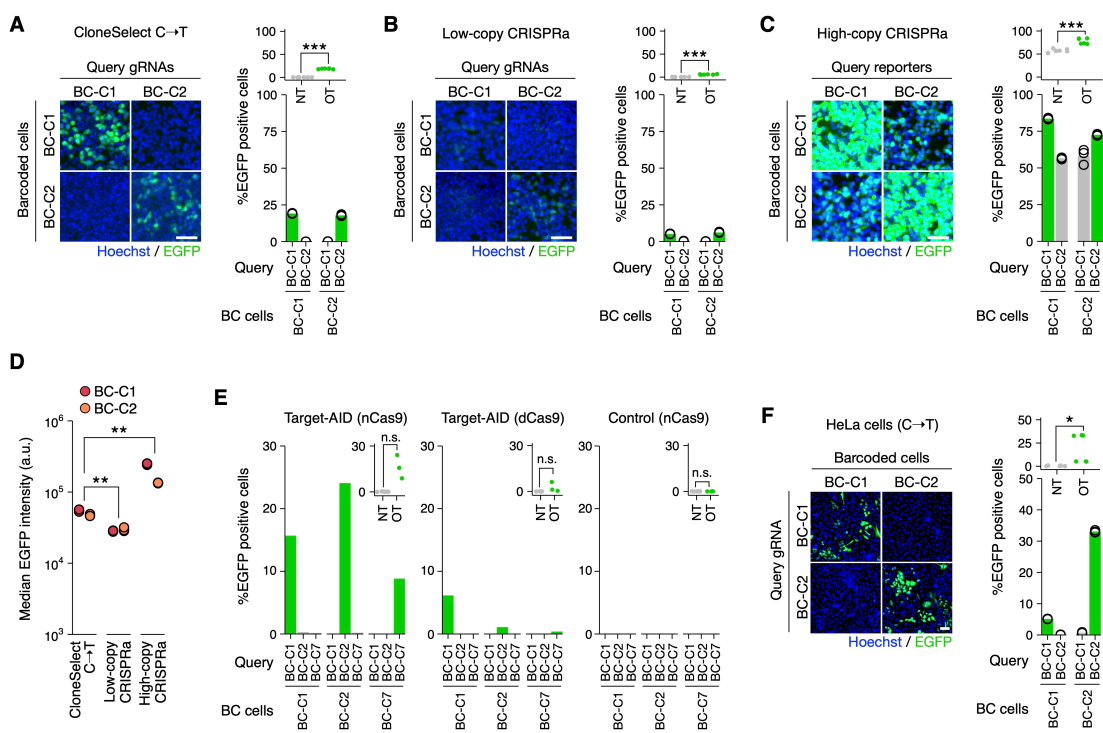


Fig. S1. Supplementary data for developing CloneSelect C→T. (A–C) Barcode-specific gRNA-dependent activation of EGFP reporters for two barcoded HEK293T strains established for each of CloneSelect C→T (A), low-copy CRISPRa (B), and high-copy CRISPRa (C) ($n=3$). Scale bar, 50 μ m. Welch's t-test was performed to compare on-target (OT) and non-target (NT) activations. (D) Median EGFP intensities of genome editing-activated EGFP positive cells ($n=3$). The Mann-Whitney U test was performed to compare two groups. (E) Comparison of Target-AID variants and a nCas9 (D10A) control in the CloneSelect C→T reporter activation for the same set of barcode-gRNA pairs ($n=1$). Welch's t-test was performed to compare OT and NT activations. (F) Reporter activation in HeLa cells by CloneSelect C→T ($n=3$). Welch's t-test was performed to compare OT and NT activations. Scale bar, 80 μ m. * $P < 0.05$; ** $P < 0.01$; *** $P < 0.001$.

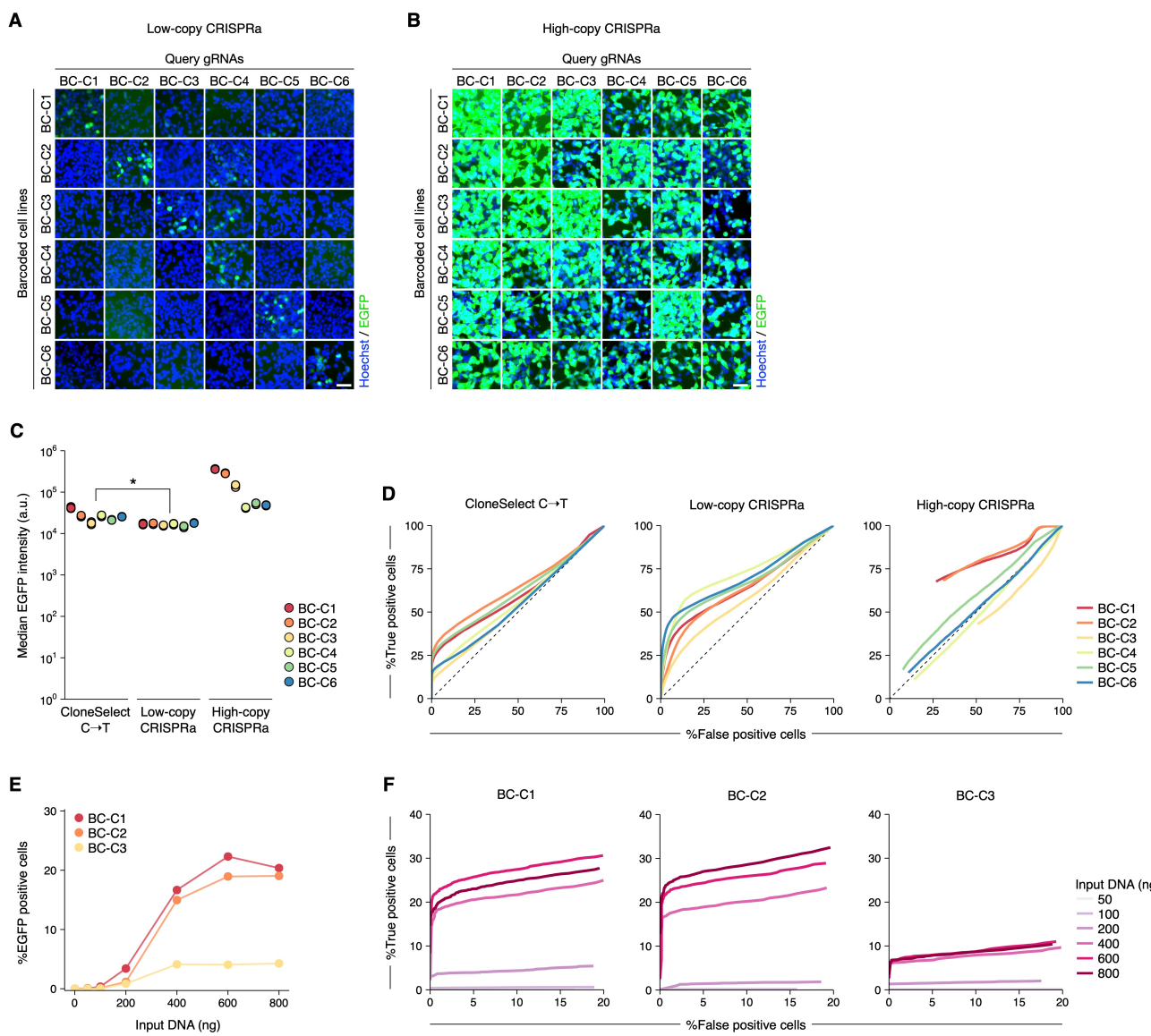


Fig. S2. Supplementary data for comparing CloneSelect C→T with CRISPRa-based circuits. (A and B) Barcode-specific gRNA-dependent reporter activation of six barcoded cell lines prepared for each of low-copy CRISPRa and high-copy CRISPRa. Scale bar, 50 μ m. (C) Median EGFP intensities of genome editing-activated EGFP positive cells ($n=3$). (D) ROC curves along varying reporter intensity thresholds for target barcoded cells. CloneSelect C→T, low-copy CRISPRa, and high-copy CRISPRa were examined for the common set of six barcodes. The Mann-Whitney U test was performed to compare two groups (* $P < 0.05$; ** $P < 0.01$; *** $P < 0.001$). (E) Frequencies of CloneSelect C→T reporter-activated cells obtained by transfection of different DNA amounts of barcode-targeting genome editing reagents. (F) ROC curve for each input DNA amount along varying reporter intensity thresholds for target barcoded cells.

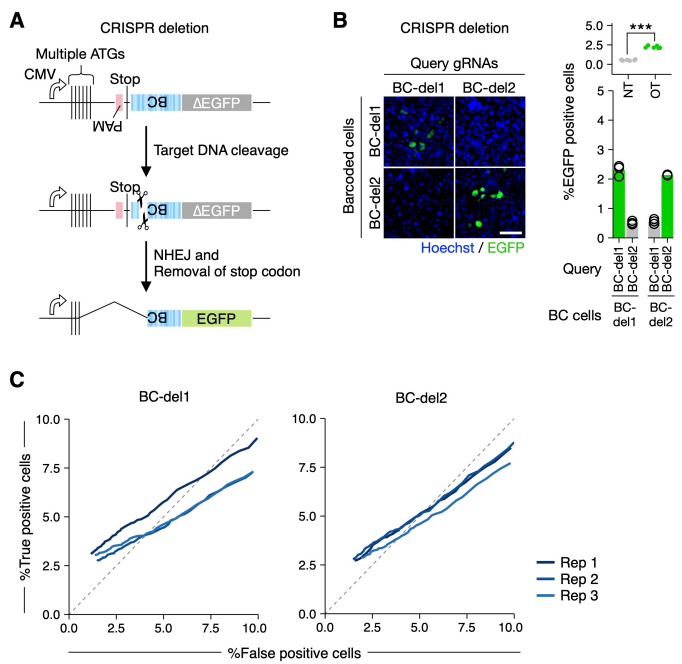


Fig. S3. DSB-based circuit. (A) Barcode-specific gRNA-dependent reporter activation circuit using wild-type Cas9. (B) Barcode-specific activation of the deletion-based reporter prepared for two barcodes (BC-del1 and BC-del2) in HEK293T cells ($n=3$). Welch's t-test was performed to compare on-target (OT) and non-target (NT) activations (* $P < 0.05$; ** $P < 0.01$; *** $P < 0.001$). Scale bar, 50 μ m. (C) ROC curves along varying reporter intensity thresholds for target barcoded cells ($n=3$).

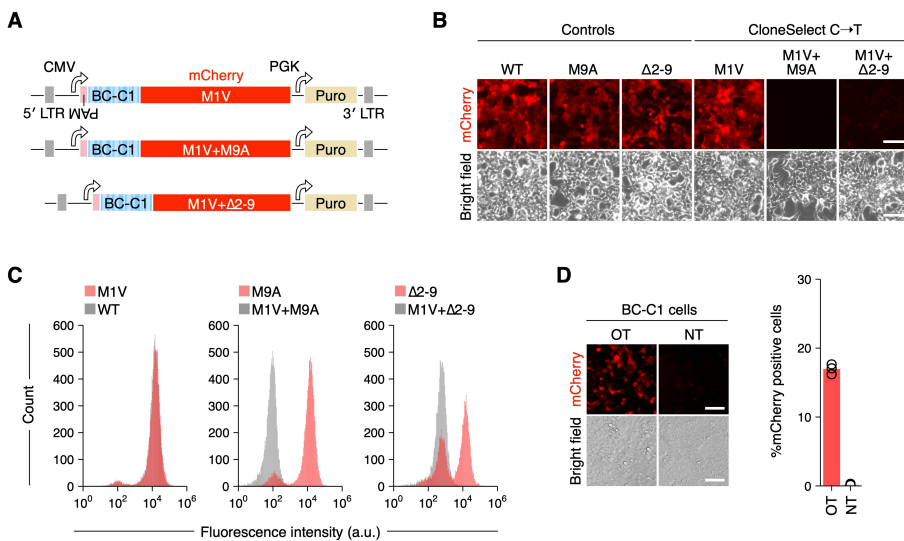


Fig. S4. mCherry reporter for CloneSelect C→T. **(A)** Different mCherry reporter variants tested to establish CloneSelect C→T. **(B and C)** mCherry expression from the different reporter variants with the first codon as GTG or ATG. Scale bar, 50 µm. **(D)** Activation of the M1V (GTG)+Δ2-9 mutant reporter with OT and NT gRNAs (n=3). Scale bar, 100 µm.

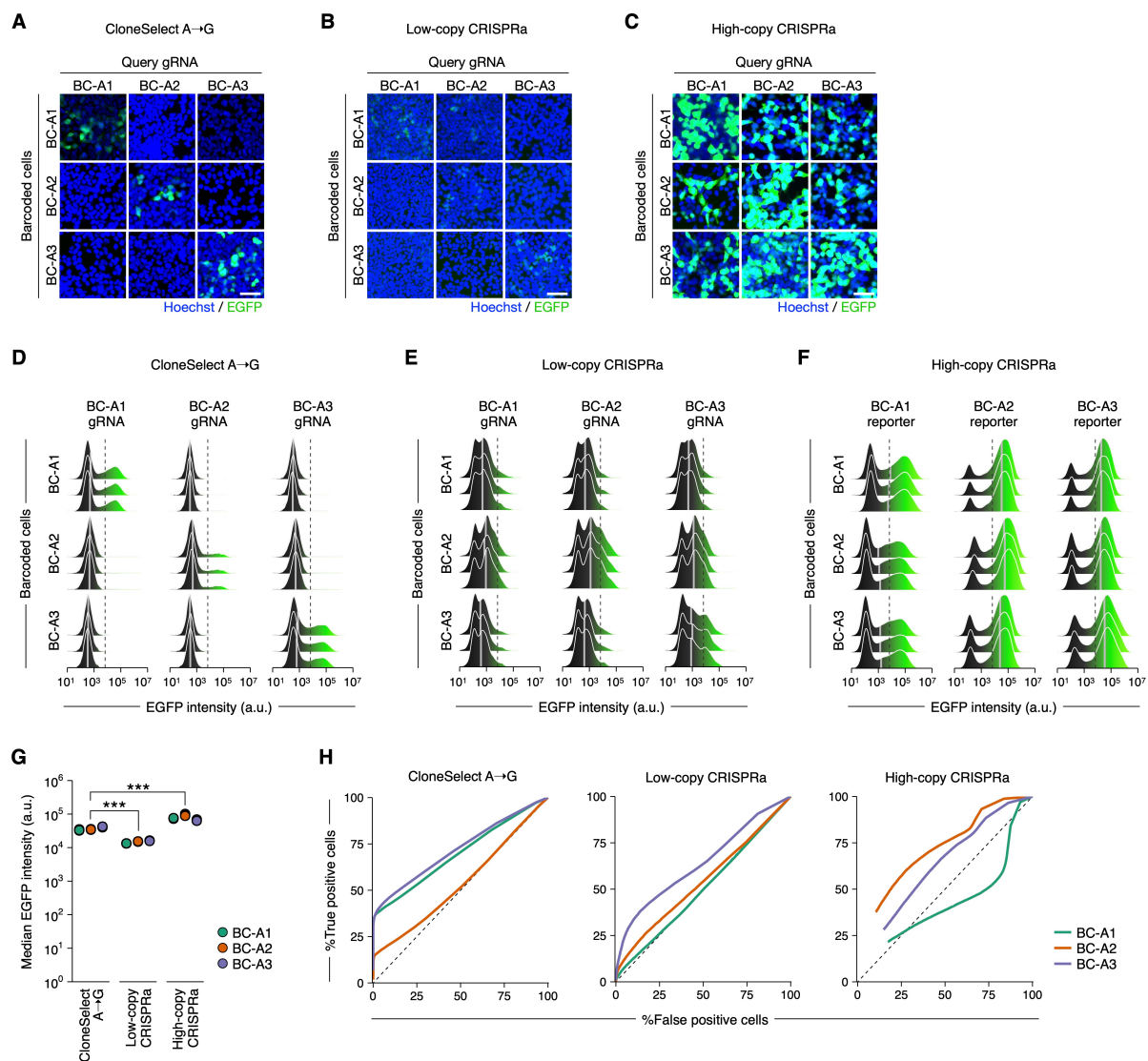


Fig. S5. Supplementary data for comparing CloneSelect A→G with CRISPRa-based circuits. (A–C) Barcode-specific gRNA-dependent reporter activation of three barcoded cell lines prepared for each of CloneSelect A→G, low-copy CRISPRa, and high-copy CRISPRa. Scale bar, 50 μ m. **(D–F)** Flow cytometry analysis of single-cell EGFP activation levels. **(G)** Median EGFP intensities of genome editing-activated EGFP positive cells ($n=3$). The Mann-Whitney U test was performed to compare two groups (* $P < 0.05$; ** $P < 0.01$; *** $P < 0.001$). **(H)** ROC curves along varying reporter intensity thresholds for target barcoded cells ($n=3$).

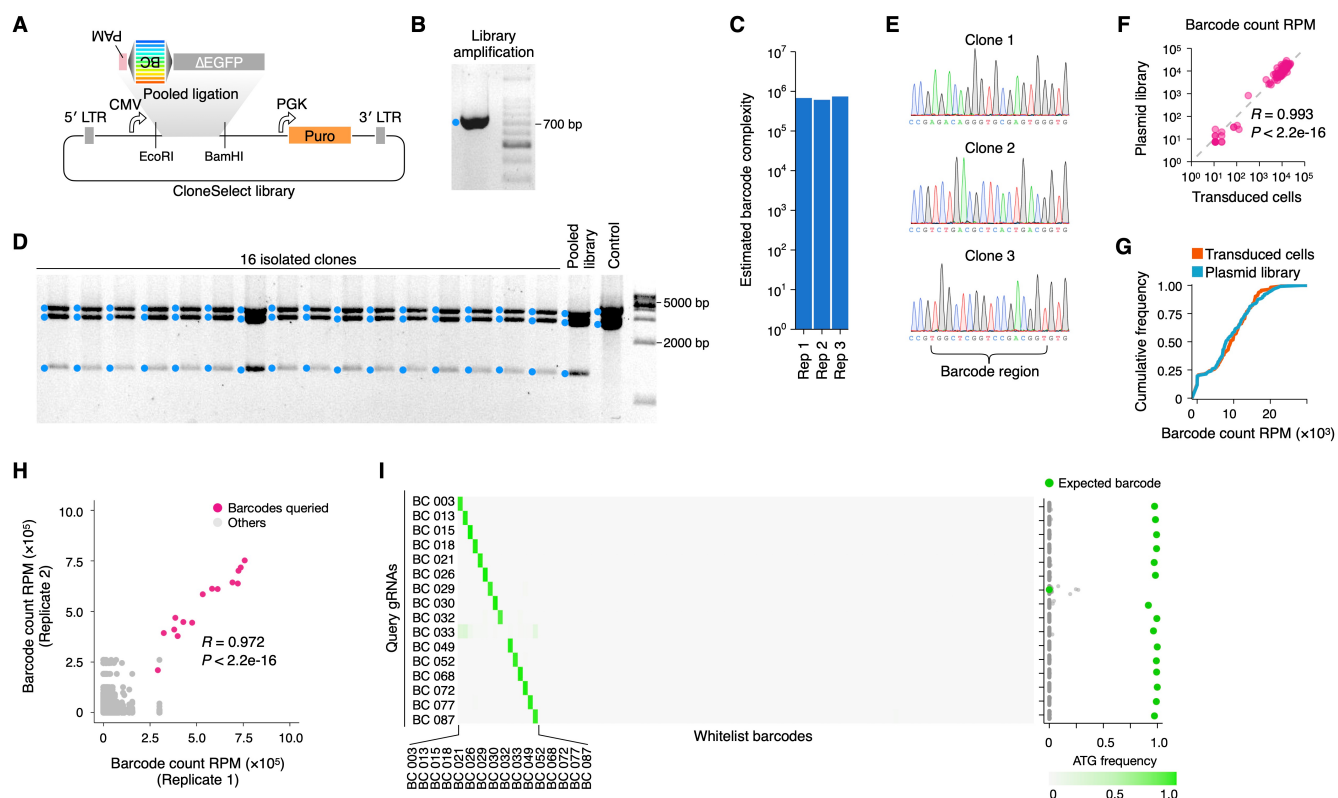


Fig. S6. Supplementary data for isolating barcoded cells using CloneSelect C \rightarrow T. (A) Schematic diagram for the barcode library construction. The ΔEGFP fragment (no start codon) was amplified by PCR using pooled forward primers encoding the PAM followed by semi-random barcode sequences encoding GTG and a common reverse primer, and enzymatically digested and ligated to the lentiviral backbone. (B) The insert PCR fragments. (C) Estimated complexities of the generated plasmid pools in triplicate. (D) Library QC by colony isolation and restriction digest by BsrGI, Clal and Pvul. (E) Sanger sequencing of the barcode region of the colony isolates. (F and G) Barcode distribution in the lentiviral plasmid DNA pool and that in the cell population transduced using the same plasmid DNA pool. (H) Barcode distribution in the EGFP-positive cell population obtained by cell sorting after barcode-specific activation by a target gRNA. The results of the 16 independent samples were combined after read count normalization for each sample. (I) Frequency of the GTG \rightarrow ATG mutation observed for each barcode after sorting of the reporter positive cells. Each row represents the GTG \rightarrow ATG mutation frequency profile obtained for each target isolation attempt.

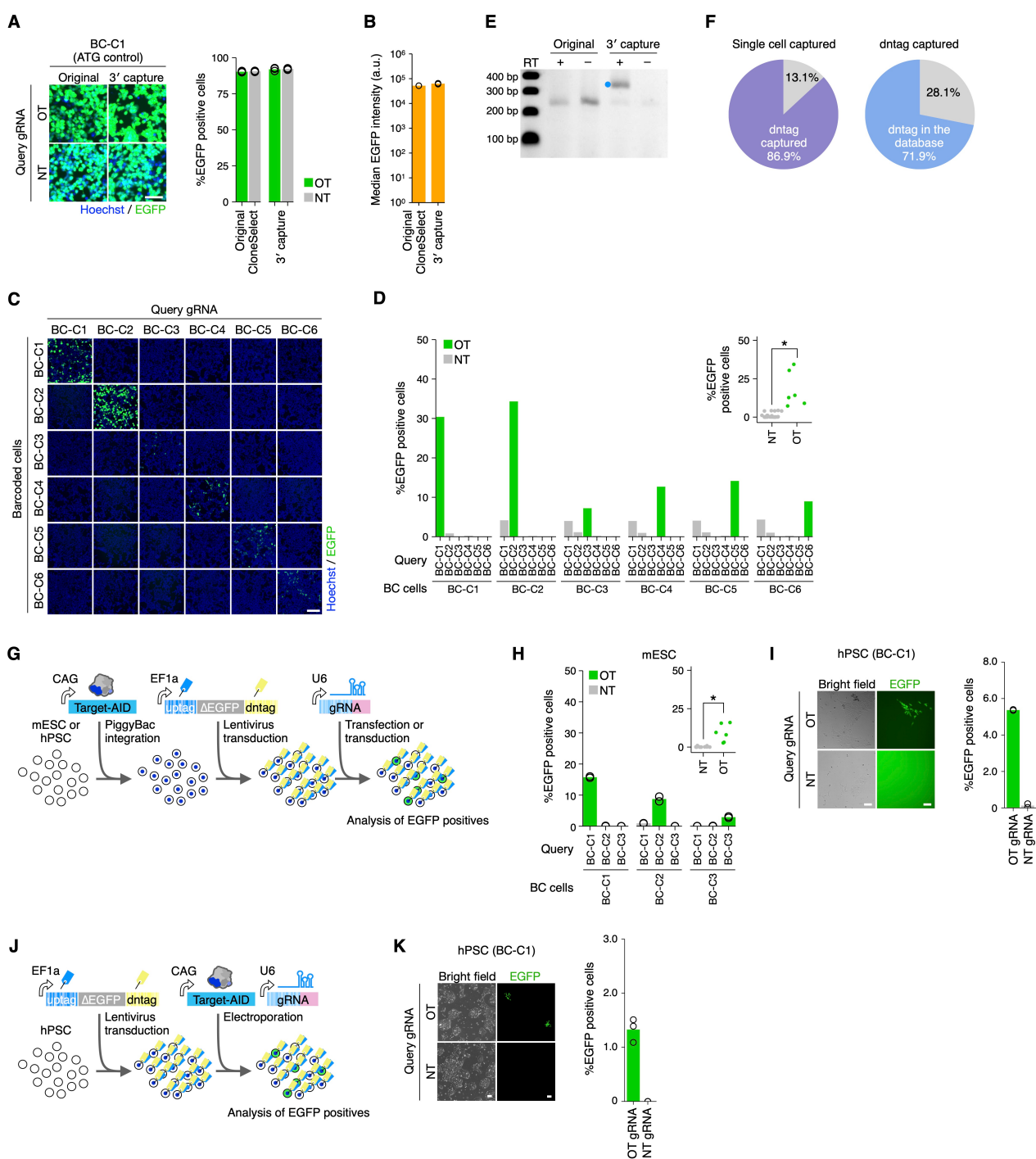


Fig. S7. Supplementary data for developing scCloneSelect. (A) EGFP-positive control expressions for the original CloneSelect C→T and scCloneSelect in HEK293T cells with the same genome editing conditions tested for the respective reporters (n=3). Scale bar, 50 μm. (B) Median EGFP intensities of base editing-activated EGFP positive cells (n=3). (C and D) Barcode-specific gRNA-dependent reporter activation of six barcoded cell lines by scCloneSelect (n=1). Welch's t-test was performed to compare on-target (OT) and non-target (NT) activations (*P < 0.05; **P < 0.01; ***P < 0.001). Scale bar, 50 μm. (E) RT-PCR of the scCloneSelect dntags in HEK293T. (F) Fraction of mESC single-cell transcriptome profiles (Drop-seq) that contained dntags and fraction of dntags reported in the uptag-dntag combination reference database. (G) Schematic representation of a scCloneSelect reporter activation assay where Target-AID was stably introduced to the cell population prior to barcoding and gRNA-dependent reporter activation. (H and I) gRNA-dependent reporter activation of target barcoded mESCs and CA1 hPSCs by scCloneSelect (n=2). Target-AID was stably integrated prior to the barcoding. Targeting

gRNAs were delivered by transfection. Welch's t-test was performed to compare OT and NT activations ($*P < 0.05$; $**P < 0.01$; $***P < 0.001$). Scale bar, 100 μ m. (J) Schematic representation of a scCloneSelect reporter activation assay where the target gRNA and Target-AID were electroporated together to the barcoded cell population. (K) gRNA-dependent reporter activation of barcoded H1 hPSCs by scCloneSelect (n=2). Targeting gRNA and Target-AID were electroporated together. Scale bar, 100 μ m.

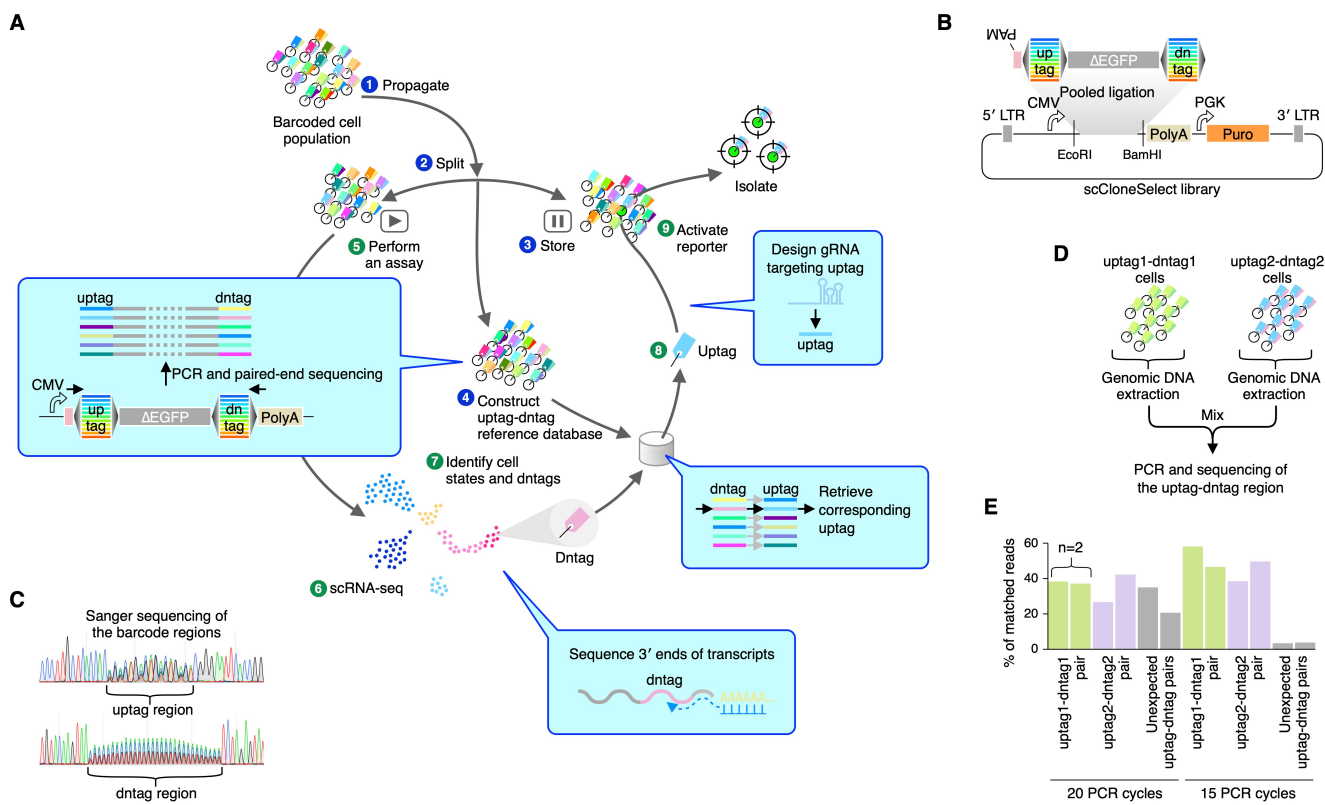


Fig. S8. The gene expression profile cytometry cell sorting concept. (A) Schematic diagram of a scCloneSelect workflow. **(B)** Preparation of barcode library for scCloneSelect. **(C)** Sanger sequencing results of the uptag and dntag regions of the constructed plasmid pool. **(D)** Mixing of genomic DNA samples from two barcoded cell lines to optimize the PCR protocol to create a library for identifying the uptag-dntag combination reference database. **(E)** Fraction of unexpected chimeric PCR recombination products in the sequencing reads.

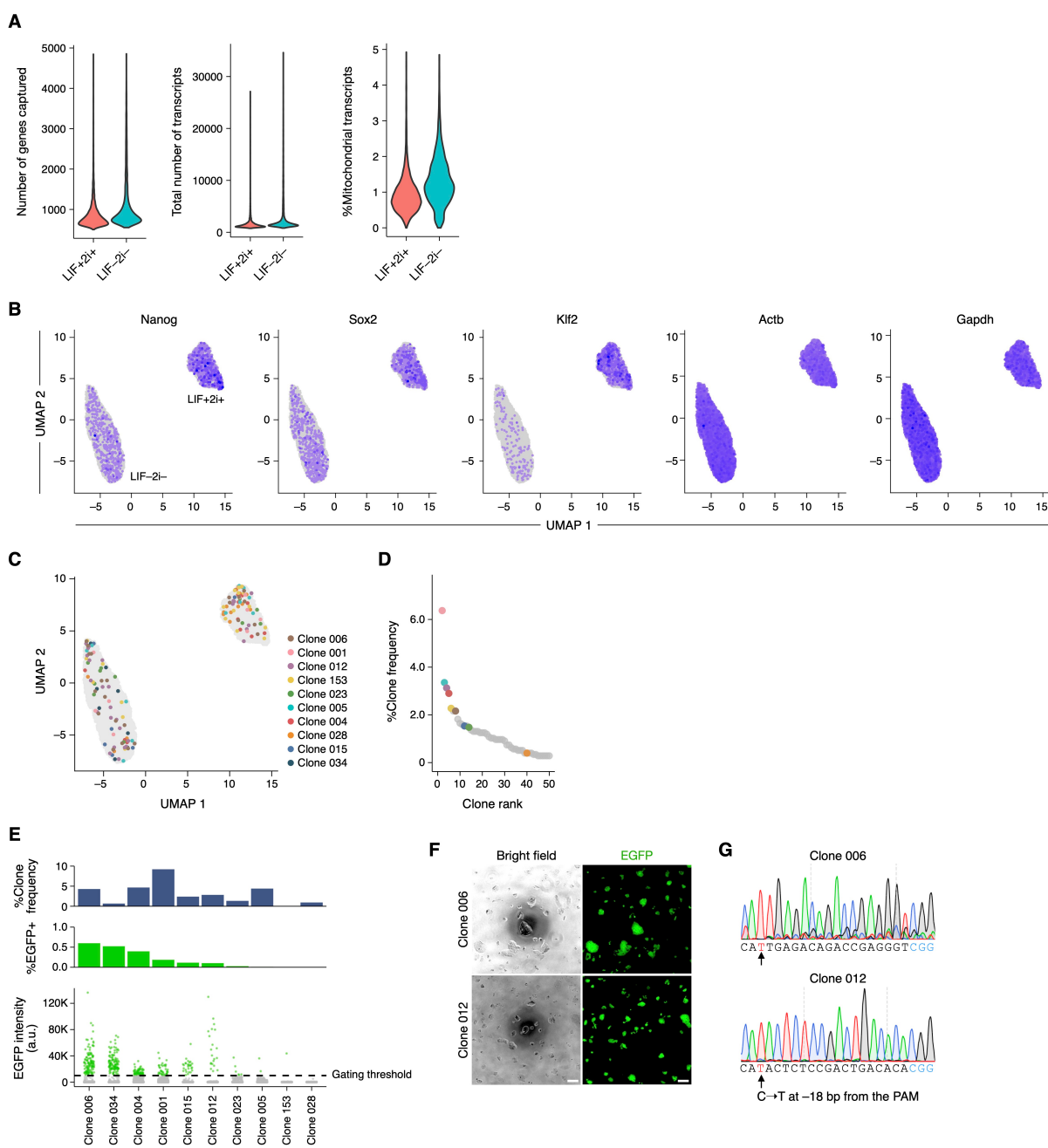


Fig. S9. Supplementary data for isolating barcoded cells identified in scRNA-seq data. (A) QC of scRNA-seq datasets obtained for the barcoded mESC population cultured with LIF and 2i and that cultured without LIF or 2i. **(B)** Single-cell expression patterns of key genes. **(C)** Distribution of cells in a two-dimensional UMAP space for all the clones targeted for isolation. **(D)** Abundances of barcoded cell clones in the mESC population. The data was generated based on dntags identified in the scRNA-seq dataset with no reamplification of the dntag reads. **(E)** gRNA-dependent activation of the reporter for each of the target clones in the initial mESC population. **(F)** Culturing of single isolated cells. Scale bar, 100 μ m. **(G)** Sanger sequencing of the barcodes for the isolated target clones expanded after clone labeling and single-cell isolation.

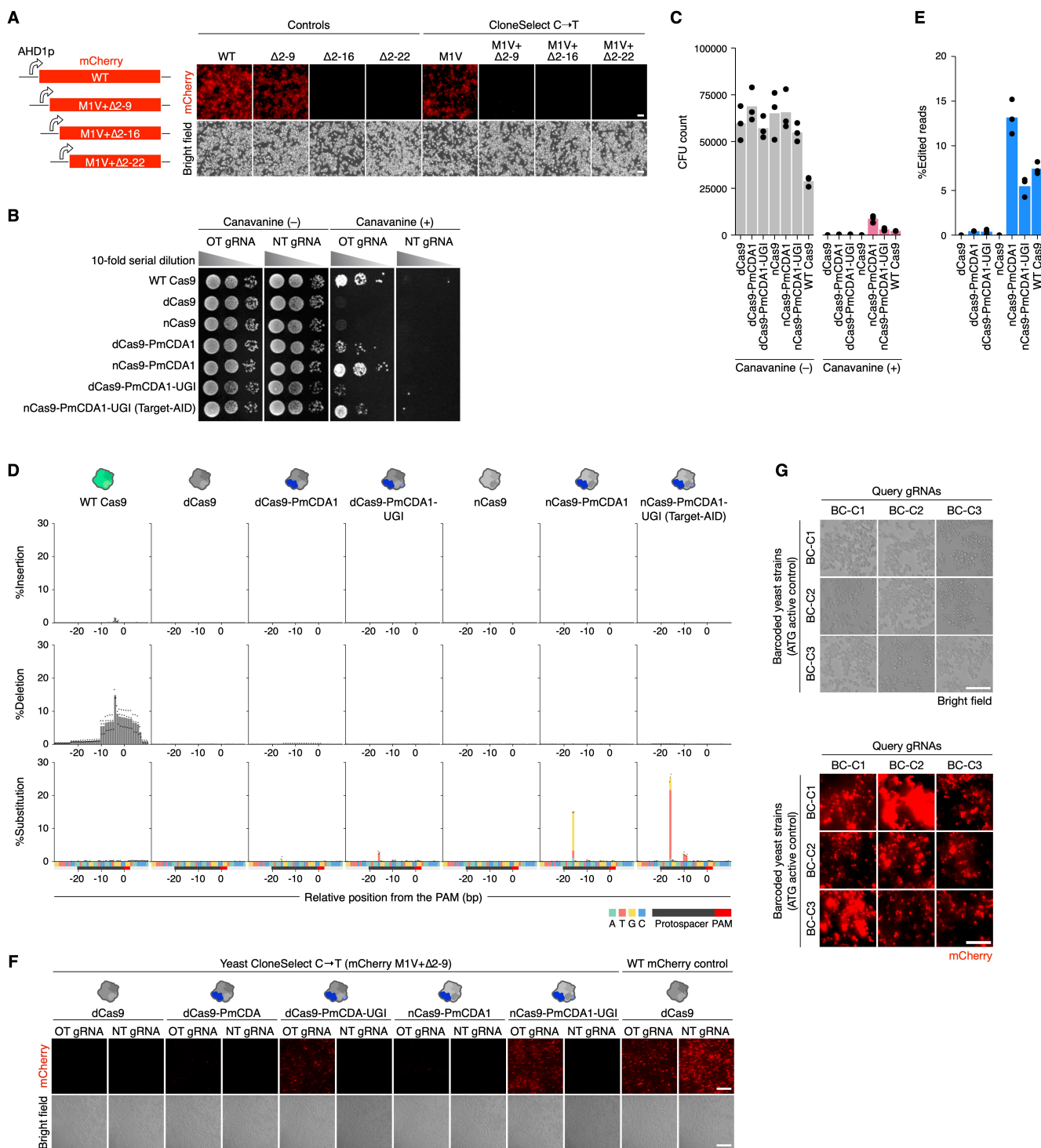


Fig. S10. Supplementary data for developing yeast CloneSelect. (A) Different mCherry reporter variants tested to establish CloneSelect C→T. The different reporter variants were tested with the first codon as GTG or ATG. Scale bar, 100 μ m. **(B)** Canavanine resistance assays for different CRISPR genome editing enzymes with a gRNA targeting CAN1 gene and a control NT gRNA. For each experiment, cell concentration was normalized to 1.0 OD_{595 nm} and serially diluted with 10-fold increments for spotting. **(C)** Estimated CFU counts for the same assay in **(B)**. **(D)** Genome editing outcomes observed by amplicon sequencing. Frequencies of mutation patterns observed across the target sequence region are shown for the same assay in **(B)**. **(E)** Genome editing frequencies at the target CAN1 locus estimated by amplicon sequencing for the different enzymes. **(F)** Activation of the mCherry M1V (GTG)+Δ2-9 mutant reporter by OT and NT gRNAs. Scale bar, 200 μ m. **(G)** mCherry-positive control

expressions for yeast CloneSelect. Yeast cells having the positive control reporters with three different barcodes (BC-C1, BC-C2, and BC-C3) were each treated by Target-AID and three different targeting gRNAs. Scale bar, 25 μm .

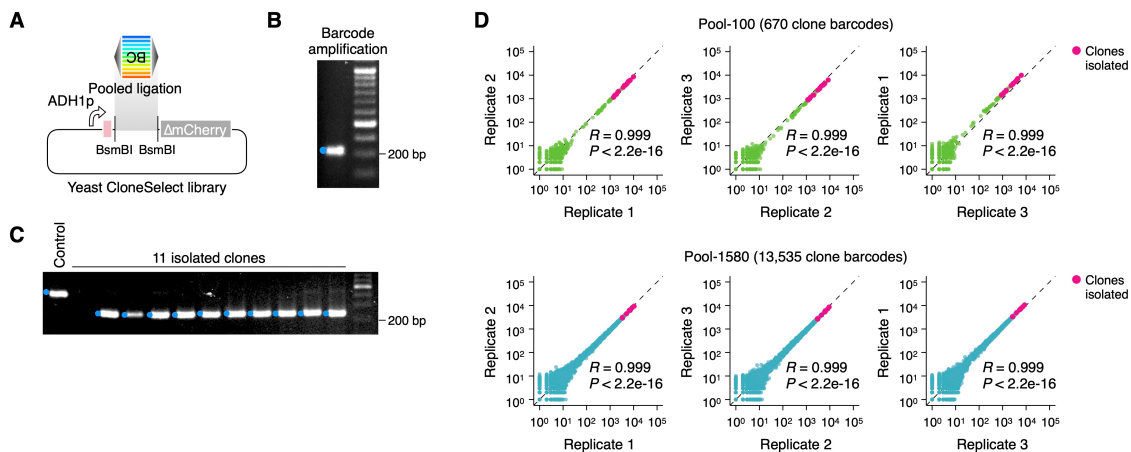


Fig. S11. Preparation of yeast CloneSelect library. **(A)** Schematic diagram for the barcode library construction. The barcode fragment pool was prepared by PCR using a common primer pair amplifying a template DNA pool encoding the PAM, WSNS semi-random repeat, and the mutated start codon GTG. The PCR product was digested and ligated to a backbone plasmid. **(B)** The insert PCR fragments (Pool-100). **(C)** Library QC by colony isolation and PCR amplification of the barcode insert (Pool-100). **(D)** Barcode abundance distribution (read per million) in the constructed barcode library pool. The sequencing library was prepared and analyzed in triplicate ($n=3$).

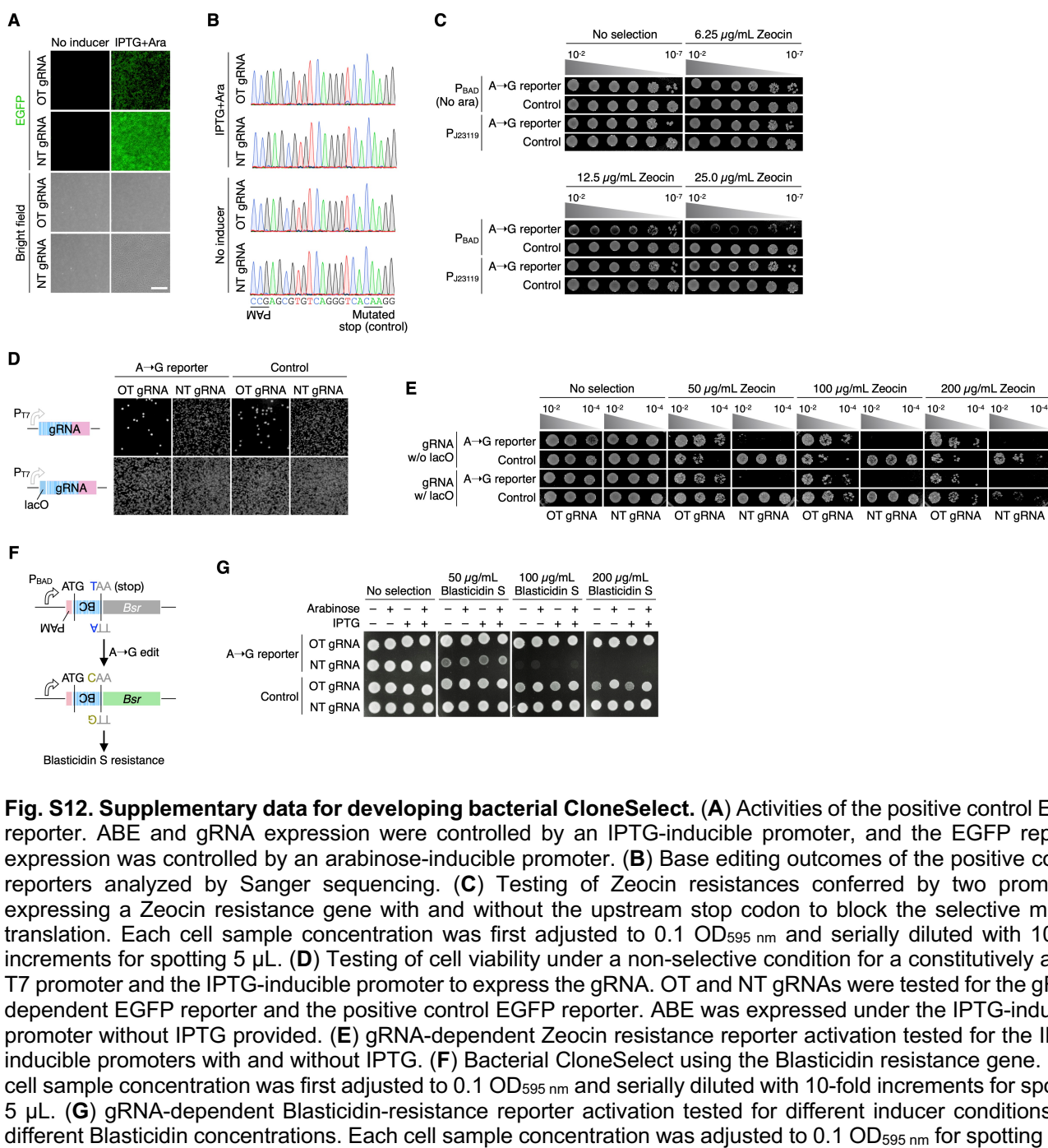


Fig. S12. Supplementary data for developing bacterial CloneSelect. (A) Activities of the positive control EGFP reporter. ABE and gRNA expression were controlled by an IPTG-inducible promoter, and the EGFP reporter expression was controlled by an arabinose-inducible promoter. (B) Base editing outcomes of the positive control reporters analyzed by Sanger sequencing. (C) Testing of Zeocin resistances conferred by two promoters expressing a Zeocin resistance gene with and without the upstream stop codon to block the selective marker translation. Each cell sample concentration was first adjusted to 0.1 OD_{595 nm} and serially diluted with 10-fold increments for spotting 5 μL. (D) Testing of cell viability under a non-selective condition for a constitutively active T7 promoter and the IPTG-inducible promoter to express the gRNA. OT and NT gRNAs were tested for the gRNA-dependent EGFP reporter and the positive control EGFP reporter. ABE was expressed under the IPTG-inducible promoter without IPTG provided. (E) gRNA-dependent Zeocin resistance reporter activation tested for the IPTG-inducible promoters with and without IPTG. (F) Bacterial CloneSelect using the Blasticidin resistance gene. Each cell sample concentration was first adjusted to 0.1 OD_{595 nm} and serially diluted with 10-fold increments for spotting 5 μL. (G) gRNA-dependent Blasticidin-resistance reporter activation tested for different inducer conditions and different Blasticidin concentrations. Each cell sample concentration was adjusted to 0.1 OD_{595 nm} for spotting 5 μL.

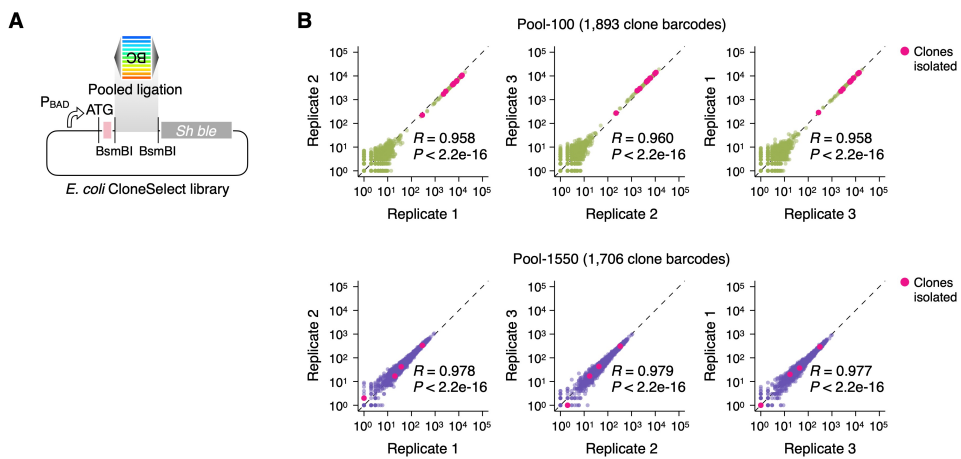


Fig. S13. Preparation of *E. coli* CloneSelect library. (A) Schematic diagram for the barcode library construction. The barcode fragment pool was prepared by PCR using a common primer pair amplifying a template DNA pool encoding the PAM, VNN repeat sequence, and the start codon TAA. The PCR product was digested and ligated to a backbone plasmid. **(B)** Barcode abundance distribution (read per million) in the constructed barcode library pool. The sequencing library was prepared and analyzed in triplicate ($n=3$).

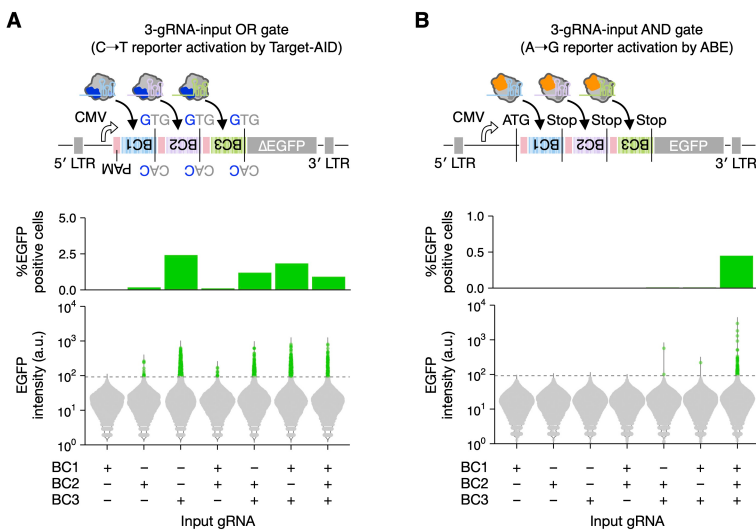


Fig. S14. Multiple gRNA-input logic gates. (A) Three-gRNA-input OR gate with CloneSelect C→T that is designed to confer the EGFP reporter expression by any of the three barcode-specific gRNA-dependent GTG→ATG mutations. (B) Three-gRNA-input AND gate with CloneSelect A→G that is designed to confer the EGFP reporter expression when all three barcode-specific gRNA-dependent TAA→CAA mutations are provided.